Contents lists available at ScienceDirect

Arabian Journal of Chemistry

journal homepage: www.ksu.edu.sa

Natural products-isoxazole hybrids: A review of developments in medicinal chemistry

Jin Wang [a,1], Dong-Bo Wang [b,1], Li-Li Sui [a], Tian Luan [a,*]

[a] Department of Pharmacy, Shenyang Medical College, Shenyang 110034, China
[b] Department of Pharmacy, Shandong Second Provincial General Hospital, Jinan 250022, China

ARTICLE INFO

Keywords:
Isoxazole
Natural products
Pharmacological activity
Structural modifications

ABSTRACT

Five-membered heterocycles containing nitrogen, oxygen atoms, especially isoxazoles, are widely present in many natural products and drugs and have relevant medical and pharmaceutical applications. Due to their rich biological activity, the development of novel isoxazole derivatives has been the focus of researchers and scientists. It is worth noting that a large number of isoxazoles have been used frequently as clinical drugs to treat various diseases, showing great development value and wide medicinal potential. In this review, the research progress of isoxazole natural products in anti-bacterial, anti-tuberculosis, anti-virus, anti-tumor, anti-inflammation, anti-diabetes, anti-parasite, anti-psychosis and other biological activities was reviewed. Finally, the research and development prospects of isoxazole natural products were prospected. This review will provide reference for the design of natural isoxazole products with stronger activity and less toxicity.

1. Introduction

N-containing heterocyclic compounds are a class of important heterocyclic compounds, that are widely used in the search for new bioactive compounds and play an important role in the fields of medicinal chemistry and organic chemistry (Sysak and Obminska-Mrukowicz, 2017). Azoles are a class of 5-membered nitrogen-containing heterocyclic compounds with one or more heteroatoms, such as nitrogen, oxygen, or sulfur (El-Garhy, 2015) (Fig. 1).

Isoxazole is a class of heterocyclic compounds widely used in drug discovery research. The structural characteristics of isoxazole make it possible for a variety of noncovalent interactions, especially hydrogen bonds (hydrogen bond receptors N and O), π-π stack (unsaturated five-membered ring), and hydrophilic interactions (cLog$P$ = 0.334 at physiological pH = 7.4) (Zhu et al., 2018). The introduction of isoxazole can improve efficacy, reduce toxicity, and improve pharmacokinetic characteristics (Sysak and Obminska-Mrukowicz, 2017; Anand and Singh, 2014; Barmade et al., 2016). Isoxazoles can interact with a wide range of protein targets, so isoxazoles have a wide range of biological activities, including anti-cancer, anti-bacterial, anti-fungal, anti-viral, anti-microbial, anti-tuberculosis, anti-inflammatory, etc. (Zhu et al., 2018). Currently, there are dozens of drugs available on the market that contain isoxazole fragments. These drugs can alleviate and eliminate the effects of various diseases, thereby safeguarding human health. (Fig. 2 and Table 1) (Thakur et al., 2022).

Natural products extracted from microorganisms, plants, and animals have significant structural diversity and biological properties, and these natural products are an important source of drug discovery (Huang et al., 2022; Chopra and Dhingra, 2021). However, most natural products have low pharmacological activity or too many adverse reactions to be used directly in the clinical treatment of diseases (Wang et al., 2023). Structural modification can improve the physical and chemical properties and biological activities of natural products, reduce adverse reactions, and improve selectivity. Furthermore, structural modifications may also exhibit biological activities completely different from those of their parent compounds (Yao et al., 2017). Isoxazole plays an important role in natural products and has significant biological activity. More and more studies have reported the modification of natural products with isoxazole (Farooq and Ngaini, 2022).

Some reviews have been conducted on the research of some isoxazole derivatives as drugs (Zhang et al., 2011; Ohnmacht and Neidle, 2014; Defossa and Wagner, 2014), but there is no systematic report on the development status of isoxazole in natural product derivatives. Given this, the research progress of isoxazole derivatives in the field of natural

* Corresponding author.
E-mail address: luantian@symc.edu.cn (T. Luan).
[1] Both authors contributed equally to this work.

https://doi.org/10.1016/j.arabjc.2024.105794
Received 19 January 2024; Accepted 13 April 2024
Available online 15 April 2024

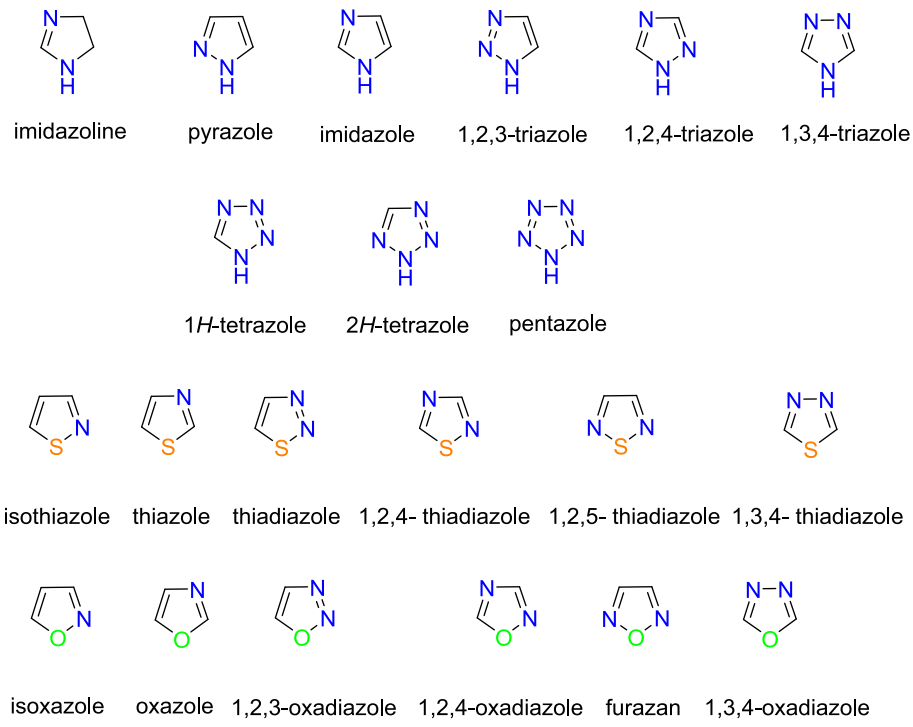

Fig. 1. Various types of azoles.

product modification in anti-microbial, anti-fungal, anti-viral, anti-tuberculosis, anti-cancer, anti-inflammatory, hypoglycemic, anti-parasitic, anti-obesity, anti-psychosis, anti-oxidation and other aspects was reviewed. The research direction of isoxazole-natural products in medicinal chemistry was explored.

2. Hybridization of natural product and isoxazole

To facilitate the classification and management of the literature, all relevant literature is divided into eleven categories according to the introduction framework: cinnamamide and cinnamic acids, chalcones, styrene and polyphenols, coumarins, lignin, quinones, flavonoids, steroids, terpenes, alkaloids, carbohydrate, and other natural components.

2.1. Cinnamamide and cinnamic acid-isoxazole hybridization

Shultz *et al.* (Shultz et al., 2011) designed and synthesized *N*-hydroxy-(4-oxime)-cinnamide derivatives containing indole. Among them, compound **1** containing isoxazole showed certain inhibitory activity against HDAC-1 with an IC_{50} value of 17 nM. The synthesis route of compound **1** is depicted in Fig. 3. Methyl 4-formylcinnamate was reacted with (2-(3,5-dimethylisoxazol-4-yl)-1*H*-indol-3-yl)methanamine via reductive amination to generate substituted methyl 4-aminomethyl cinnamates, which were then converted to the corresponding hydroxamates using aqueous hydroxylamine in methanolic sodium methoxide. Histone deacetylases (HDACs) are enzymes involved in chromatin remodeling that play a key role in epigenetic regulation of gene expression. HDAC catalyzes the removal of acetyl groups from core histones and other lysine residues that control cell functions such as proliferation, migration, differentiation, and cell death. Therefore, inhibition of HDAC is a practical treatment for the discovery of new targeted anticancer drugs (Bolden et al., 2006). Giannini *et al.* (Giannini et al., 2009) designed a series of compounds with a *N*-hydroxy-(4-oxime)-cinnamide scaffold. The cytotoxic activity of the compounds against the NB4, H460 and HCT116 cell lines and their inhibitory activity against class I, II, and IV HDacs were evaluated. Compound **2**, which contains isoxazole, exhibited significant inhibitory activity against HCT116 and NCI-H460 cell lines with IC_{50} values of 7.0 and 4.0 μM, respectively. Compound **2** also demonstrated good inhibitory activity against HDAC6 and HDAC8 with IC_{50} values of 0.175 and 0.127 μM, respectively.

Botulinum neurotoxin (BoNTs) is the most toxic protein known to man, and exposure to it can cause flaccid paralysis. Because these proteins are extremely potent, they have been studied as possible bioterrorism weapons. Smith *et al.* (Smith et al., 2012) reported a series of 2,4-dichloro cinnamyl hydroxamate derivatives and tested their inhibition of the BoNT/A light chain metalloprotease. Compound **3**, which contains isoxazole, exhibited a certain inhibitory effect on BoNT/A with an IC_{50} value of 1.16 μM.

EP3 antagonists have the potential to reduce the risk of atherosclerotic thrombosis without increasing the risk of bleeding. Singh *et al.* (Singh et al., 2010) reported on the pharmacological effects of a series of EP3 receptor antagonists. In the absence of serum protein, compound **4** containing isoxazole showed some binding capacity to hEP3 with an IC_{50} value of 14.5 μM.

Shultz *et al.* (Shultz et al., 2011) described the design, synthesis, and biological evaluation of a novel isoindolyl hydroxate. Compound **5** containing isoxazole inhibited HDAC1 with an IC_{50} of 0.17 μM. The proliferation of HCT116 cells was inhibited with an IC_{50} of 2.2 μM. The synthesis route of the compound is shown in Fig. 4. Starting with 5-Bromoisoindoline-1,3-dione as the starting material, it was converted to *tert*-butyl carbamate through reduction and Boc protection. A subsequent Heck reaction with methyl acrylate was followed by removal of the Boc protecting group. The isoxazole fragment was then introduced through a nucleophilic substitution reaction. Finally, compound **5** was obtained by treating the methyl esters with hydroxylamine in the presence of sodium methoxide.

Sunduru *et al.* (Sunduru et al., 2015) designed and synthesized a series of salicylhydrazide sulfonamides and investigated the *in vitro* replication activity of these compounds against *Chlamydia trachomatis* (*C. trachomatis*) and *Chlamydia pneumoniae* (*C. pneumoniae*) in HeLa cells. Compound **6** showed an inhibitory effect on *C. trachomatis* at a concentration of 50 μM with an inhibitory rate of 33.4 %. Compound **7** showed inhibitory effects on *C. trachomatis* and *C. pneumoniae* at a

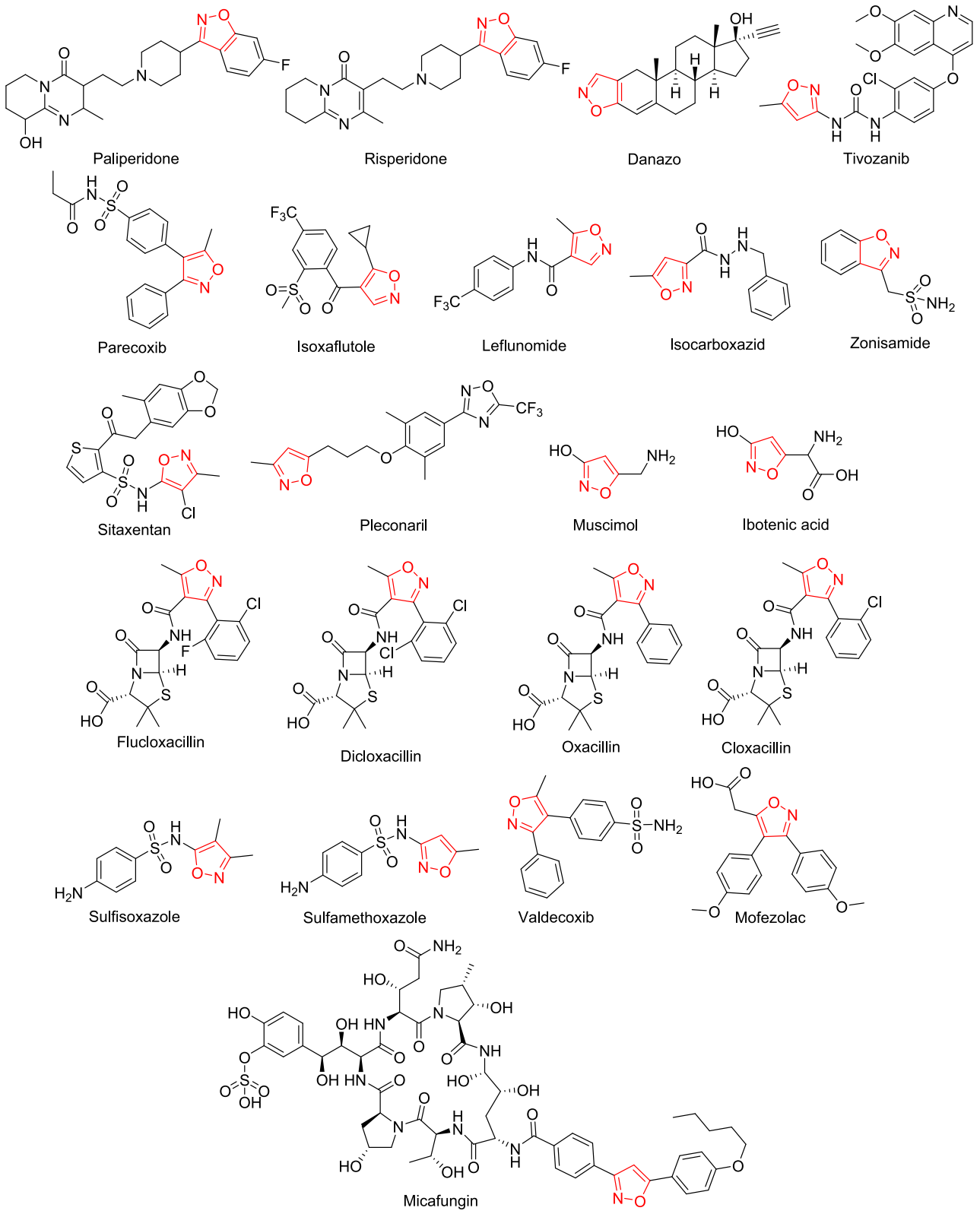

Fig. 2. Isoxazole-based commercially available drugs.

concentration of 50 μM, and inhibitory rates were 28.0 % and 22.4 %. Furthermore, compound **7** inhibits T3S in *Yersinia pseudotuberculosis* (*Y. pseudotuberculosis*) in a dose-dependent manner.

Marwaha *et al.* (Marwaha et al., 2014) found that acylated sulfonamides are novel growth inhibitors of the sexually transmitted pathogen *C. trachomatis*. Compounds **8**–**12** showed significant inhibitory effects on *C. trachomatis* with MIC values of 12 μM. These compounds showed strong inhibitory effects on *C. trachomatis* and *C. pneumoniae* with an IC_{50} ranging from 4.2 to 7.7 μM. There was no significant toxicity to host cells (HeLa: $IC_{50} > 50$ μM).

Caffeic acid sulfonamide derivatives were synthesized by coupling sulfonamide compounds to the caffeic acid main chain. Free radical

Table 1
Isoxazole-based commercially available drugs.

Drug	Pharmacological mechanism	Treatment/ Purpose	Ref.
Paliperidone	Dopamine type 2 receptor blockade	Schizophrenia	(Dolder et al., 2008)
Risperidone	Serotonin 5-HT2 receptor blockade	Schizophrenia	(Megens et al., 1994)
Danazol	Gonadotropin inhibitor	Endometriosis	(Andrews and Wentz, 1975)
Tivozanib	VEGF-TKI with high selectivity for VEGF receptors 1–3	Renal cell carcinoma	(Salgia et al., 2020)
Parecoxib	COX-2 inhibitor	Anti-inflammatory	(Urdaneta et al., 2009)
Isoxaflutole	Hydroxyphenylpyruvate dioxygenase (HPPD) inhibitor	Herbicidal	(Pallett et al., 1997; Viviani et al., 1998)
Leflunomide	Interfere with the metabolism of pyrimidine nucleotides	Rheumatoid arthritis	(Greene et al., 1995)
Isocarboxazid	The monoamine oxidase inhibitor	Treatment-resistant depression	(Larsen et al., 2015)
Zonisamide	It is likely to involve blockade of both sodium and T-type calcium channels	Anti-epileptic	(Mimaki, 1998)
Sitaxentan	Highly selective endothelin (ET) A receptor antagonist	Pulmonary arterial hypertension	(Scott, 2007)
Pleconaril	Pleconaril integrates into the capsid of picornaviruses, including enteroviruses and rhinoviruses, preventing the virus from attaching to cellular receptors and uncoating to release RNA into the cell	Enterovirus infections	(Rotbart et al., 2001)
Muscimol	GABAA-agonist	Anticonvulsant	(Allen et al., 2008; Collins, 1980)
Ibotenic acid	Aspartic acid receptor agonists	Hallucinogens	(Stebelska, 2013; Krogsgaard-Larsen et al., 1980)
Flucloxacillin	β-lactamase inhibitor	Anti-bacterial	(Lima et al., 2020)
Dicloxacillin	β-lactamase inhibitor	Anti-bacterial	(Lima et al., 2020)
Oxacillin	β-lactamase inhibitor	Anti-bacterial	(Lima et al., 2020)
Cloxacillin	β-lactamase inhibitor	Anti-bacterial	(Lima et al., 2020)
Sulfisoxazole	Endothelin receptor antagonist	Anti-bacterial	(Syed et al., 2006; Uchino et al., 2008)
Sulfamethoxazole	Competitive antagonists of *para*-aminobenzoic acid (PABA)	Anti-bacterial	(Yang et al., 2017; Brain et al., 2008)
Valdecoxib	COX-2 inhibitor	Anti-inflammatory	(Talley et al., 2000; Nussmeier et al., 2005)
Mofezolac	COX-1 inhibitor	Anti-inflammatory	(Pati et al., 2019; Cingolani et al., 2017)
Micafungin	Inhibiting the production of 1,3-β-*D*-glucan	Anti-fungal	(Wasmann et al., 2018)

scavenging ability was determined by the DPPH method. CASMZ (**13**) has a certain ability to clear DPPH, and the IC_{50} value is 42.2 μM, close to the activity of caffeic acid (IC_{50} value 40.9 μM). The pretreatment of cells with CASMZ (**13**) inhibited the viability of H_2O_2-induced cells, decreased ROS and MDA production, increased antioxidant enzyme activity, and further up-regulated the expression of Nrf2 and its target genes (Peng et al., 2020) (Fig. 5).

Darwish *et al.* (Darwish et al., 2014) synthesized a variety of heterocyclic compounds containing sulfonamides and evaluated the antibacterial and anti-fungal activities of the compounds newly synthesized *in vitro*. Compounds **14** and **15** containing cinnamic acid showed significant inhibitory activity against a variety of bacteria and fungi. The diameters of the inhibited region of **14** and **15** on *Bacillus subtilis* (RCMB-010067) are 18.20 cm and 18.30 cm. The diameters of the inhibition zone of *Geotricum candidum* (RCMB-05097) are 18.30 and 19.00 cm.

Mohamed *et al.* (Mohamed et al., 2021) designed and synthesized a series of heterocyclic cyanoacrylamide and tested the anti-tumor activity of these compounds against four cell lines (A549, MCF-7, HepG-2, and Wi38). Compounds **16** and **17** containing isoxazole exhibited varying degrees of inhibitory activity against A549, MCF-7, HepG-2, and WI38 cell lines with an IC_{50} ranging from 187.1 to 1057 μg/mL. Compound **16** had the most obvious inhibitory effect on A549 cells with an IC_{50} value of 187.1 μg/mL. Compounds **16** and **17** increased the expression of apoptotic genes (BAX and P53) and decreased the expression of anti-apoptotic genes (Bcl2 and CDK4). Compounds **16** and **17** also increased caspase-3, -8, and -9 activity. Flow cytometry showed that compound 6 induced cell cycle arrest in the S phase and compound **17** induced cell cycle arrest in the G2/M phase. Compounds **16** and **17** caused significant DNA breaks in HepG-2 cells compared to control cells. Therefore, compounds **16** and **17** inhibit liver cancer growth by inducing endogenous and exogenous pathways of the apoptosis process (Fig. 6).

Kamal *et al.* (Kamal et al., 2015) synthesized isoxazole-linked aryl cinnamic acid conjugates. Inhibition of these compounds on the growth of multiple human cancer cell lines (HeLa, DU-145, A549, and MDA-MB231) was evaluated. Among them, **18**–**20** showed good cytotoxicity in HeLa and MD-MB231 cells, with IC_{50} values between 2.3 and 3.3 μM. The preliminary structure–activity relationship indicated that the activity could be enhanced by introducing electron-donating groups at both the meta and *para*-positions of the phenyl group.

Kumar *et al.* (Kumar et al., 2017) synthesized a series of arylisoxazole-oxyindole derivatives and evaluated the anti-proliferative activity of these compounds against A549, HeLa, MCF-7, and DU-145 cell lines. Ethyl 2,4-dioxo-4-(substituted phenyl)butanoates were obtained by reacting 1-(3,4,5-trimethoxyphenyl)ethan-1-one with diethyl oxalate in the presence of sodium ethanolate in ethanol. Further cyclization was achieved by $NH_2OH{\bullet}HCl$ in ethanol to produce ethyl 3-substituted phenylisoxazole-5-carboxylate. The carboxylates were then reduced to (3-substituted phenylisoxazol-5-yl)methanol using $LiAlH_4$. The resulting compounds were selectively oxidized to 3-arylisoxazole-5-carbaldehyde by IBX in DMSO. Finally, the target compounds were synthesized through the Knoevenagel reaction between equimolar mixtures of 3-arylisoxazole-5-carbaldehyde and oxindoles (Fig. 7). Compounds **21**–**23** have excellent to moderate cytotoxicity, with IC_{50} values ranging from 0.82 to 2.59 μM. Compounds **22** and **23** showed the strongest inhibitory effects on A549 cells, with IC_{50} values of 0.91 and 0.82 μM, respectively.

Cheng *et al.* (Cheng et al., 2006) reported the design and synthesis of a series of Malonyl-Coa decarboxylase (MCD) inhibitors. Compound **24** contains a C_3-conjugated ethyl acrylate isoxazole fragment, showing strong inhibitory activity against MCD with an IC_{50} value of 3.16 μM.

To obtain new PDHK inhibitors, Meng *et al.* (Meng et al., 2014) designed and synthesized a series of diarylisoxazole HSP90 inhibitors using the homology of the ATP binding bag between HSP90 and PDHK. The starting material was reduced using $LiAlH_4$ conditions to obtain the corresponding alcohol, which was subsequently oxidized with activated

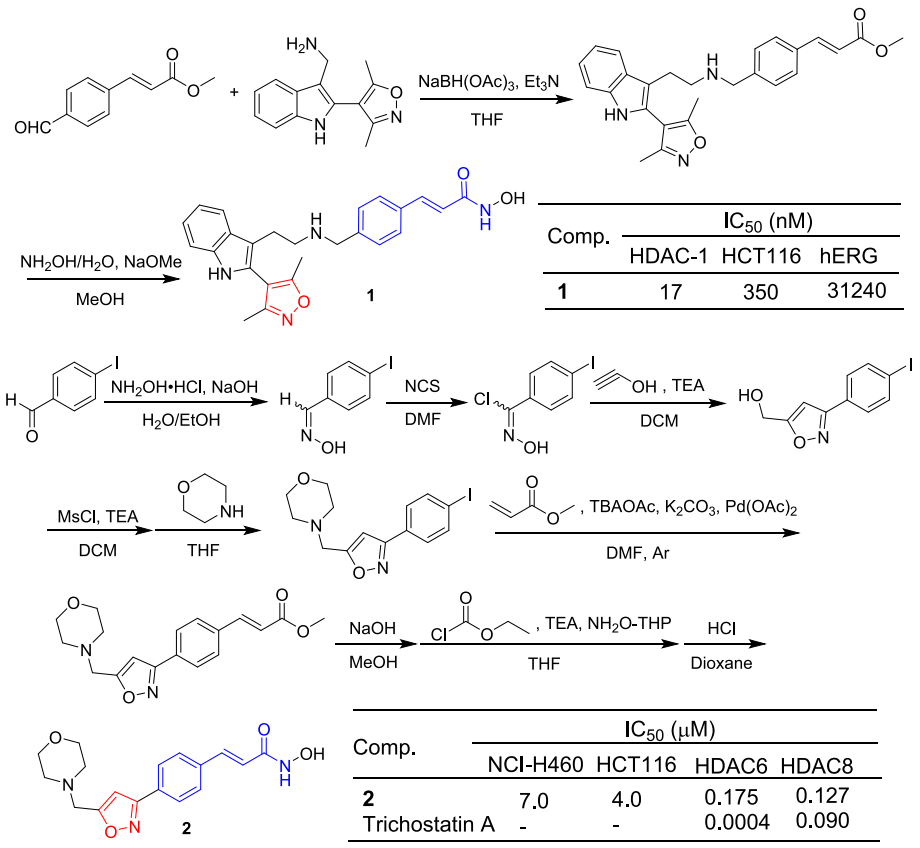

Comp.	IC50 (nM)		
	HDAC-1	HCT116	hERG
1	17	350	31240

Comp.	IC50 (μM)			
	NCI-H460	HCT116	HDAC6	HDAC8
2	7.0	4.0	0.175	0.127
Trichostatin A	-	-	0.0004	0.090

Fig. 3. Cinnamamide-isoxazole derivatives **1**–**2**.

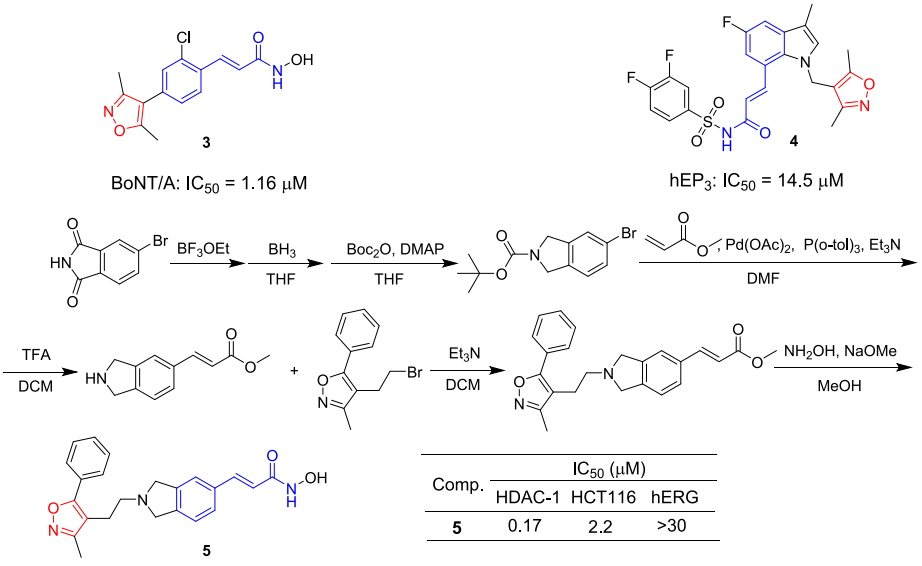

Comp.	IC50 (μM)		
	HDAC-1	HCT116	hERG
5	0.17	2.2	>30

Fig. 4. Cinnamamide-isoxazole derivatives **3**–**5**.

MnO_2 to yield the aldehyde. Following this, the Horner-Wadsworth-Emmons reaction was employed to generate an α,β-unsaturated ester. Hydrolysis of this ester with aqueous sodium hydroxide resulted in the formation of an acid. Subsequent amidation with various substituted piperazines and debenzylation using boron trichloride provided compounds **25**–**28**. These compounds were further demethylated utilizing boron tribromide to produce phenolic compounds **29**–**31** (Fig. 8). The 3-linked acrylamide compounds **25**, **26**, and **29** of isoxazole showed significant inhibitory activity against PDHK1, with IC_{50} values ranging from 0.491 to 0.604 μM. Compounds **27**, **28**, **30**, and **31** showed significant inhibitory activity against HSP90 with IC_{50} values ranging from 0.491 to 0.604 μM. Furthermore, compound **29** has greater cellular activity and can effectively regulate the metabolic profile of cancer cells and inhibit cancer cell proliferation, which can be demonstrated by increasing oxidative phosphorylation, reducing glycolysis, and related oxidative stress. The preliminary structure–activity relationship suggests that, for PDHK1, the introduction of substituting phenyl groups on piperazine demonstrates superior inhibitory activity compared to

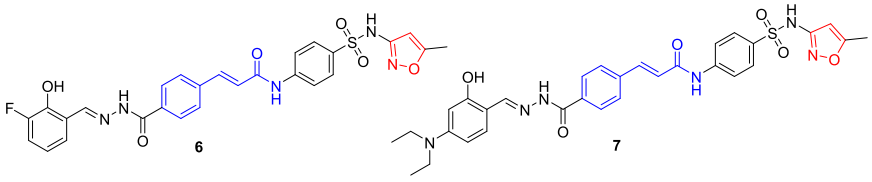

Comp.	50 μM, Inhibition (%)	
	C. trachomatis	*C. pneumoniae*
6	33.4	-
7	28.0	22.4

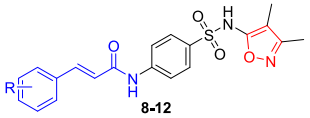

Comp.	*C. trachomatis*		*C. pneumoniae*	
	IC_{50} (μM)	MIC (μM)	IC_{50} (μM)	MIC (μM)
8	4.9	12	3.2	50
9	6.0	12	7.8	50
10	5.5	12	4.7	>50
11	4.2	12	4.7	25
12	6.5	12	7.7	>50

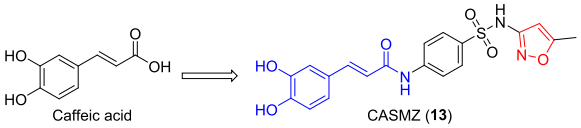

Comp.	IC_{50} (μM)
CASMZ (**13**)	42.2
Caffeic acid	40.9

Fig. 5. Cinnamamide-isoxazole derivatives **6**–**13**.

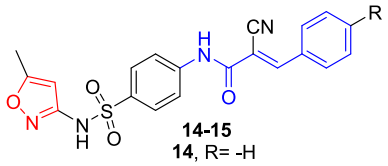

Comp.	Inhibition Zone Diameter (mm)			
	Streptococcus pneumoniae (RCMB-010010)	*Bacillis subtilis* (RCMB-010067)	*Pseudomonas aeruginosa* (RCMB-010043)	*Escherichia coli* (RCMB-010052)
14	16.90	18.20	10.70	11.90
15	16.30	18.30	11.60	15.40
Amphotericin B	22.6	18.2	13.8	15.3
	Aspergillus fumigatus (RCMB-02568)	*Syncephalastrum racemosum* (RCMB-05922)	*Geotricum candidum* (RCMB-05097)	*Candida albicans* (RCMB-05036)
14	15.70	13.80	18.30	15.20
15	17.30	12.60	19.00	16.90
Sulfamethoxazole	23.7	19.7	28.7	25.4

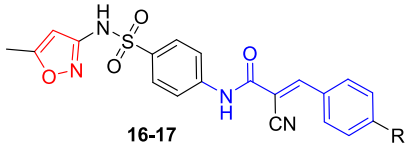

Comp.	IC_{50} (μg/mL)			
	A549	MCF-7	HepG-2	WI38
16	287.5	187.1	325.7	1057
17	412.8	229.8	207.1	799.6
5-Fluorouracil	205.4	178	237	-

Fig. 6. Cinnamamide-isoxazole derivatives **14**–**17**.

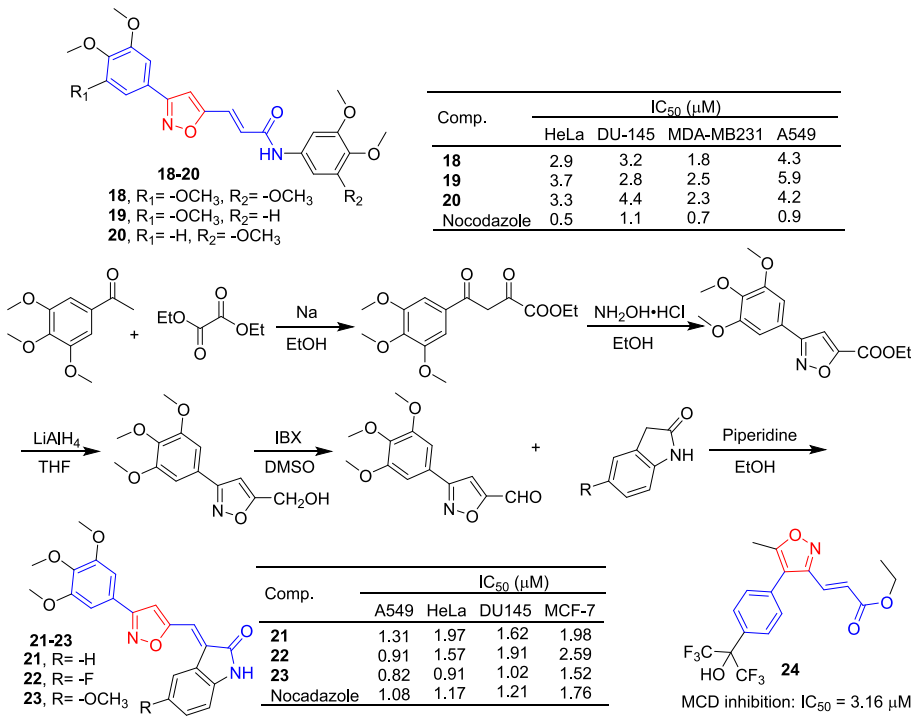

Comp.	IC50 (μM)			
	HeLa	DU-145	MDA-MB231	A549
18	2.9	3.2	1.8	4.3
19	3.7	2.8	2.5	5.9
20	3.3	4.4	2.3	4.2
Nocodazole	0.5	1.1	0.7	0.9

Comp.	IC50 (μM)			
	A549	HeLa	DU145	MCF-7
21	1.31	1.97	1.62	1.98
22	0.91	1.57	1.91	2.59
23	0.82	0.91	1.02	1.52
Nocadazole	1.08	1.17	1.21	1.76

Fig. 7. Cinnamamide and cinnamic acid-isoxazole derivatives **18**–**24**.

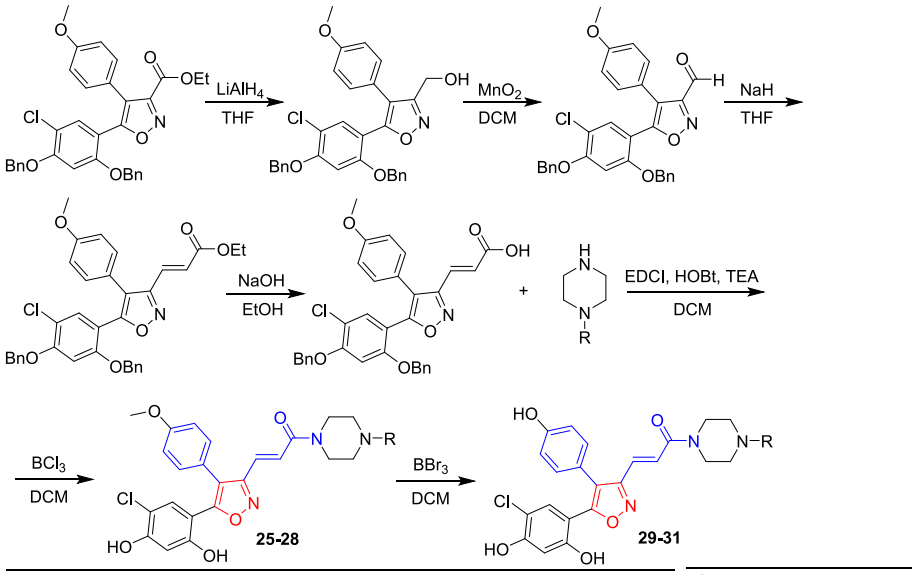

Comp.	R	Comp.	R	Comp.	R	Comp.	R
25		**26**		**27**		**28**	
29		**30**		**31**			

Comp.	IC50 (μM)	
	PDHK1	HSP90
25	0.557	0.700
26	0.491	0.718
27	1.050	0.215
28	1.070	0.208
29	0.604	0.512
30	0.878	0.357
31	0.521	0.338

Fig. 8. Cinnamamide-isoxazole derivatives **25**–**31**.

heterocyclic groups. Conversely, for HSP90, the introduction of heterocyclic groups on piperazine exhibits enhanced inhibitory activity relative to substituting phenyl groups.

Pfizer (formerly Agouron) has developed AG-7088, a peptide-aldehyde that targets the 3C protease of human rhinovirus (HRV) with the potential to treat the common cold (Witherell, 2000; McKinlay, 2001). Studies have shown that AG7088 is effective against EV6 and EV9, with EC_{50} of 43 nM and 15 nM, respectively (Binford et al., 2005). Based on the crystal structure of the RV 3C protease complex with AG7088, Kuo *et al.* (Kuo et al., 2008) designed and synthesized a series of AG7088 analogs and further tested their antiviral activity. The starting material was condensed with benzyloxycarbonyl (Cbz)-

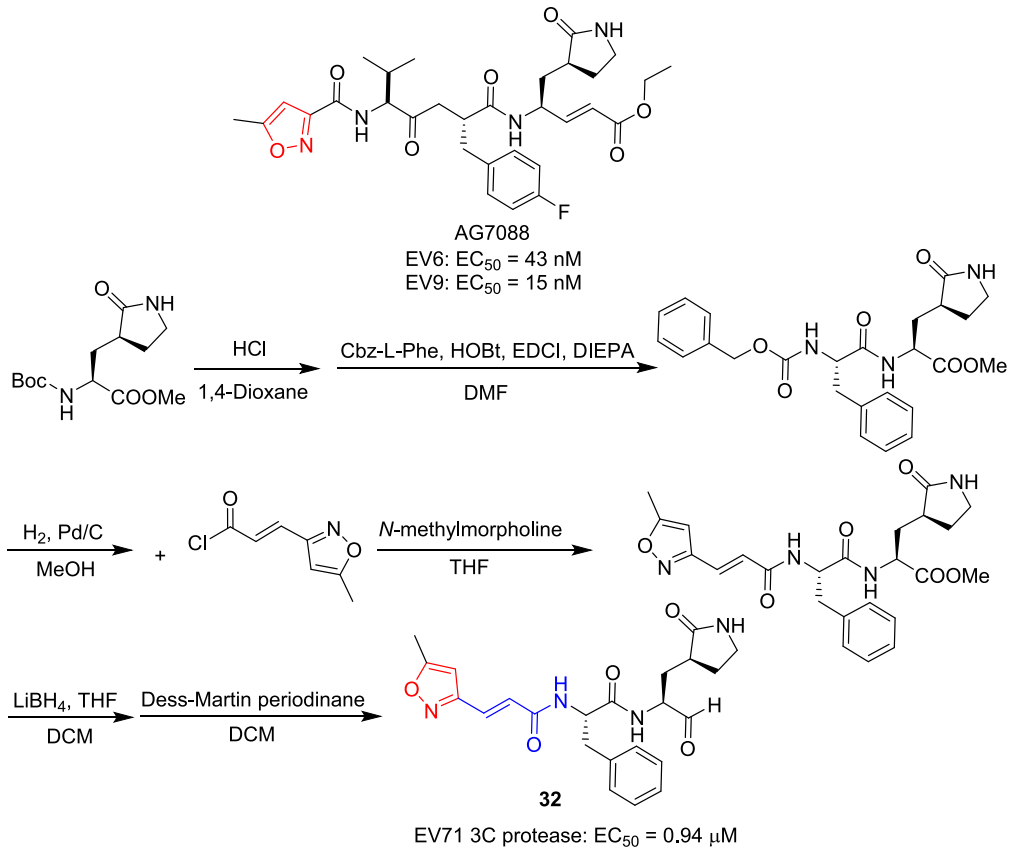

Fig. 9. Cinnamamide-isoxazole derivative **32**.

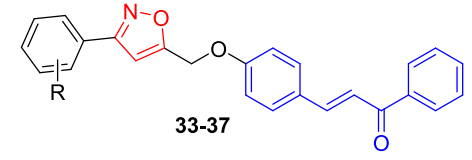

33, R= 4-F
34, R= 3,4-F
35, R= 3,4-Cl
36, R= 4-Cl
37, R= 4-Cl-3-F

Comp.	Tyrosinase activity EC_{50} (μM)
33	6.4
34	2.5
35	3.0
36	1.3
37	8.1
8-methoxypsoralen	14.8

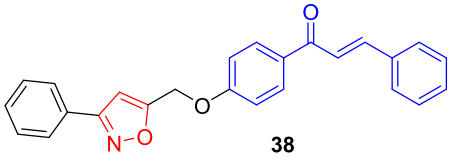

Comp.	50 μM	
	Tyrosinase activity	Melanin content
38	135.7%	199.8%
8-methoxypsoralen	120.1%	127.9%

Fig. 10. Chalcone-isoxazole derivatives **33**–**38**.

protected Phe to form the corresponding amide intermediate. Subsequently, derivative **32** was synthesized through the addition of 3-(5-methylisoxazol-3-yl)acryloyl chloride, followed by reduction and oxidation. The derivative **32** containing isoxazole showed a certain inhibitory effect on EV71 3C protease, with EC_{50} of 0.98 μM and no obvious toxicity (CC_{50} > 25 μM) (Fig. 9).

Summary: Cinnamamide and cinnamic acid-isoxazole hybridization natural products mainly have anti-tumor, anti-pathogen, and antioxidant activities. Among the anti-tumor activities, compound **1** showed the strongest inhibitory effect on the HCT116 cell line with an IC_{50} value of 0.35 μM, and compound **23** showed the strongest inhibitory effects on A549 and HeLa cells, with IC_{50} values of 0.82 and 0.91 μM, respectively. Therefore, the cinnamamide-linked isoxazole derivatives have the value of further research in the field of anti-tumor. Cinnamamide-isoxazole hybrid sulfonamide structure (compounds **8**–**12**) has the best anti-chlamydia activity, and preliminary structure–activity relationship showed that introducing the electron-donating group was superior to the electron-withdrawing group in the *para*-position of the phenyl group of cinnamamide.

2.2. *Chalcone-isoxazole hybridization*

Niu *et al.* (Niu et al., 2016) designed and synthesized a series of chalcone derivatives containing isoxazole groups and evaluated their activity on melanin synthesis in mushroom tyrosinase and mouse B16 cells. **33**–**37** activity was stronger and EC_{50} was between 1.3–8.1 μM, which was significantly better than 8-methoxypsoralan (EC_{50} = 14.8 μM). The activity of these compounds with different substitutions on the benzene ring was found to be in the following order: 4-Cl > 3,4-F > 3,4-Cl > 4-F > 4-Cl, 3-F. In B16 cells, all compounds exhibited higher

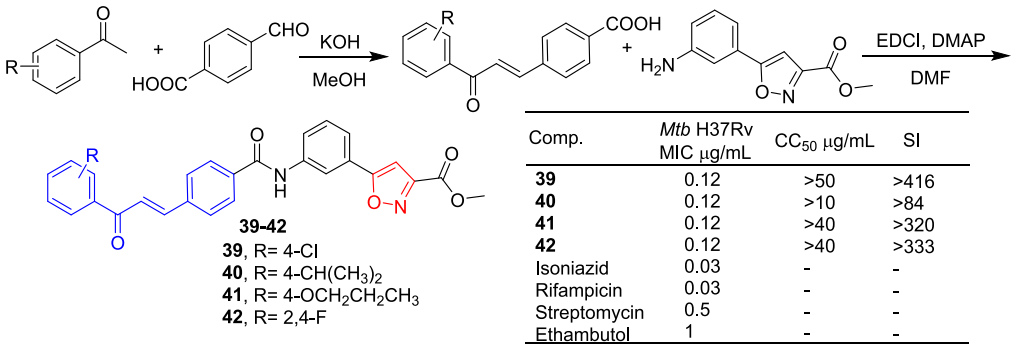

Comp.	*Mtb* H37Rv MIC μg/mL	CC_{50} μg/mL	SI
39	0.12	>50	>416
40	0.12	>10	>84
41	0.12	>40	>320
42	0.12	>40	>333
Isoniazid	0.03	-	-
Rifampicin	0.03	-	-
Streptomycin	0.5	-	-
Ethambutol	1	-	-

Fig. 11. Chalcone-isoxazole derivatives **39**–**42**.

melanin-producing activity compared to 8-methoxypsoralan, with compound **34** (463 %) being three times more potent than the control 8-methoxypsoralan (115 %) (Fig. 10).

Li *et al.* (Yin et al., 2017) reported a new isoxazole chalcone derivative **38**. Pharmacological experiments showed that compound **38** (50 μM, 135.7 %) had a stronger inhibitory effect on tyrosinase in mouse B16 melanoma cells than 8-methoxy psoralen (50 μM, 120.1 %). Compound **38** can promote melanin synthesis in B16 cells and its activity (50 μM, 199.8 %) is better than that of 8-methoxypsoralen (50 μM, 127.9 %). Western blot experiments have shown that compound **38** promotes melanin production through Akt and GSK3β signaling pathways and has the potential to be developed as a drug for the treatment of vitiligo.

Sahoo *et al.* (Sahoo et al., 2021) designed and synthesized a series of 5-phenyl-3-isoxazolecarboxylic acid methyl ester-chalcone hybrids and evaluated their antimicrobial activity. As shown in Fig. 11, a series of chalcone acids were synthesized through aldol condensation of 4-formyl benzoic acid and various substituted acetophenones in the presence of potassium hydroxide as a base in methanol. The synthesized chalcone acids were then reacted with methyl 5-(3-aminophenyl)isoxazole-3-carboxylate using DMAP as a base and EDCI to form the target hybrid products, which are isoxazole methyl ester-chalcone derivatives. Compounds **39**–**42** showed strong *in vitro* activity against *Mycobacterium tuberculosis* H37Rv (*Mtb* H37Rv) with a MIC of 0.12 μg/mL. Cell viability tests in Vero cells did not show cytotoxicity of these compounds (CC_{50} > 10 μg/mL, SI > 320). Compound **41** has the strongest anti-drug activity against drug-resistant *Mtb* H37Rv with a MIC of 0.03–0.5 μg/mL.

Sunitha *et al.* (Sunitha et al., 2018) synthesized a series of diisooxazol-like chalcones and tested their anti-bacterial and anti-fungal activities. Compounds **43**–**46** were highly active at concentrations of 75 and 100 μg/mL against eight bacteria [*Micrococcus luteus* (*M. luteus*), *Methicillin-resistant Staphylococcus aureus* (*S. aureus*), *Bacillus subtilis* (*B. subtilis*), *Bacillus cereus* (*B. cereus*), *Pseudomonas aeruginosa* (*P. aeruginosa*), *Klebsiella pneumoniae* (*K. pneumoniae*), *Escherichia coli* (*E. coli*), *Proteus vulgaris* (*P. vulgaris*], three fungi (*Microsporum canis*, *Microsporum gypseum*, *Epidermophyton floccosum*) (Fig. 12). The structure–activity relationship demonstrates that R_1 is the electron-withdrawing group, while R_2 is the electron-donating group, which is beneficial to the activity..

Sunitha *et al.* (Sunitha et al., 2018) synthesized a series of monoisooxazol-like chalcones and tested their antibacterial activities. Compounds **47**–**50** were highly active at concentrations of 75 and 100 μg/mL against *M.s luteus*; *S. aureus*, *B. subtilis*, *B. cereus*, *P. aeruginosa*, *K. pneumoniae*, *E. coli*, and *P. vulgaris* (Fig. 13). The structure–activity relationship demonstrates that compounds with strong electron-withdrawing substituents on the phenyl ring attached to isoxazole enhance the antibacterial activity of the compounds.

Wan *et al.* (Wan et al., 2014) synthesized a series of isoxazoly-chalcone and evaluated the anti-tumor activity of H1792, H157, A549, and Calu-1 cancer cells *in vitro*. The IC_{50} values of compounds **51** and **52** against H1792, H157, A549, and Calu-1 cells were 1.35–19.63 μM. Among them, compounds **51** and **52** induce apoptosis of A549 cells through an exogenous pathway mediated by the death receptor 5 (DR5).

Shaik *et al.* (Shaik et al., 2020) designed and synthesized chalcone containing an isoxazole ring and determined its anti-bacterial, anti-oxidant, and anti-cancer activities. Compounds **53**–**55** exhibited potent antibacterial activity with MIC values ranging from 1 to 16 μg/mL, and the introduction of more electron-donating groups onto the phenyl moiety was found to enhance their activity. The compounds **56**–**58** and **54** exhibited potent antioxidant activity, with IC_{50} values ranging from 5 to 8 μg/mL. Compounds **55** and **59**–**60** demonstrated potent anti-tumor activity against DU-145 cells, with an IC_{50} range of 5–8 μg/mL (Fig. 14).

Summary: Chalcone-isoxazole hybridization natural products mainly have anti-pathogen and anti-tumor activities. Compounds **39**–**42** have strong anti-tuberculosis activity and low toxicity *in vitro*. The structure–activity relationship demonstrates that nonpolar groups, such as halogens and alkyls, exhibit potent inhibitory capacity. Among them, compound **41** is valuable for further research in the development of anti-tuberculosis drugs. In terms of anti-tumor activity, these compounds did not reach the nanomolar level of IC_{50} values for cancer cells.

2.3. Styrene and polyphenols-isoxazole hybridization

Rodrigues *et al.* (Rodrigues et al., 2021) synthesized a derivative **61** containing isoxazole using curcumin as the skeleton (Fig. 15). Compound **61** showed strong inhibitory activity against the MCF-7 cell line, with IC_{50} = 3.97 μM, exceeding that of curcumin (IC_{50} = 21.89 μM). Compound **61** also showed significant inhibitory activity against the SKBR3 cell line with an IC_{50} value of 4.00 μM. However, it did not exceed curcumin (IC_{50} = 2.11 μM) (Amolins et al., 2009).

According to another study, compound **61** showed strong inhibitory effects on HA22T/VGH, MCF-7, and MCF-7R cell lines with IC_{50} values of 12.8, 13.1, and 12.0 μM, respectively, surpassing the activity of curcumin (HA22T/VGH: IC_{50} = 17.4 μM; MCF-7: IC_{50} = 29.3 μM; MCF-7R: IC_{50} = 26.2 μM) (Simoni et al., 2008).

Actin and tubulin are contractile proteins and established targets for the development of anticancer drugs. Replacing the diketone portion of curcumin with isoxazole increased the stability of curcumin. Compound **61** retained actin polymerization inhibitory activity similar to that of curcumin. Additionally, compound **61** exhibited significant antioxidant activity, demonstrating a notable inhibition rate on DPPH with an EC_{50} value of 8 μM, which was higher than that of curcumin (EC_{50} = 40 μM) (Dhar et al., 2015; Chakraborti et al., 2013; Sherin and Rajasekharan, 2015). Kumboonma *et al.* (Kumboonma et al., 2019) found that compound **61** showed some inhibition activity of HDAC, with an inhibition rate of 54 % at 100 μM, which was lower than curcumin (62 %).

Curcumin binds to amyloid β peptide (Aβ) and inhibits or regulates the metabolism of amyloid precursor protein (APP). Compound **61** showed inhibitory activity on Aβ secretion, reducing the cleavage of Aβ38, Aβ40 and Aβ42 sites to varying degrees, with IC_{50} values of 6.1, 7.4 and 6.8 μM, respectively. It is a potent gamma-secretase inhibitor

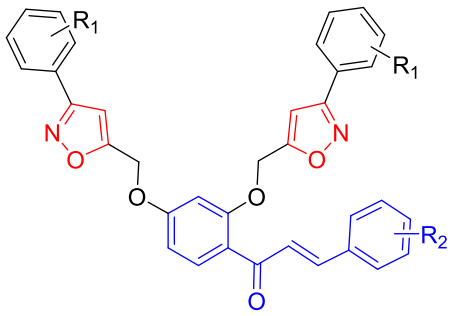

43-46

43, R_1= 4-Cl, R_2= 4-OCH_3
44, R_1= 4-Br, R_2= 4-OCH_3
45, R_1= 4-NO_2, R_2= 4-H
46, R_1= 4-NO_2, R_2= 4-OCH_3

Comp.	Concentration (μg/mL)	Zone of inhibition, mm			
		Gram positive bacteria			
		Micrococcus luteus	*Methicillin-resistant Staphylococcus aureus*	*Bacillus subtilis*	*Bacillus cereus*
43	75	36	35	36	31
	100	40	49	49	34
44	75	33	30	28	29
	100	36	33	31	32
45	75	25	27	27	28
	100	28	31	30	31
46	75	32	28	26	27
	100	35	32	28	30
Nystatin	75	27	31	30	31
	100	30	33	33	34

		Gram negative bacteria			
		Pseudomonas aeruginosa	*Klebsiella pneumoniae*	*Escherichia coll*	*Proteus vulgaris*
43	75	31	33	30	28
	100	33	36	33	31
44	75	29	30	31	30
	100	31	33	34	33
45	75	26	24	26	25
	100	29	26	30	28
46	75	26	26	28	27
	100	29	29	31	30
Nystatin	75	28	27	31	29
	100	31	30	33	31

		Fungus		
		Microsporum canis	*Microsporum gypseum*	*Epidermophytnn floccosum*
43	75	25	22	22
	100	28	26	24
44	75	24	19	18
	100	27	22	21
45	75	19	17	16
	100	22	20	19
46	75	21	17	16
	100	24	20	18
Nystatin	75	25	20	10
	100	28	24	23

Fig. 12. Chalcone-isoxazole derivatives **43**–**46**.

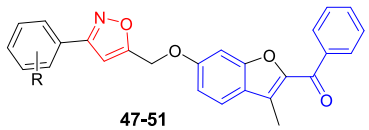

47-51
47, R= 3-NO_2
48, R= 4-NO_2
49, R= 4-OCH_3
50, R= 3,4-OCH_3
51, R= 3-OCH_3

Comp.	Concentration (μg/mL)	Zone of inhibition, mm			
		Gram positive bacteria			
		Micrococcus luteus	*Staphylococcus aureus*	*Bacillus subtilis*	*Bacillus cereus*
47	75	31	28	26	27
	100	33	31	29	30
48	75	32	28	26	27
	100	35	32	28	30
48	75	26	28	27	28
	100	29	31	30	31
49	75	28	29	26	28
	100	31	32	29	31
50	75	22	26	24	27
	100	25	29	27	30
Nystatin	75	27	31	30	31
	100	30	33	33	34

		Gram negative bacteria			
		Pseudomonas aeruginosa	*Klebsiella pneumoniae*	*Escherichia coll*	*Proteus vulgaris*
47	75	26	27	29	28
	100	29	31	33	31
48	75	26	26	28	27
	100	29	29	31	30
48	75	26	24	24	26
	100	29	28	27	29
49	75	27	28	30	29
	100	30	31	33	32
50	75	23	20	26	23
	100	26	23	29	26
Nystatin	75	28	27	31	29
	100	31	30	33	31

Fig. 13. Chalcone-isoxazole derivatives **47**–**50**.

with an affinity for Aβ42 aggregates (IC_{50} = 138 nM), but with no significant activity against tau aggregates (Narlawar et al., 2008).

The curcumin IC_{50} on chloroquine-sensitive (CQ-S) and chloroquine-resistant (CQ-R) *Plasmodium falciparum* (*P. falciparum*) growth was 3.25 μM (MIC = 13.2 μM) and 4.21 μM (MIC = 14.4 μM). Mishra *et al.* (Mishra et al., 2008) synthesized a series of curcumin derivatives and evaluated their ability to inhibit the growth of *P. falciparum*. The IC_{50} of CQ-S *P. falciparum* and CQ-R *P. falciparum* were 8.44 and 7.92 μM, respectively, and the activity of derivative **61** was weaker than that of curcumin.

Mechanisms by which calcium/calmodulin-dependent protein kinase II (CaMKII) is involved in higher-order brain functions, such as learning and memory. Mayadevi *et al.* (Mayadevi et al., 2012) found that curcumin and its analogues inhibit Ca^{2+}-dependent and independent kinase activity of CaMKII. The Ca^{2+}-dependent activity of CaMKII was inhibited by compound **61** with an IC_{50} value of 11.37 μM. In autophosphorylation, CaMKII autophosphorylation, Ca^{2+} dependent, and Ca^{2+} independent activities were inhibited by compound **61** with IC_{50} values of 24.44 and 0.68 μM, respectively. Compound **61** inhibited the autophosphorylation of CaMKII in PSD and cytoplasm (IC_{50} = 22.79 μM), as well as Ca^{2+} dependent (IC_{50} = 22.87 μM) and Ca2 + independent activity (IC_{50} = 18.88 μM). Therefore, compound **61** is a potent CaMKII inhibitor.

Ahmed *et al.* (Ahmed et al., 2018) synthesized curcumin derivatives

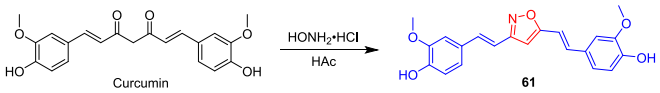

Cytotoxicity

Comp.	IC_{50} (μM) MCF-7	Ref.
Curcumin	21.89	[67]
61	3.97	
Doxorubicin	0.0652	

Cytotoxicity

Comp.	IC_{50} (μM) MCF-7	IC_{50} (μM) SKBR3	Ref.
Curcumin	5.58	2.11	[68]
61	1.76	4.00	

Cytotoxicity

Comp.	HA22T/VGH IC_{50} (μM)	HA22T/VGH IC_{70} (μM)	MCF-7 IC_{50} (μM)	MCF-7 IC_{70} (μM)	MCF-7R IC_{50} (μM)	MCF-7R IC_{70} (μM)	Ref.
Curcumin	17.4	24.6	29.3	51.7	26.2	46.2	[69]
61	12.8	18.3	13.1	23.2	12.0	24.7	

Fig. 15. Styrene and polyphenol-isoxazole derivative **61**.

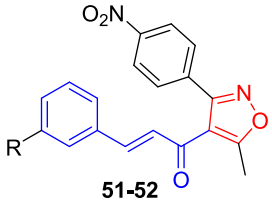

51-52

51, R= -Cl
52, R= -Br

Comp.	IC_{50} (μM) H1792	H157	A549	Calu-1
51	19.30	1.35	1.48	2.07
52	19.63	7.27	11.07	8.98

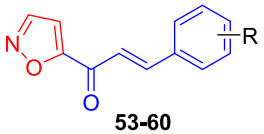

53-60

53, R= 2,4-OCH_3
54, R= 2,4,6-OCH_3
55, R= 2-Cl, 4,6-OCH_3
56, R= 2,3,4-OCH_3
57, R= 2,4,5-OCH_3
58, R= 3,4,5-OCH_3
59, R= 3,4-OCH_3
60, R= 2-F, 3,4-OCH_3

Antibacterial and antifungal activities

Comp.	MIC (μg/mL) *S. aureus*	*P. aeruginosa*	*A. niger*	*C. tropicalis*
53	2	4	8	16
54	1	1	2	2
55	2	2	4	4
Ciprofloxacin	2	2	-	-
Fluconazole	-	-	1	1

DPPH assay

Comp.	IC_{50} (μg/mL)
56	6
57	7
54	5
55	8
Gallic acid	5

Cytotoxicity

Comp.	IC_{50} (μg/mL) DU-145	L02
59	6	>40
55	8	>40
60	5	>40
Docetaxel	5	-

Fig. 14. Chalcone-isoxazole derivatives **51**–**60**.

HDAC inhibitory activity

Comp.	Inhibition of DPPH IC_{50} (μM)	Ref.
Curcumin	40	[72]
61	8	

HDAC inhibitory activity and *in vitro* antioxidant activities

Comp.	%HDAC inhibition (100 μM)	DPPH IC_{50} (μM)	RP EC_{50} (μM)	TA EC_{50} (μM)	Ref.
Curcumin	62	6	11	43	[73]
61	54	7	22	51	

Activity of curcumin and **61** on the secretion of $A\beta_{42}$ and $A\beta$

Comp.	$A\beta_{42}$ affinity assay IC_{50} (nM)	$A\beta$ secretion IC_{50} (μM) $A\beta_{38}$	$A\beta_{40}$	$A\beta_{42}$	Ref.
Curcumin	107	>20	>20	>20	[74]
61	138	6.1	7.4	6.8	

Plasmodium falciparum

Comp.	CQ-S IC_{50} (μM)	CQ-S MIC (μM)	CQ-R IC_{50} (μM)	CQ-R MIC (μM)	Ref.
Curcumin	3.25	13.2	4.21	14.4	[75]
61	8.44	27.3	7.92	25.3	

Inhibition of activity of CaMKII by **61**

Comp.	IC_{50} (μM)	Ref.
Ca^{2+}-dependent activity of CaMKII	11.37	[76]
Ca^{2+}-dependent activity of autophosphorylated CaMKII	24.44	
Ca^{2+}-independent activity of autophosphorylated CaMKII	0.68	
CaMKII autophosphorylation	18.01	
Cytosol CaMKII Ca^{2+}-dependent activity	28.9	
Cytosol CaMKII Ca^{2+}-independent activity	13.68	
Cytosol CaMKII autophosphorylation	17.10	
PSD CaMKII Ca^{2+}-dependent activity	22.87	
PSD CaMKII Ca^{2+}-independent activity	18.88	
PSD CaMKII autophosphorylation	22.79	

Anti-inflammatory activity and antinociceptive activity, COX-2 inhibitory

Comp.	Anti-inflammatory activity Paw edema in mm (% inhibition) 0 h	1 h	2 h	3 h	Antinociceptive activity Total writhing count (% inhibition)	Comp.	% inhibition of COX-2 at 10 μM	Ref.
61	1.93 (-)	2.89 (7.7)	2.83 (35.7)	2.80 (66.1)	22.4 (61.0)	**61**	49.3	[77]
Curcumin	1.99 (-)	2.80 (22.1)	2.75 (45.7)	2.72 (71.6)	24.1 (58.1)	Curcumin	19.1	
Indomethacin	1.94 (-)	2.85 (12.5)	2.63 (50.7)	2.34 (84.4)	-	Celecoxib	76.5	
Diclofenac sodium	-	-	-	-	18.9 (67.1)	Diclofenac sodium	-	
Control	1.95 (-)	2.99 (-)	3.35 (-)	4.52 (-)	-			

Anti-oxidant, COX-1, COX-2 inhibitory and anti-inflammatory activities

Comp.	Anti-oxidant activity IC_{50} (μM)	ARP (1/ED_{50})	% Inhibition (100 μM) COX-1	COX-2	Anti-inflammatory activity % Inhibition at 75 mg/kg	Ref.
Curcumin	11.06	5.4	80.5	35.0	61.4	[78]
61	10.71	5.6	80.8	58.1	60.3	
Trolox	13.1	4.5	-	-	-	
Celecoxib	-	-	77.6	2.05	71.9	
Ibuprofen	-	-	14.4	265.5	54.5	

Fig. 16. Multiple pharmacological activities of derivative **61**.

containing isoxazole and evaluated their anti-inflammatory and anti-nociceptive activities in experimental animal models. *In vivo* anti-inflammatory studies showed that the inhibition rate of compound **61** in induced edema was 66.1 %, which was lower than curcumin (71.6 % inhibition) and diclofenac sodium (84.4 % inhibition). Compound **61** has a relatively strong preventive effect on the onset of the torsional body, and its anti-nociceptive activity is 61 %. This was better than curcumin (58.1 % inhibition) but less than diclofenac sodium (67.1 % inhibition). The results of the *in vitro* COX-2 inhibition experiments showed that the inhibitory effect of compound **61** was stronger (49.3 % inhibition) than that of curcumin (19.1 % inhibition).

The ketoenol of curcumin is replaced by isoxazole to give compound **61**. Compound **61** showed a strong scavenging ability for DPPH free radicals with an IC_{50} value of 10.71 μM. The activity was slightly higher than that of curcumin (IC_{50} = 11.06 μM). The inhibitory activities of the compounds in COX-1 and COX-2 were tested at 100 μM, and the compounds **61** and curcumin were equivalent to the COX-1 enzyme (compound **61**: 80.8 %; curcumin: 80.5 %). The inhibitory activity of compound **61** on the COX-2 enzyme was significantly increased (compound **61**: 58.1 %; curcumin: 35.0 %) and the COX-2/COX-1 ratio (0.72) was significantly increased (Selvam et al., 2005) (Fig. 16).

The IC_{50} of derivative **62** against the MCF-7 and MCF-7R cell lines was 13.1 and 12.0 μM, respectively, surpassing the activity of curcumin (MCF-7: IC_{50} = 29.3 μM; MCF-7R: IC_{50} = 26.2 μM). The derivative **62** is similar to curcumin and is not cleared from cells by the P-gp protein (Poma et al., 2007).

Changtam *et al.* (Changtam et al., 2010) synthesized a series of curcumin derivatives and evaluated their activity against *Mtb* H37Rv. The synthesis method is similar to compound **61**, and among them, compound **64** exhibits the highest activity with an MIC of 0.09 μg/mL. It is 1131 times more active than curcumin and about 18 times more active than the standard drugs kanamycin and isoniazid, respectively. The compound **64** also has strong activity against multidrug-resistant (MDR) *M. tuberculosis* isolated from patients (MIC = 0.195–3.125 μg/mL). Compounds **63**, **65**, and **66** also exhibited significant inhibitory activity against *M. tuberculosis* H37Ra, with a MIC of 0.39, 0.78, and 0.39 μg/mL, respectively. Compounds **63**, **65**, and **66** also showed high activity against clinical isolates of MDR-TB with a MIC ranging from 0.39 to 12.5 μg/mL.

The protein kinase C (PKC) family of serine/threonine kinases is an attractive drug target because it is involved in the regulation of various cellular functions, including cell growth, differentiation, metabolism, and apoptosis. To develop curcumin derivatives as effective PKC modulators, Das *et al.* (Das et al., 2011) found that the EC_{50} of curcumin derivatives **61** and **67** for protein fluorescence quenching varied in the range of 3.16–25.23 μM. These derivatives bind to PKChC1B to a higher degree than PKCdC1B and PKCeC1B.

Taka *et al.* (Taka et al., 2014) reported that a series of curcumin derivatives improved telomerase activity *in vitro* TRAP assays. Compound **68** increased telomerase activity by about 3 times at 60 μM (Fig. 17).

Compound **69** showed the highest anti-fungal activity against

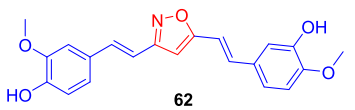

62

Comp.	Cytotoxicity IC$_{50}$ (μM) MCF-7	MCF-7R
Curcumin	29.3	26.2
62	13.1	12.0

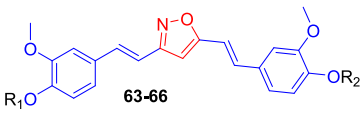

63-66

63, R_1= -$CH_2CH_2CH_2CH_2CH_3$, R_2= -H
64, R_1= -CH_3, R_2= -H
65, R_1= -H, R_2= -CH_3
66, R_1= -CH_3, R_2= -CH_3

Comp.	*M. tuberculosis* H37Ra strain MIC (μg/mL)
Curcumin	100
63	0.39
64	0.09
65	0.78
66	0.39

Code	Isolate resistant profile	MIC (μg/mL) **63**	**64**	**65**
H37Ra	Pan sensitive	0.39	0.09	0.78
M3	INH, RIF, SM	0.39	0.195	0.78
M4	INH, RIF, EMB, SM	1.56	1.56	6.25
M5	INH, RIF, SM	1.56	3.125	12.5
M6	INH, RIF	0.78	0.39	1.56
M8	INH, RIF, EMB, SM	3.125	3.125	12.5
M11	INH, RIF	3.125	3.125	12.5
M16	INH, RIF, EMB	1.25	1.56	12.5
M21	INH, RIF, EMB, SM	3.125	3.125	12.5
M22	INH, RIF	0.78	0.39	1.56
M27	INH, RIF	0.39	0.195	0.78
M46	INH, RIF, EMB, SM, OFX, CIP	1.56	1.56	6.25
M48	INH, RIF, EMB, SM, OFX, CIP	3.125	1.56	12.5
M53	INH, RIF, EMB, SM, OFX, CIP	3.125	3.125	12.5

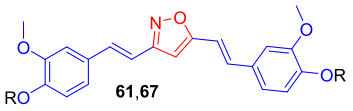

61,**67**

61, R= -H
67, R= -$CH_2CH_2CH_2CH_3$

Comp.	δC1B EC$_{50}$	n	εC1B EC$_{50}$	n	θC1B EC$_{50}$	n
Curcumin	10.67	1.00	8.81	1.00	11.08	1.00
61	11.55	1.03	11.81	1.14	3.16	1.46
67	25.23	0.89	23.38	0.76	7.14	0.51

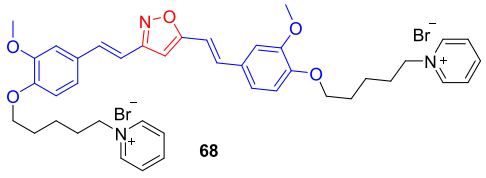

68

Fig. 17. Styrene and polyphenols-isoxazole derivatives **62**–**68**.

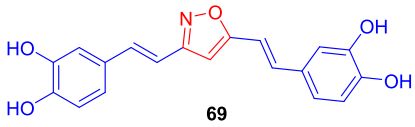

69

Comp.	MIC$_{80}$ (μg/mL) *Candida albicans* 103 With FLC	FICI	Mode	*Candida tropicalis* 087 With FLC	FICI	Mode	*Candida kruseii* 2159 With FLC	FICI	Mode
69	1	0.094	Synergy	1	0.07	Synergy	0.5	0.563	Independent
Curcumin	8	0.125	Synergy	8	0.125	Synergy	8	0.125	Synergy

Fig. 18. Styrene and polyphenol-isoxazole derivative **69**.

C. albicans (MIC$_{80}$ (alone) = 32 μg/mL, MIC$_{80}$ (in combination) = 1 μg/mL) (CCM: MIC$_{80}$ (alone) > 64 μg/mL, MIC$_{80}$ (in combination) = 8 μg/mL. It showed strong synergistic antibacterial activity against *C. krusei* when combined with FLC (MIC$_{80}$ = 0.5 μg/mL). It also showed strong synergistic antibacterial activity against *C. tropicalis* (MIC$_{80}$ = 1 μg/mL). Furthermore, compound **69** showed strong antibacterial activity against *C. krusei* when used alone (MIC$_{80}$ = 1 μg/mL). For *C. tropicalis*, compound **69** also showed the strongest synergistic anti-fungal activity (MIC$_{80}$ = 1 μg/mL) (Fig. 18) (Dong et al., 2021).

Changtam *et al.* (Lal et al., 2013) synthesized a series of curcumin derivatives and evaluated their anti-bacterial and anti-tumor activities. Curcumin derivative **70** containing isoxazole: *S. aureus* (ATCC 11632), *B. cereus* (MTCC 7350), *S. typhi* (ATCC 23564), *P. aeruginosa* (ATCC 15499), and *E. coli* (ATCC 35218) showed significant inhibitory activity with MIC values of 20 μM. The derivative **70** showed moderate inhibitory activity against *A. niger* (MTCC 1108) with a MIC value of 40 μM. The IC$_{50}$ values of derivative **70** against HepG-2, QG-56, and HCT116 cell lines were 25, 50, and 25 μM, respectively. Cytotoxicity was stronger than curcumin (HepG-2: IC$_{50}$ = 50 μM; QG-56: IC$_{50}$ = 100 μM; HCT116: IC$_{50}$ = 50 μM).

Ahmed *et al.* (Ahmed et al., 2018) used curcumin scaffolds to synthesize sulfonamides, among which compound **71** containing isoxazole had the highest inhibitory activity against carbonic anhydrase isoenzyme I (human), with an IC$_{50}$ value of 2.11 μM. The activity was similar to that of Acetazolamide (IC$_{50}$ = 2.17 μM). Additionally, compound **71** showed good inhibitory activity against bCAII with an IC$_{50}$ of 0.87 μM, the activity was better than Acetazolamide (IC$_{50}$ = 0.94 μM). The kinetic study of compound **71** on the bCAII enzyme showed that the Ki value was 0.71 μM (Fig. 19).

Balaji *et al.* (Balaji et al., 2019) synthesized several isoxazole-Hispolon derivatives. Among them, derivative **72** showed the best anti-tuberculosis activity against *Mtb H37Rv* (MIC = 1.6 μg/mL).

Reddy *et al.* (Reddy et al., 2020) synthesized a series of isoxazole derivative methyl β-orsellinate and evaluated its *in vitro* anti-

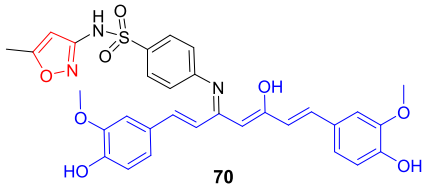

70

Comp.	MIC (μM)				
	Gram-(+) bacterial strains		Gram-(-) bacterial strains		
	S. aureus (ATCC 11632)	*B. cereus* (MTCC 7350)	*S. typhi* (ATCC 23564)	*P. aeruginosa* (ATCC 15499)	*E. coli* (ATCC 35218)
70	20	20	20	20	20
Sulfanilamide	-	-	-	-	-
Sulfamethoxazole	>160	-	>160	-	>160
Sulfapyridine	-	-	-	-	>160
Sulfamethoxypyridazine	>80	>160	>160	>160	>160
Sulfadimidine	-	-	>160	-	>160
Curcumin	80	>80	>80	>80	>80
Ciprofloxacin	1.25	0.63	2.5	1.25	1.25

Comp.	IC_{50} (μM)			
	HeLa	HepG-2	QG-56	HCT116
70	50	25	50	25
Curcumin	50	50	100	50
Adriamycin	5.0	2.5	2.5	5.0

Comp.	MIC (μM)			
	A. niger (MTCC 1108)	*A. flavus* (MTCC 1021)	*C. lunata* (MTCC 581)	*T. viride* (MTCC 1107)
70	40	>80	80	80
Curcumin	-	-	>80	>80
Fluconazole	-	>80	20	20

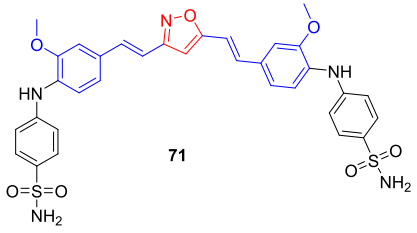

71

Comp.	IC_{50} (μM)		hCAI			bCAII		
	hCAI	bCAII	$K_{m\ (app)}$	$V_{max\ (app)}$	Ki	$K_{m\ (app)}$	$V_{max\ (app)}$	Ki
71	2.11	0.87	7.18	19.11	0.99	7.03	12.34	0.71
Sulfanilamide	11.42	1.38	-	-	-	-	-	-
Sulfacetamide	15.53	2.21	-	-	-	-	-	-
Hydrochlorothiazide	2.12	1.23	-	-	-	-	-	-
Acetazolamide	2.17	0.904	7.69	19.84	1.01	8.80	14.18	0.63

Fig. 19. Styrene and polyphenols-isoxazole derivatives **70**–**71**.

proliferative activity against four human cancer cells and the normal cell line HEK-293 T(embryonic kidney). Compound **75** exhibits excellent anti-proliferative activity against the MCF-7 cell line with an IC_{50} of 7.9 μM, 5 times that of methyl β-orsellinate (IC_{50} = 46.63 μM). Compounds **73** and **75** showed inhibitory effects on MIAPACA cells with IC_{50} values of 9.862 and 9.442 μM. Compound **74** showed an inhibitory effect on IMR-32 cells with an IC_{50} value of 9.792 μM. Flow cytometry showed that compound **75** induced apoptosis of MCF-7 cells and kept the cell cycle in the G2/M phase.

The gallic acid derivative JEZTC (**76**) containing an isoxazole structure has anti-arthritic and cartilage protective effects. JEZTC (**76**) can significantly inhibit the expression of MMP and intracellular ROS, and significantly increase the expression of the metalloproteinase-1 (TIMP-1) gene in tissue. Additionally, there was less cartilage degradation *in vivo* in the JEZTC (**76**) group compared to the PBS group. The results also showed that JEZTC (**76**) activated the NF-κB pathway by regulating the MAPK and PI3K/Akt signaling pathways, resulting in the down-regulation of MMP, thus affecting osteoarthritis. The chondroprotective effect of JEZTC (**76**) may be related to its ability to inhibit chondrocyte apoptosis by reducing ROS production (Lu et al., 2018).

Mahapatra *et al.* (Mahapatra et al., 2022) synthesized a series of *N*-heteroaryl substituted gallamide derivatives. The antibacterial activity of three strains (*S. aureus*; *E. coli*, and *Streptococcus pyogenes*) was evaluated with compounds. JEZTC (**76**) was found to exhibit more inhibitory action against all three bacterial strains with the highest inhibition zone at 24, 24, and 25 mm; and had produced MIC at concentrations of 6.25 μg/mL with *S. aureus*, *E.coli*, and *S. pyogenes* (Fig. 20).

He *et al.* (He et al., 2016) synthesized a variety of stilbene derivatives containing isoxazole and determined the inhibitory activities of protein tyrosine phosphatase 1B (PTP1B) and TCPTP by colorimetry. Among them, compound **77** has the best inhibitory activity with IC_{50} values of 0.91 and 5.19 μM, respectively, which is stronger than that of the lead compound lithocholic acid (IC_{50} = 12.54 μM). Compound **78** showed remarkable activity and best selectivity (TCPTP/PTP1B = 20.7). The structure–activity relationship reveals that the introduction of electron-withdrawing groups, such as halogens, onto phenyl moieties can significantly enhance the inhibitory potency against PTP1B.

Pyrczak-Felczykowska *et al.* (Pyrczak-Felczykowska et al., 2019) synthesized a series of usnic acid derivatives and evaluated the anti-proliferation capacity of various cancer cells. Compounds **79** and **80** inhibit the survival of all cancer cell lines tested in a dose- and time-dependent manner. After 48 h of action, their IC_{50} value was approximately 3 μM for MCF-7 and PC-3 cells, and approximately 1 μM for HeLa cells. Both compounds **79** and **80** can induce G0/G1 blockade and decrease the proportion of HeLa cells in the S phase and the G2/M phase. Compounds **79** and **80** reduce the clonal potential of cancer cells, induce

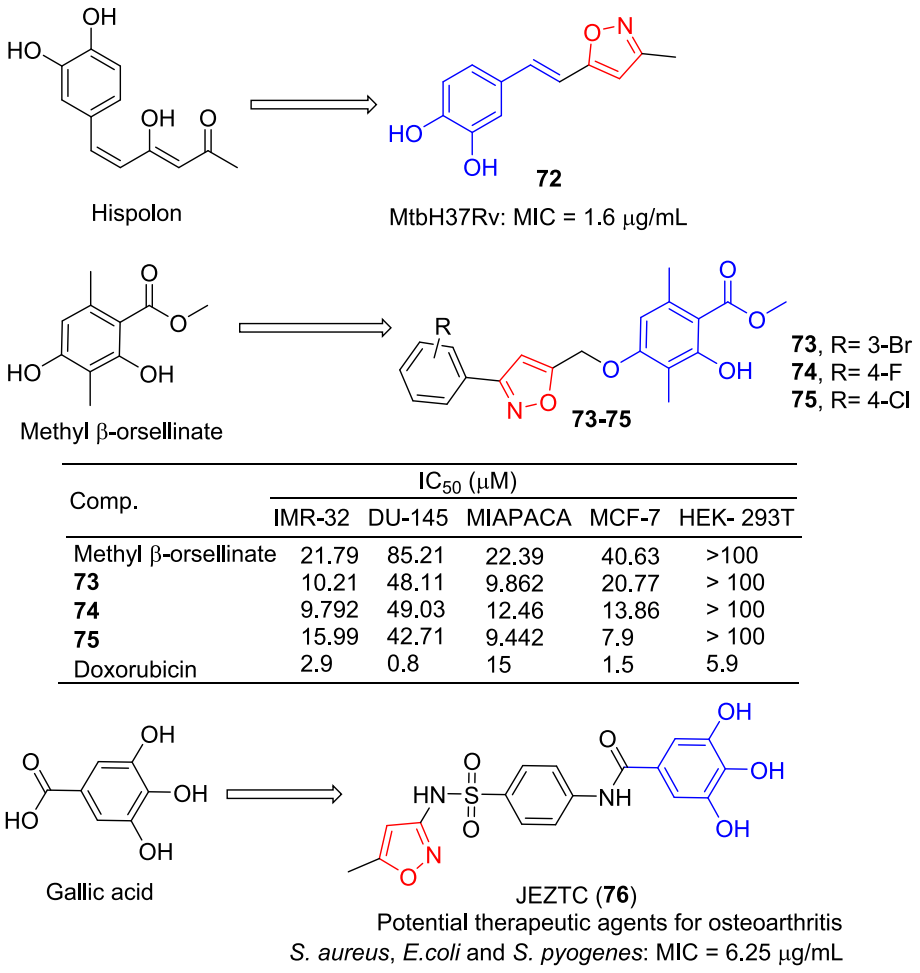

Comp.	IC_{50} (μM)				
	IMR-32	DU-145	MIAPACA	MCF-7	HEK- 293T
Methyl β-orsellinate	21.79	85.21	22.39	40.63	>100
73	10.21	48.11	9.862	20.77	> 100
74	9.792	49.03	12.46	13.86	> 100
75	15.99	42.71	9.442	7.9	> 100
Doxorubicin	2.9	0.8	15	1.5	5.9

Fig. 20. Polyphenols-isoxazole derivatives **72**–**76**.

cell cycle arrest in the G0/G1 phase, and apoptosis of MCF-7 cells. In addition, they induced a large amount of cytoplasmic vacuolation through kinetoprotein-dependent endocytosis (Fig. 21).

Summary: Curcumin, Resveratrol, Gallic acid, and Usnein are all polyphenols. The compounds summarized in this section combine isoxazole in the above natural products and their derived structures. These compounds have a variety of pharmacological activities by binding to different targets, including anti-tumor, anti-pathogen, antioxidant, anti-inflammatory, anti-arthritic, anti-nociceptive, and diuretic activities. Since curcumin and resveratrol have various pharmacological activities, these pharmacological activities are often improved after the hybridization of isoxazole. Similarly, the anti-tumor activity of gallic acid and usnein was significantly improved after the hybridization of isoxazole.

2.4. *Flavone-isoxazole resveratrol*

Wogonin (5, 7-dihydroxy-8-methoxy-flavonoids) has anticancer activity, and many results have shown that wogonin has strong anti-tumor activity *in vivo* and *in vitro* (Li-Weber, 2009; Baumann et al., 2008; Polier et al., 2011). Bian *et al.* (Bian et al., 2017) introduced isoxazole at site 7 of wogonin to obtain derivative **81** and tested its anti-tumor activity. Compound **81** showed some inhibitory activity in HepG-2 cells with an IC_{50} value of 21.66 μM. The activity was lower than wogonin (IC_{50} = 19.0 μM) and 5-fluorouracil (IC_{50} value 17.2 μM).

Rao *et al.* (Rao et al., 2018) designed and synthesized a series of heterocyclic flavono-isoxazole compounds and determined their anti-proliferative activity against MCF-7 by sulforhodamine B assay (SRB) and turbidimetry. Compound **82** showed a certain inhibitory effect on MCF-7 cells with an IC_{50} value of 34.2 μM. Compound **82** also showed moderate antibacterial activity, with an inhibitory rate of 41.7 % at a concentration of 30 μM (Fig. 22).

The flavonoid hydnocarpin, derived from the seeds of *Hydnocarpus wightiana* Blume, was chemically linked to isoxazole by Arya et al. (Arya et al., 2019) in order to synthesize a series of derivatives. These derivatives were subsequently evaluated for their anti-proliferative activity against A375, A549, and WI-38 cells. During the process of synthetic modification, the primary hydroxyl group at the C-9′ position of Hydnocarpin was initially transformed into its corresponding aldehyde via Moffatt oxidation. Subsequently, a one-pot [3 + 2] cycloaddition reaction was employed for synthesizing hydnocarpin-isoxazole derivatives. Compounds **83**–**86** exhibited significant inhibitory effects on A375 and A549 cells with IC_{50} values ranging from 0.65 to 7.5 μM (Fig. 23).

3-*O*-[(*E*)-4-(4-cyanophenyl)-2-oxobut-3-en-1-yl] kaempferol is a lead compound with anti-diabetic and anti-obesity activities. Nie *et al.* (Nie et al., 2020) reported a novel isoxazole derivative **87** based on this lead compound, which improves glucose consumption in insulin-resistant (IR) HepG-2 cells at the nanomolar level (EC_{50} = 0.8 nM). The methylation of kaempferol was achieved by subjecting it to dimethyl sulfate. For demethylation, anhydrous aluminum bromide in acetonitrile was employed as the chosen condition, resulting in the formation of the corresponding 3-hydroxyflavone. Subsequently, compound **87** underwent a nucleophilic substitution reaction followed by cyclization with chloro-benzaldoxime to yield isoxazole derivative (Fig. 24). Compound **87** significantly improved the level of AMPK phosphorylation (AMP-activated protein kinase) in HepG-2 cells. The levels of PEPCK (phosphoenolpyruvate carboxykinase) and G6Pase (glucose 6-

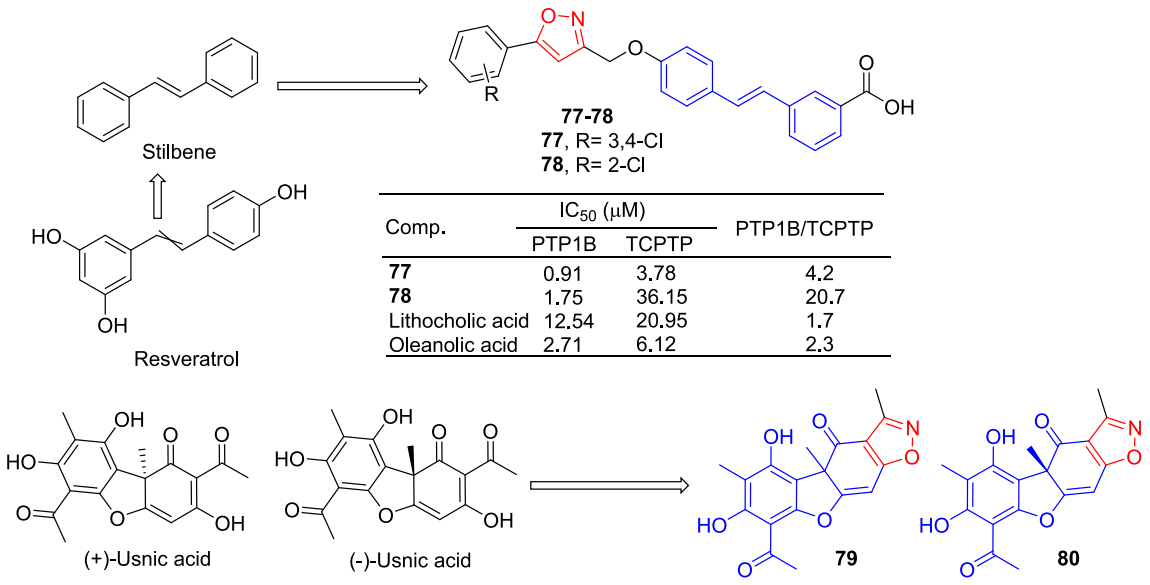

Comp.	IC_{50} (μM)		PTP1B/TCPTP
	PTP1B	TCPTP	
77	0.91	3.78	4.2
78	1.75	36.15	20.7
Lithocholic acid	12.54	20.95	1.7
Oleanolic acid	2.71	6.12	2.3

Comp.	IC_{50} (μM)							
	MCF-7		HeLa		PC-3		HDFa	
	24 h	48 h	24 h	48 h	24 h	48 h	24 h	48 h
(-)-usnic acid	> 10	> 10	> 10	> 10	> 10	> 10	> 10	> 10
(+)-usnic acid	> 10	> 10	> 10	> 10	> 10	> 10	> 10	> 10
79	3.1	2.9	1.0	1.0	3.4	2.8	> 10	5.9
80	3.2	2.5	1.0	1.0	3.2	3.1	9.2	3.0

Fig. 21. Styrene and polyphenols-isoxazole derivatives **77**–**80**.

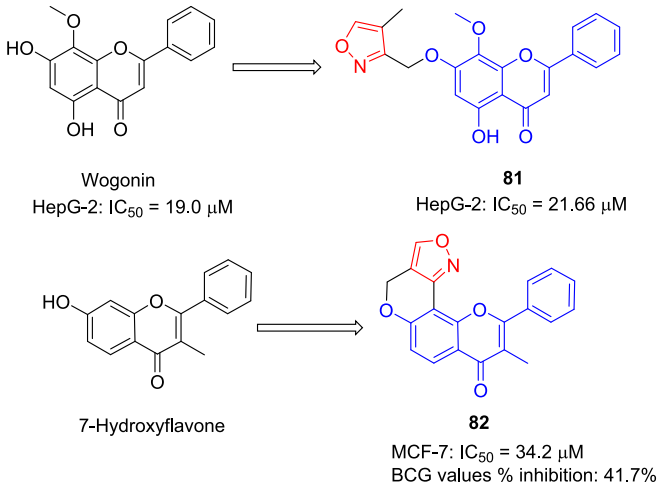

Fig. 22. Flavono-isoxazole derivatives **81**–**82**.

phosphatase) were decreased. The molecular mechanism of **87** may be related to the activation of the AMPK/PEPCK/G6Pase pathway.

Inhibition of alpha-amylase is considered a therapeutic strategy for the treatment of glucose absorption disorders. Flavonoids, isoxazoles, and their halogenated derivatives have become the focus of pharmaceutical chemistry research because of their high biological activity. Saidi *et al.* (Saidi et al., 2022, 1247) designed and synthesized a series of novel halogenated flavonoid isoxazoles and evaluated their inhibitory potential against α-amylase. The α-amylase inhibitory activity of compound **88** (IC_{50} = 16.2 μM) was the highest *in vitro*, which was comparable to that of acarbose (IC_{50} = 15.7 μM). Compounds **89**–**91** were slightly less active than **88**, with IC_{50} values of 17.33, 17.58, and 18.36 μM, respectively. The above results suggest that the incorporation of electron-withdrawing groups in the *para*-position of the benzene ring confers enhanced activity.

Rongmao *et al.* (Qiu et al., 2018) designed and synthesized a series of isoflavone analogs and evaluated their lipid-lowering activities. Most of the compounds significantly reduced lipid accumulation in 3 T3-L1 adipocytes, and four compounds **92**–**95** had stronger inhibitory effects than GW4064. Compound **95** showed agonistic activity against FXR in cell-based luciferase reporting tests. At the same time, the expression of the FXR, SHP, and BSEP genes was up-regulated and the mRNA expression of the lipogenic gene SREBP-1c was down-regulated on **95**. The safety of **95** in the HepG-2 cytotoxicity test also exceeds GW4064 (Fig. 25).

Asha Bhanu *et al.* (Asha Bhanu et al., 2020) designed and synthesized 7-hydroxyflavone derivatives and evaluated their anti-bacterial activity (Fig. 26). Compounds **96**–**98** showed strong antibacterial activity, exceeding or approaching that of standard drugs (Streptomycin and Cycloheximide).

Gu *et al.* (Gu et al., 2017) designed and synthesized a series of dihydroflavone derivatives and evaluated their anti-psychotic activities *in vitro* and *in vivo*. In brief, dihydroflavones with various substitutions were first synthesized, followed by the acquisition of the target compounds through a three-step nucleophilic substitution reaction (Fig. 27). The activity of the D2 receptor/G protein α16a cotransfected into HEK293 cells was significantly reduced by compounds **99**–**101**, exhibiting IC_{50} values ranging from 0.0513 to 0.116 μM. Moreover, compounds **99**–**101** effectively suppressed lipopolysaccharide/interferon-gamma-induced excess nitric oxide production by BV-2 microglia. In mice, the increase in motor activity induced by MK-801 (an antagonist of NMDA receptors) was reversed by gavage of **99**–**101**. Reduce the overactivity of climbing behavior induced by apomorphine (a dopamine receptor agonist).

Nifantev *et al.* (Nifantev et al., 2015) synthesized dihydroquercetin aryl derivatives and determined the cytotoxicity of these compounds in HeLa cells and murine fibroblasts. The derivative **102** containing isoxazole showed weak HeLa cytotoxicity, with a survival rate of 50 % at 100 μM. At the same concentration, the survival rate of murine

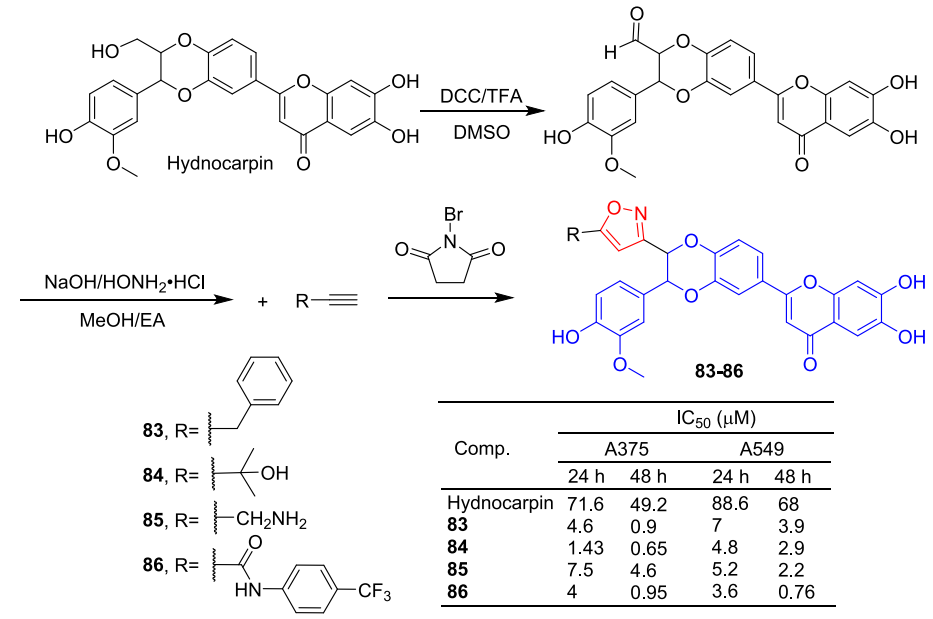

Comp.	IC_{50} (μM)			
	A375		A549	
	24 h	48 h	24 h	48 h
Hydnocarpin	71.6	49.2	88.6	68
83	4.6	0.9	7	3.9
84	1.43	0.65	4.8	2.9
85	7.5	4.6	5.2	2.2
86	4	0.95	3.6	0.76

Fig. 23. Flavono-isoxazole derivatives **83**–**86**.

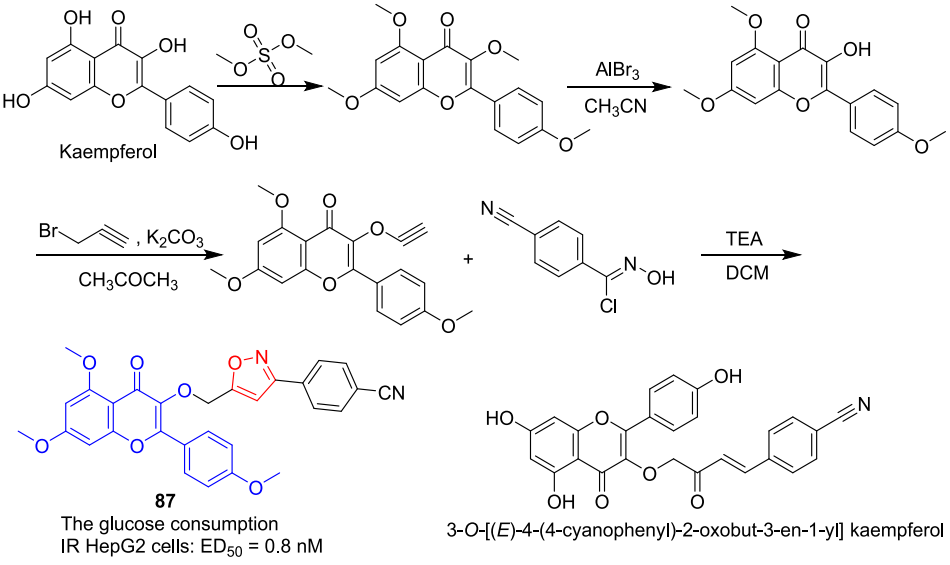

Fig. 24. Flavono-isoxazole derivative **87**.

fibroblasts was 83 %.

Badadhe *et al.* (Badadhe et al., 2013) designed and synthesized a series of novel isoxazol pigment compounds and evaluated their anti-bacterial activities. Pharmacological experiments showed that compounds **103**–**105** had moderate anti-bacterial activity against Gram-positive bacteria.

Dengale *et al.* (Dengale et al., 2022) designed and synthesized a series of 2-(4,5,6,7-tetrahydrobenzo[c]isoxazol-3-yl)-4*H*-chromen-4-ones. Compounds **106**–**108** exhibited moderate anti-inflammatory activity compared to the standard drug diclofenac sodium and showed antioxidant activity comparable to the standard drug ascorbic acid. In terms of anti-inflammatory activity, the preliminary structure–activity relationship revealed that the presence of an electron-withdrawing group (R_1) was conducive to enhanced activity, while the presence of an electron-donating group (R_2) was detrimental to activity.

Diabetic retinopathy (DR) is one of the leading causes of blindness. Rho-associated coiled coils containing serine/threonine protein kinases (ROCKs) are considered potential targets for DR therapy. Zhao et al. designed and synthesized a new class of ROCK inhibitor 4H-chromen-4-one derivative. Compound **109** containing isoxazole can reduce ROCK I and ROCK II activity with IC_{50} values of 0.068 and 0.005 μM, respectively (Zhao et al., 2019) (Fig. 28).

Abu-Bakr *et al.* (Abu-Bakr et al., 2019) synthesized a series of furo [3,2-g]chromones derivatives and screened for their inhibitory capacity in three human cancer cell lines, HFT-116, MCF-7, and HepG-2. Compound **110** showed a strong inhibitory effect on the HepG-2 cell line with an IC_{50} of 7.9 μg/mL. Compounds **111** and **112** showed strong inhibitory effects on the HCT116 cell line with an IC_{50} of 4.7 and 7.8 μg/mL, respectively.

Kaushik *et al.* (Kaushik et al., 2019) designed and synthesized a series of isoxazolylchromones, compound **113** showed obvious cytotoxicity in MCF-7 cells with an IC_{50} value of 31.25 μg/mL. The ERα selectivity of the ligand was confirmed by ERα silencing experiments. Deactivation of compound **113** showed that ERα luciferase reporter gene expression was

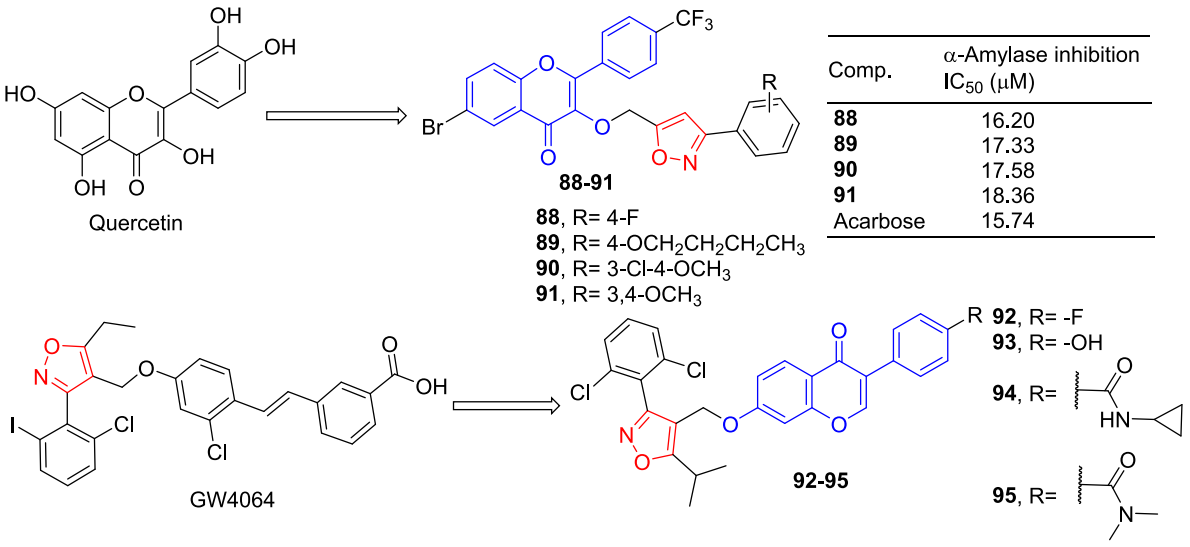

Comp.	α-Amylase inhibition IC_{50} (μM)
88	16.20
89	17.33
90	17.58
91	18.36
Acarbose	15.74

Fig. 25. Flavono-isoxazole derivatives **88**–**95**.

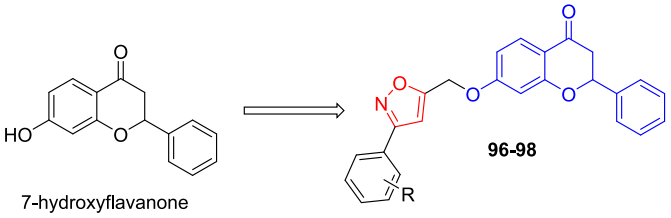

Comp.	Zone of inhibition, mm					
	Gram positive bacteria		Gram negative bacteria		Fungus	
	Staphylococcus aureus	*Bacillus subtilis*	*Escherichia coll*	*Pseudomonas aeruginosa*	*Aspergillus niger*	*Aspergillus fumigates*
96	12.26	12.33	12.16	16.82	13.53	12.50
97	13.50	12.80	12.30	17.80	14.10	13.97
98	13.66	12.83	12.53	17.60	14.26	14.05
Streptomycin	14.26	13.23	12.76	16.76	-	-
Cycloheximide	-	-	-	-	14.53	13.7

Fig. 26. Flavono-isoxazole derivatives **96**–**98**.

negatively regulated and ERβGFP was induced in treated cells. The cell cycle showed an increase in sub-G0/G1 populations in the compound **113** treatment group. Compound **113** also induces cell death through apoptosis. Similar to tamoxifen, **113**-induced cell death is mediated by an increase in ROS. Compared to tamoxifen-induced autophagy, compound **113** induced mitochondrial transmembrane potential loss and caspase activation without signs of autophagy.

Awadallah *et al.* (Awadallah et al., 2015) synthesized a series of isoxazole-containing pigment compounds and evaluated their cytotoxic activity against MCF-7 and A-549 cells. Compounds **114**–**116** showed weak inhibitory activity against the off-target cytoplasmic isomers hCA I and hCA II, but showed significant inhibitory activity against tumor-associated hCA IX and hCA XII. Compound **114** showed high inhibitory effects on MCF-7 and A-549 cell lines with IC_{50} of 25.80 and 57.23 μM, respectively (Fig. 29).

Summary: Flavone-isoxazole hybridization natural products mainly have anti-tumor, anti-psychotic, and lipid-lowering activities, and these compounds can also be used to treat diabetic retinopathy. Compound **87** exhibits promising potential as a valuable candidate in the quest to develop novel anti-diabetic drugs. Compounds **99**–**101** possess potential antipsychotic effects and may be beneficial in the treatment of schizophrenia. In terms of anti-tumor activity, most of the hybrid isoxazole derivatives showed no significant improvement in activity compared to the lead compounds. However, hydnocarpin derivatives (**83**–**86**), showed significantly improved anti-tumor activity. To some extent, the structure of isoxazole is an important pharmacophore for the anti-tumor effect of these hydnocarpin derivatives. Among these derivatives, compound **84** showed the strongest inhibitory effect on A375 cells with an IC_{50} of 0.65 μM, which is valuable for further study.

2.5. Coumarin-isoxazole hybridization

Shi *et al.* (Shi et al., 2017) designed and synthesized a series of coumarin-isoxazole compounds, and measured their anti-cancer activity against HCT116, Hun7, and SW620 cells *in vitro* by the MTT assay. Compound **118** showed inhibitory effects on HCT116, Hun7, and SW620 cell lines with IC_{50} values of 10.3, 12.1 and 10.5 μM, respectively. The IC_{50} values of compound **117** for these three cell lines were 9.21, 8.76, and 9.83 μM, respectively. Compounds **118** and **117** were less toxic to normal cells (HFL-1: The IC_{50} values were 90.9 and 74.2 μM, respectively).

Shakeel-u-Rehman *et al.* (Shakeel et al., 2014) designed and synthesized a series of 6-hydroxycoumarin isoxazoles. Compounds **119** and **120** showed the strongest inhibitory activity against PC-3 cells, with IC_{50} values of 8.2 and 13.6 μM, respectively.

The isoxazole-coumarin derivative **121** showed certain inhibitory

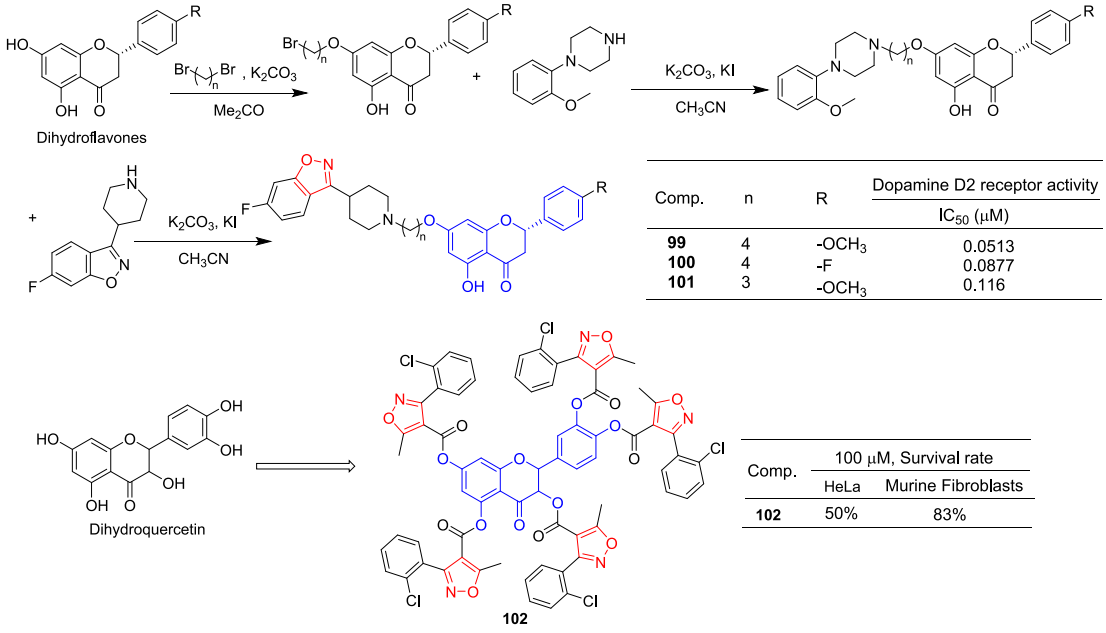

Comp.	n	R	Dopamine D2 receptor activity IC50 (μM)
99	4	-OCH_3	0.0513
100	4	-F	0.0877
101	3	-OCH_3	0.116

Comp.	100 μM, Survival rate	
	HeLa	Murine Fibroblasts
102	50%	83%

Fig. 27. Flavono-isoxazole derivatives **99**–**102**.

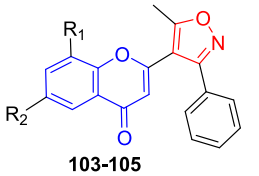

103-105

103, R_1= -CH_3, R_2= -H
104, R_1= -CH_3, R_2= -CH_3
105, R_1= -H, R_2= -Br

Comp.	Zone of inhibition (MIC, μg/mL)			
	B. subtilis	*S. aureus*	*S. typhi*	*P. aeroginosa*
103	13.8 (10)	13.3 (10)	15.1 (13)	14.9 (14)
104	14.3 (10)	14.1 (10)	12.8 (15)	12.7 (15)
105	13.4 (10)	13.7 (10)	15.1 (15)	14.8 (15)
Streptomycin	15.1 (10)	14.9 (10)	16.4 (10)	16.1 (10)
Ampicillin	14.3 (10)	14.7 (10)	16.3 (10)	15.9 (10)

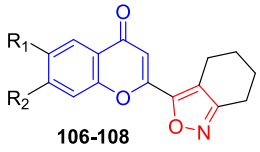

106-108

106, R_1= -Cl, R_2= -CH_3
107, R_1= -F, R_2= -H
108, R_1= -Cl, R_2= -H

Comp.	Anti-inflammatory Percent of inhibition	Anti-oxidant MIC in μg/mL
106	41.18%	650.475
107	48.72%	628.325
108	49.75%	NT
Diclofenac sodium	77.78%	-
Ascorbic acid	-	41.69611

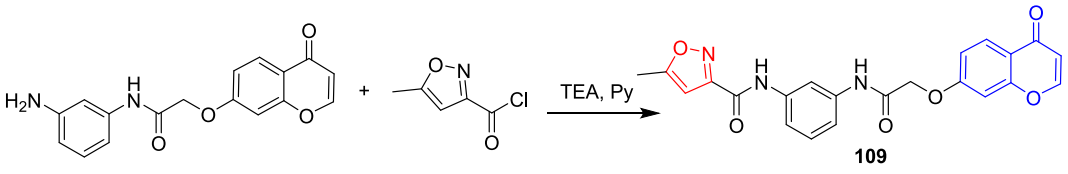

109

ROCK I: IC_{50} = 0.068 μM
ROCK II: IC_{50} = 0.005 μM

Fig. 28. Chromone-isoxazole derivatives **103**–**109**.

activity against the HepG-2 cell line with an IC_{50} value of 15.3 μM (Gomha et al., 2015).

Krishna *et al.* (Krishna et al., 2017) synthesized isoxazole fused coumarin analogs and tested their anti-tumor activity *in vitro*. Compounds **122** and **123** showed moderate inhibitory effects on the Colo-205 cell line with IC_{50} values of 28.5 and 30.1 μM, respectively (Fig. 30).

Ghorab *et al.* (Ghorab et al., 2016) designed and synthesized a series of sulfanilyl coumarin derivatives. The anti-tumor activity of all compounds against the breast cancer cell line (T47D) was evaluated *in vitro*. Compound **124** containing isoxazole showed a moderate inhibitory effect on the T47D cell line with an IC_{50} of 68.4 μM.

Wang *et al.* (Wang et al., 2013) reported that a series of coumarin-containing sulfa compounds inhibited two human carbonic anhydrases. The starting diverse substituted malonic acid mono phenol esters were synthesized under solvent-free conditions using Meldrum's acid and various substituted phenols, followed by cyclization with Eaton's reagent to yield the corresponding 4-hydroxycoumarin. The different substituted 3-formyl-4-chlorocoumarins were obtained through Vilsmeiere-Haack reactions. Finally, compounds **125**–**127** were prepared by reacting with sulfamethoxazole in ethanol (Fig. 31). These three compounds, which contain isoxazole, exhibited significant inhibitory effects on hCA II and hCA IX as well as on B16-F10 and MCF-7 cell

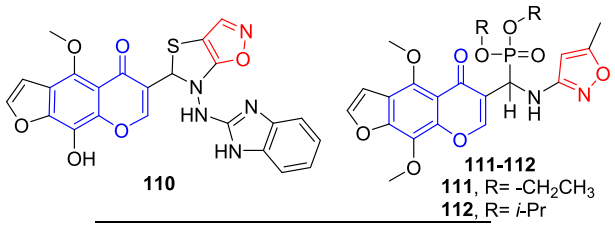

110

111-112
111, R= -CH_2CH_3
112, R= *i*-Pr

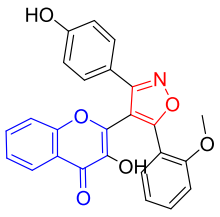

113
MCF-7: IC_{50} = 31.25 μg/mL

Comp.	IC_{50} (μg/mL)		
	HCT116	MCF-7	HepG-2
110	7.8	28.1	7.9
111	4.7	28.2	12.7
112	7.8	30.6	9.4
Doxorubicin	5.5	15.6	6.1

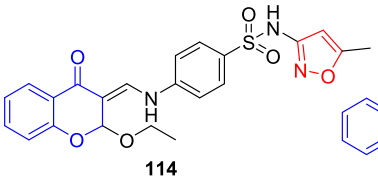

114

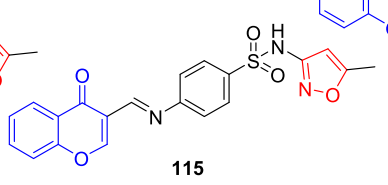

115

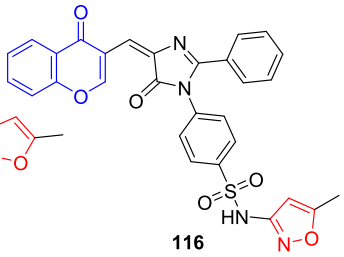

116

Comp.	IC_{50} (μM)		K_i (nM)	
	MCF-7	A549	hCA IX	hCA XII
114	25.80	57.23	23.84	424.40
115	34.50	59.66	32.09	10.76
116	30.01	>100	25.24	9.71
Doxorubicin	33.13	26.81	-	-
Acetazolamide	-	-	25.00	5.70

Fig. 29. Chromone-isoxazole derivatives **110**–**116**.

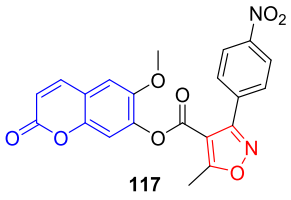

117

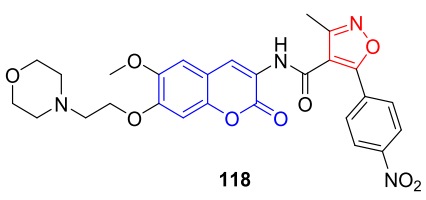

118

Comp.	IC_{50} (μM)			
	HCT116	Huh7	SW620	HFL-1
117	9.21	8.76	9.83	90.9
118	10.3	12.1	10.5	68.52
Scopoletin	>25	>25	>25	-
Sunitinib	5.62	3.03	6.25	-

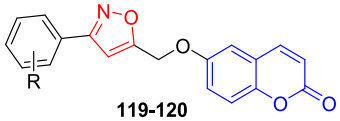

119-120
119, R= 2-NO_2
120, R= 2-CN

Comp.	IC_{50} (μM)
	PC-3
119	8.2
120	13.6

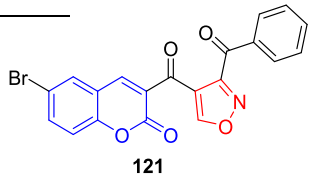

121
HepG-2: IC_{50} = 15.3 μM

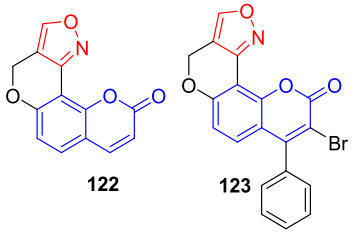

122

123

Comp.	IC_{50} (μM)		
	Colo-205	HepG-2	HeLa
122	28.5	68.4	65.6
123	30.1	61.7	81.4
Etoposide	0.42	4.77	22.5

Fig. 30. Coumarin-isoxazole derivatives **117**–**123**.

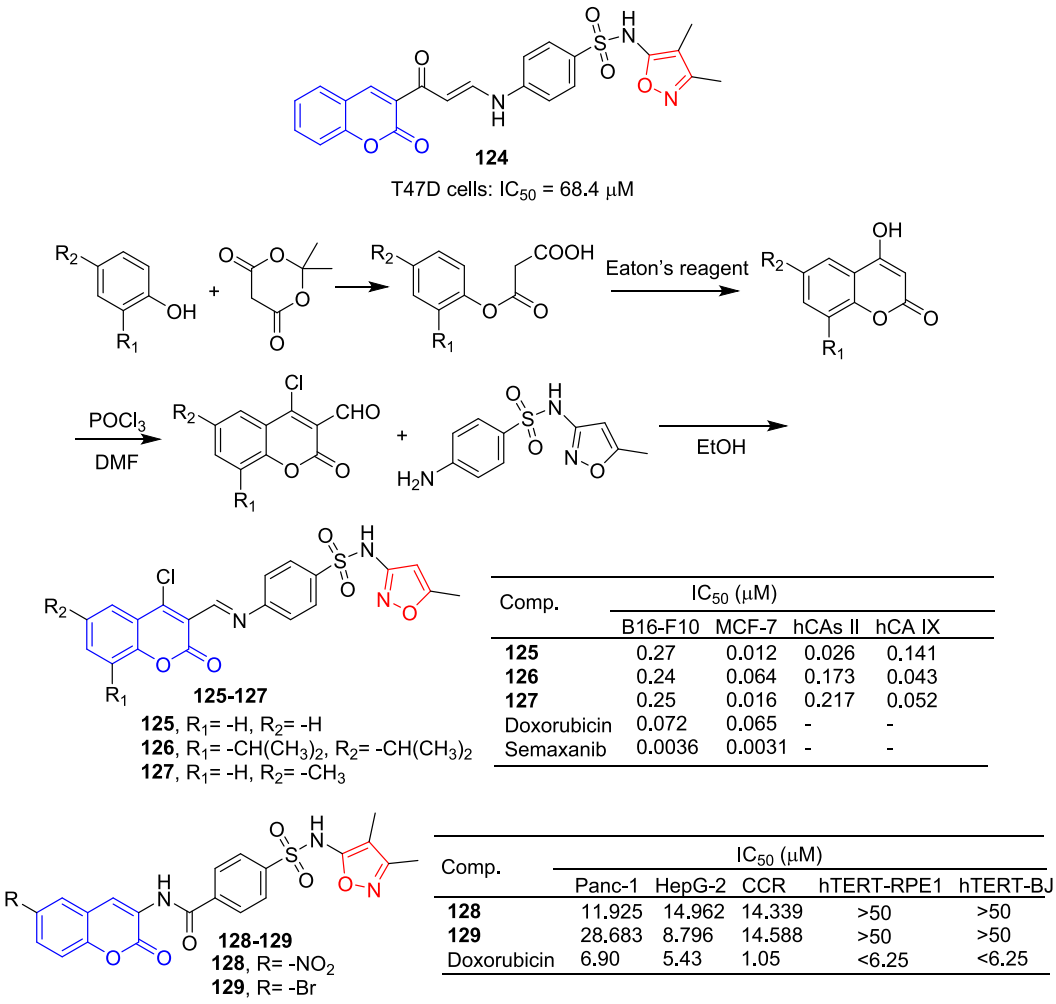

Comp.	IC50 (μM)			
	B16-F10	MCF-7	hCAs II	hCA IX
125	0.27	0.012	0.026	0.141
126	0.24	0.064	0.173	0.043
127	0.25	0.016	0.217	0.052
Doxorubicin	0.072	0.065	-	-
Semaxanib	0.0036	0.0031	-	-

Comp.	IC50 (μM)				
	Panc-1	HepG-2	CCR	hTERT-RPE1	hTERT-BJ
128	11.925	14.962	14.339	>50	>50
129	28.683	8.796	14.588	>50	>50
Doxorubicin	6.90	5.43	1.05	<6.25	<6.25

Fig. 31. Coumarin-isoxazole derivatives **124**–**129**.

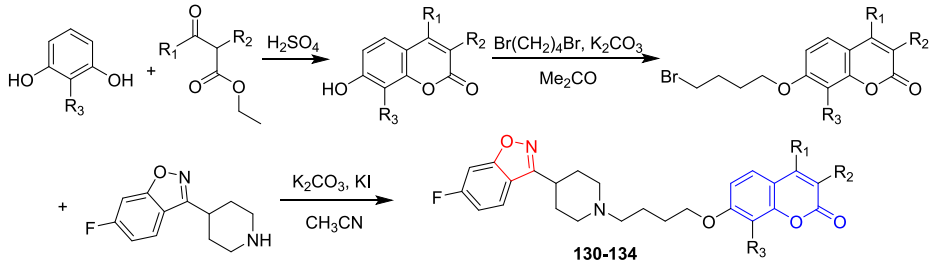

Comp.	Receptor affinity K_i (nM)		
	D_2	5-HT_{1A}	5-HT_{2A}
130	4.9	3.5	8.4
131	3.9	409.5	30.8
132	4.0	16.7	0.3
133	2.6	3.3	0.3
134	5.3	12.9	0.9

Fig. 32. Coumarin-isoxazole derivatives **130**–**134**.

lines. Compound **125** had the strongest inhibitory effect on the MCF-7 cell line and hCA II, with IC_{50} values of 0.012 and 0.026 μM. Compound **126** had the strongest inhibitory effect on hCA IX with an IC_{50} of 0.043 μM. As hCA II inhibitors, the substituted moieties on the benzene ring of the coumarin exhibit an active gradient of –H > $-^tBu$ > $–CH_3$. However, for hCA IX, it is $-^tBu$ > $–CH_3$ > -H.

Nasr *et al.* (Nasr et al., 2018) synthesized a series of derivatives of coumarin hydrazone and evaluated the anti-tumor activity of Panc-1, HepG-2, and CCR cell lines *in vitro*. Compound **128** containing isoxazole had the strongest inhibitory effect on Panc-1 cells with an IC_{50} value of 11.925 μM. Compound **129** had the strongest inhibitory effect on HepG-2 cells with an IC_{50} of 8.796 μM.

Chen *et al.* (Chen et al., 2013) synthesized novel anti-psychotic coumarin derivatives with potent dopamine D_2, D_3, and serotonin 5-HT_{1A}, 5-HT_{2A} receptor properties. The starting 7-hydroxycoumarin intermediates were obtained via the Pechmann reaction, and the target

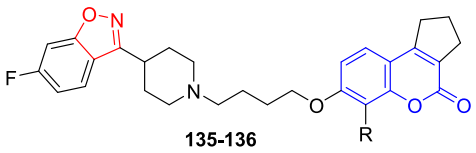

135-136

135, R= -CH_3
136, R= -Cl

Comp.	Receptor affinity K_i (nM)				
	D_2	5-HT_{1A}	5-HT_{2A}	D_3	H_1
135	12.7	7.8	2.2	13.6	1825.3
136	18.9	11.4	5.3	13.9	13.6
Ripersidone	-	-	-	10.1	22.9
Clozapine	-	-	-	260.1	6.8

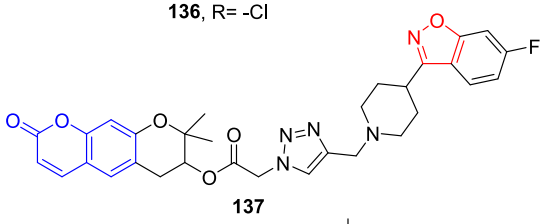

137

Comp.	IC_{50} (μM)	
	AChE	BuChE
Galantamine	1.7	9.4
Decursinol	93.4	>810
α-lipoic acid	>200	>200
137	61.91	14.64

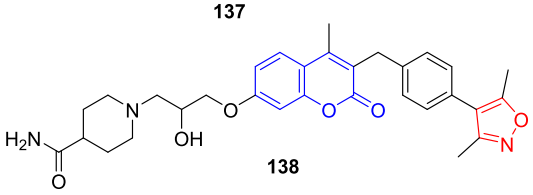

138

Comp.	IC_{50} (μM)		A549 CC_{50} (μM)
	EBOV	MARV	
138	5.2	3.2	36.9

Fig. 33. Coumarin-isoxazole derivatives **130**–**138**.

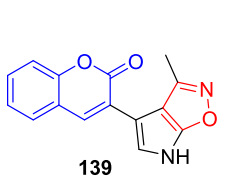

139
EACs: IC_{50} = 52.65 μg/mL

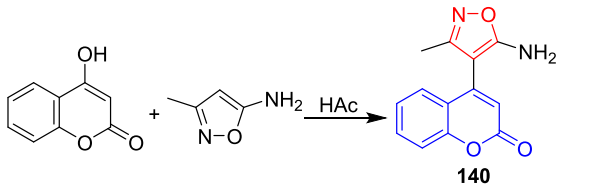

140
EAC assay: IC_{50} = 0.21 μM

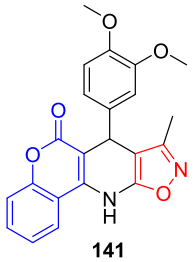

141
α-glucosidase inhibition: IC_{50} = 56.043 μg/mL

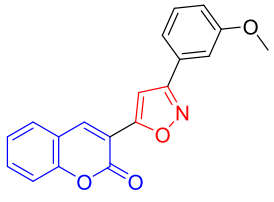

142
Edema formation inhibition rate = 42.87%

Fig. 34. Coumarin-isoxazole derivatives **139**–**142**.

compounds were subsequently prepared through a two-step nucleophilic substitution reaction (Fig. 32). The isoxazole-piperidine derivative **130** has a high affinity for the D_2, 5-HT_{1A}, and 5-HT_{2A} receptors (K_i of 4.9, 3.5, and 8.4 nM, respectively). The derivative **130** has a higher affinity for the 5-HT_{1A} receptor than risperidone (K_i = 180 nM). The titer of compound **132** against the D_2 and 5-HT_{2A} receptors exceeds **130** (D_2, K_i = 4.0 nM; 5-HT_{2A}, K_i = 0.3 nM), and the affinity of the 5-HT_{1A} receptor did not change. The derivatives **133** and **134** have the highest affinity for the 5-HT_{2A} receptor (**133**: K_i = 0.3 nM; **134**: K_i = 0.9 nM). Compounds **131**, **133**, and **134** exhibit high affinity for the D_2 receptor with K_i of 3.9, 2.6, and 5.3 nM, respectively. Compound **133** has a higher affinity for the D_2 receptor than compound **130** (K_i = 4.9 nM) and risperidone (K_i = 3.7 nM). Furthermore, compound **133** has a low affinity for the 5-HT_{2C} and H_1 receptors (which reduce the risk of obesity associated with chronic treatment) and the hERG channels (which reduce the incidence of point twisting). In animal models, compound **133** inhibited diamorphine-induced climbing behavior at the highest dose, hyperactivity and conditioned avoidance responses induced by MK-801, and no significant narcolepsy. Furthermore, in trials measuring prolactin secretion and weight gain, there were fewer preclinical adverse events at compound **133** compared to risperidone. The structure–activity relationship is as follows: the substitution at the 4-position (R_1) with methyl as the favored substituent; the substitution at the 3-position (R_2) with either unsubstituted or substituted (methyl) being preferred; and the substitution at the 8-position (R_3) with an electron-withdrawing group (chloro) as the favored substituent.

Coumarin derivatives combine the properties of dopamine receptors D_2, D_3, and serotonin 5-HT_{1A}, 5-HT_{2A}. Compounds **135** and **136** were synthesized by the same research team using a similar synthetic approach to compounds **130**–**134**. Compounds **135** and **136** have high affinity for dopamine D_2, D_3, and 5-HT_{1A}, 5-HT_{2A} receptors (K_i between 2.2–18.9 nM). Compound **135** has a low affinity for H_1 receptors (reducing the risk of obesity under chronic treatment). In animal models, compound **135** inhibited apomorphine-induced climbing and hyperactivity induced by MK-801 at the highest dose without significant paralysis (Chen et al., 2014).

Park *et al.* (Park et al., 2016) synthesized a series of decursinol derivatives using the ka-reaction method and evaluated their biological activities. Compound **137** containing isoxazole has inhibitory activity in acetylcholinesterase (AChE) and butyrylcholinesterase (BuChE) with IC_{50} values of 61.91 and 14.64 μM, respectively.

Filoviruses, including Ebolavirus (EBOV), Marburgvirus (MARV) and

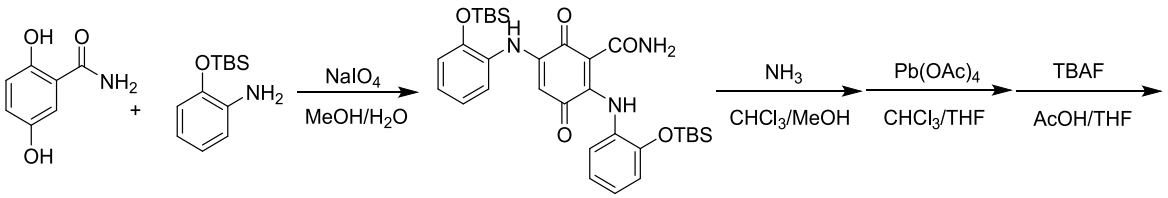

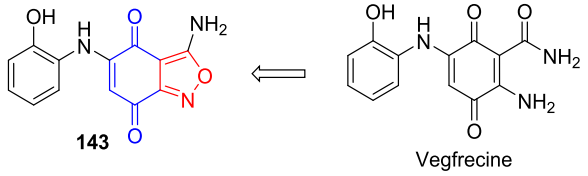

Comp.	IC_{50} (μM)			
	VEGFR-1	VEGFR-2	NIH3T3/ VEGFR-1 (Flt-1)	NIH3T3/ VEGFR-2 (KDR)
Vegfrecine	0.018	0.011	3.7	12.8
143	0.65	7.1	7.5	8.3

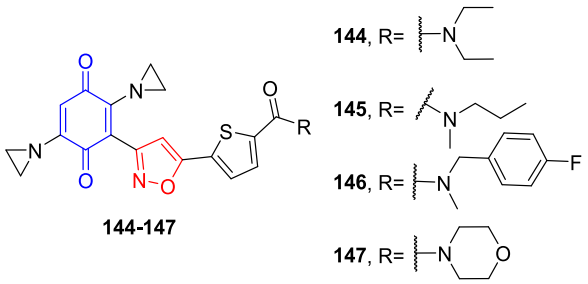

Antimicrobial activity

Comp.	MIC (μg/mL)					
	Staphylococcus aureus MTCC 96	*Bacillus subtilis* MTCC 121	*S. aureus* MLS16 MTCC 2940	*Micrococcus luteus* MTCC 2470	*Klebsiella planticola* MTCC 530	*Candida albicans* MTCC 3017
145	7.8	3.9	15.6	15.6	7.8	7.8
147	3.9	3.9	3.9	15.6	7.8	7.8
Mitomycin C	1.9	0.45	1.9	0.9	1.9	>500
Miconazole	-	-	-	-	-	-
Ciprofloxacin	0.9	0.9	0.9	0.9	0.9	7.8

Biofilm inhibition

Comp.	IC_{50} (μM)				
	Bacillus subtilis MTCC 121	*Staphylococcus aureus* MTCC 96	*S. aureus* MLS16 MTCC 2940	*Micrococcus luteus* MTCC 2470	*Klebsiella planticola* MTCC 530
145	2.2	4.6	10.6	8.9	3.5
147	2.8	2.5	1.9	9.8	5.1
Mitomycin C	0.3	1.1	0.9	0.9	1.1
Ciprofloxacin	0.5	0.7	0.6	0.8	0.6

Antifungal activity

Comp.	MIC (μg/mL)											
	C.a MTCC 183	*C.a* MTCC 227	*C.a* MTCC 1637	*C.a* MTCC 3018	*C.a* MTCC 3958	*C.a* MTCC 4748	*C.a* MTCC 7315	*Candida parapsilosis* MTCC 1744	*Candida aaseri* MTCC 1962	*Candida glabrata* MTCC 3019	*Candida krusei* MTCC 3020	*Issatchenkia hanoiensis* MTCC 4755
145	31.2	62.5	62.5	62.5	31.2	31.2	15.6	15.6	7.8	15.6	15.6	15.6
147	15.6	7.8	7.8	31.2	62.5	31.2	62.5	15.6	31.2	31.2	7.8	15.6
Miconazole	7.8	7.8	7.8	7.8	7.8	7.8	7.8	7.8	7.8	7.8	7.8	7.8

Fig. 35. Benzoquinone-isoxazole derivatives **143**–**147**.

Cuevavirus cause hemorrhagic fevers in humans with a mortality rate of up to 90 %. Gao *et al.* (Gao et al., 2020) designed and synthesized a piperidine-coumarin derivative and evaluated its anti-viral activity. Compound **138** containing isoxazole showed inhibitory activity against EBOV and MARV (EBOV: IC_{50} = 5.2 μM; MARV: IC_{50} = 3.2 μM). Compound **138** did not exhibit significant toxicity to host cells (A549: IC_{50} = 36.9 μM) (Fig. 33).

Derivative **139** exhibited moderate anti-tumor activity against the Ehrlich ascite cells (EAC) model *in vitro*, with an IC_{50} of 52.65 μg/mL (W. S. Hamama, M.E. Ibrahim, H.H. Zoorob, Synthesis, DFT Study, 2017). Derivative **140** was synthesized by reacting 4-hydroxycoumarin with 5-amino-3-methylisoxazole in glacial acetic acid and exhibited significant anti-tumor activity; with an IC_{50} of 0.21 μM (Ibrahim et al., 2016).

Suresh *et al.* (Suresh et al., 2017) synthesized dihydro-6H-chromeno [4,3-b]isoxazolo[4,5-e] pyridine heterocycles. The anti-diabetic activity of the compounds on type 2 diabetes mellitus was evaluated. Compound **141** showed the strongest inhibitory effect on α-amylase activity with an IC_{50} value of 56.043 μg/mL.

In a rat model of carrageenan-induced metatarsal edema, the anti-inflammatory activity of the compound was evaluated at 100 mg/kg of body weight. The isoxazole-containing derivative **142** showed moderate anti-inflammatory activity, with a 42.87 % inhibition of edema

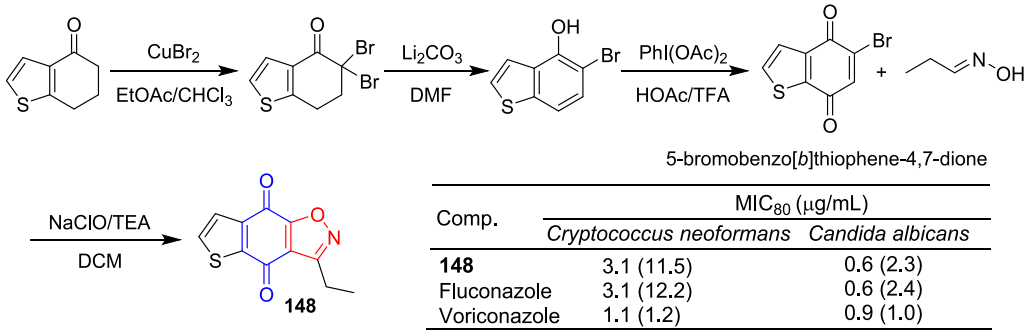

Comp.	MIC$_{80}$ (μg/mL)	
	Cryptococcus neoformans	*Candida albicans*
148	3.1 (11.5)	0.6 (2.3)
Fluconazole	3.1 (12.2)	0.6 (2.4)
Voriconazole	1.1 (1.2)	0.9 (1.0)

Fig. 36. Benzoquinone-isoxazole derivative **148**.

formation compared to the control agent ibuprofen (100 mg/kg) (Dixit et al., 2013) (Fig. 34).

Summary: Coumarin-isoxazole hybridization natural products mainly have anti-tumor, anti-inflammatory, anti-viral, anti-diabetic, and anti-psychotic activities. Carbonic anhydrase is a target for the development of anti-tumor chemotherapeutics, in terms of anti-tumor activity, compound **125** showed the strongest inhibitory activity against MCF-7 cells while inhibiting carbonic anhydrase, with IC$_{50}$ values of 12 nM. In addition, the compound did not exhibit cytotoxic activity against macrophages. The results indicate that sulfonamides containing coumarin-isoxazole moieties have the potential to be potent and novel anti-tumor agents. Compared to the compounds in the previous sections, coumarin-isoxazole derivatives also have anti-psychotic activity by inhibiting central dopamine and serotonin receptors. Among them, compound **133** may constitute a new class of drugs for the treatment of schizophrenia.

2.6. Quinonoids-isoxazole hybridization

Vegfrecine has shown effective *in vitro* inhibitory activity against VEGFR-1 and VEGFR-2 tyrosine kinases, so vegfrecine becomes a VEGF receptor tyrosine kinase inhibitor. Adachi *et al.* (Adachi et al., 2021) synthesized a derivative of vegfrecine containing isoxazole rings. Compound **143** showed moderate inhibitory activity against VEGFR-1 tyrosine kinase (IC$_{50}$ = 0.65 μM) and slightly lower inhibitory activity against VEGFR-2 tyrosine kinase (IC$_{50}$ = 7.1 μM). The synthesis of the intermediate was carried out through oxidative amination of 2,5-dihydroxybenzamide in the presence of 2-((*tert*-butyldimethylsilyl)oxy)aniline. Subsequent ammonolysis of the intermediate yielded the 1-carbamoyl-2-aminoquinone derivative, which was then subjected to oxidative cyclization between the 1-carbamoyl group and 2-amino group using lead acetate to form the isoxazole ring-fused quinone. The TBS group of the isoxazole quinone derivative was deprotected to provide compound **143** (Fig. 35).

Swapnaja *et al.* (Swapnaja et al., 2016) introduced quinone into the isoxazole structure and obtained a series of compounds with good activity against the tested strains. Compounds **145** and **147** have good bacteriostatic activity. Compound **145** can inhibit *S. aureus* MTCC 96, MIC values of *B. subtilis* MTCC 121 and *Klebsiella planticola* MTCC 530 were 7.8, 3.9, and 7.8 mg/mL, and IC$_{50}$ values were 4.6, 2.2, and 3.5 μM, respectively. Compound **147** is associated with *S. aureus* MTCC 96, *S. aureus* MLS-16 MTCC 2940, MIC values of *B. subtilis* MTCC 121, and *Klebsiella planticola* MTCC 530 were 3.9, 3.9, 3.9, and 7.8 mg/mL, and IC$_{50}$ values were 1.9, 2.5, 2.8, and 5.1 μM, respectively.

Li *et al.* (Li et al., 2019) synthesized a series of sampangine derivatives containing isoxazole. 6, 7-Dihydrobenzo[*b*]thiophen-4(5*H*)-one was used as the starting material to obtain the intermediate (5-bromobenzo[*b*]thiophene-4,7-dione) via three steps. Then, the target compound was prepared by reacting the intermediate with propionaldehyde oxime through a [1 + 2] cycloaddition reaction in the presence of NaClO. Compound **148** has strong anti-fungal activity against *Cryptococcus neoformans* (*C. neoformans*) (MIC$_{80}$ = 0.031 μg/mL) higher than that of fluconazole (MIC$_{80}$ = 2 μg/mL) and voriconazole (MIC$_{80}$ = 0.12 μg/mL). Furthermore, compound **148** had a strong inhibitory effect on the important virulence factors (biofilm, melanin, and urease) of *C. neoformans*. The mechanism study showed that compound **148** could induce apoptosis of *C. neoformans* cells and keep the cell cycle in the G1/S phase. For the C$_3$ substituents of isoxazole, alkyl substitutions were more favorable for anti-cryptococcal activity than heterocyclic and substituted phenyl derivatives. Among these, ethyl substitution yielded the best results (Fig. 36).

Santos *et al.* (Santos et al., 2010) synthesized a series of naphtho[2,3-*d*]isoxazole-4,9-diones by reacting 2,3-dichloro-1,4-naphthoquinone with nitromethyl derivatives in the presence of a base. Furthermore, they conducted an evaluation on the antifungal activity exhibited by these compounds. The MIC$_{50}$ values of compound **149** for *Candida parapsilosis* PYCC 2545 and *Candida glabrata* PYCC 2418T were as low as 0.2 μg/mL. The MIC$_{50}$ values of compound **150** for *C. albicans* PYCC 3436 and *C. parapsilosis* PYCC 2545 were 0.2 and 0.3 μg/mL.

Rajanarendar *et al.* (Rajanarendar et al., 2013) synthesized a series of isoxazole-indole-triones and evaluated the anti-inflammatory and analgesic activities of the resulting compounds. Compounds **151**–**153** exhibit significant anti-inflammatory activity by reducing the volume of foot PAWS produced by carrageenan. Compounds **151**–**153** significantly reduced the number of twists in mice and showed significant analgesic activity.

Uysal *et al.* (Uysal et al., 2021) designed and synthesized a series of novel 4-aminobenzenesulfonamide/carboxamide derivatives containing naphthoquinone pharmacophore, and evaluated their proteasomal inhibitory and anti-proliferative activities against the MCF-7. Compound **154** containing isoxazole showed significant inhibitory activity against the MCF-7 cell line with IC$_{50}$ of 10.15 μM. Compound **154** showed some inhibitory activity in ChT-L (β5), C-L (β1), and T-L (β2) of proteasome at a concentration of 10 μM, with inhibition rates of 18.89 %, 8.39 %, and 6.55 %.

Lawrence *et al.* (Lawrence et al., 2010) synthesized isoxazole-containing compounds **155** and **156** and tested their inhibition of T-L and peptidyl glutamyl peptide hydrolase (PGPH). Compounds **155** and **156** significantly inhibited the activity of three proteasomes (CT-L, T-L, and PGPH), and the combined IC$_{50}$ values of **155** for CT-L and T-L were 3.9 and 9.25 μM. The IC$_{50}$ value of compound **156** for PGPH was 16.7 μM (Fig. 37).

Yang *et al.* (Yang et al., 2011) synthesized a series of rhein derivatives and determined their cytotoxicity to HeLa and MOLT4 cell lines by the MTT assay. Rhein derivative **157** containing isoxazole showed inhibitory effects on HeLa and MOLT4 cell lines with IC$_{50}$ values of 16 and 14 μM. More than emodin activity (HeLa: IC$_{50}$ > 100 μM; MOLT4: IC$_{50}$ = 37 μM).

Lee *et al.* (Lee et al., 2012) synthesized a series of 1,2-diaminoquinone derivatives and evaluated drug-induced cytotoxicity by SRB assay. The IC$_{50}$ value of compound **158** containing isoxazole against the PC-3 cell line was 3.78 μM (Fig. 38).

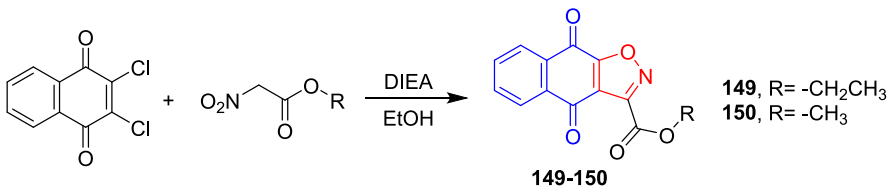

Comp.	MIC$_{50}$ μg/mL (μM)					
	C. albicans ATCC 90028	*C. albicans* PYCC 3436T	*C. krusei* PYCC 3341	*C. parapsilosis* PYCC 2545	*C. parapsilosis* ATCC 22019	*C. glabrata* PYCC 2418T
149	3.1 (11.5)	0.5 (1.8)	0.6 (2.3)	0.2 (0.6)	0.5 (1.7)	0.2 (0.6)
150	3.1 (12.2)	0.2 (0.7)	0.6 (2.4)	0.3 (1.3)	0.5 (1.8)	0.7 (2.6)
Amphotericin B	1.1 (1.2)	0.5 (0.5)	0.9 (1.0)	0.4 (0.5)	0.4 (0.5)	0.3 (0.4)

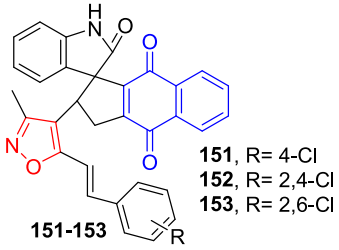

Anti-inflammatory activity

Comp.	Paw volume (mL of Hg)				
	0 h	1 h	2 h	4 h	6 h
151	0.27	0.54	0.69	0.65	0.41
152	0.25	0.57	0.71	0.54	0.32
153	0.27	0.54	0.70	0.67	0.40
Control	0.36	0.90	1.07	1.2	0.96
Ibuprofen	0.30	0.66	0.70	0.60	0.40

Analgesic activity

Comp.	No. of writhings	% inhibition
151	21.5	50.41
152	20.4	44.80
153	22.88	48.30
Control	41	-
Diclofenac	19	53.65

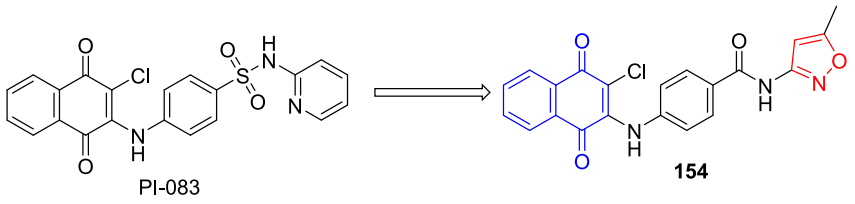

Cytotoxicity

Comp.	IC$_{50}$ (μM)
	MCF-7
154	10.15
PI-083	1.96
Doxorubicin	0.93

20S proteasome β5, β1 and β2 subunits inhibition

Comp.	Inhibition % (10 μM)		
	ChT-L (β5) activity	C-L (β1) activity	T-L (β2) activity
154	18.89	8.36	6.55
PI-083	36.76	18.81	29.59
Doxorubicin	38.23	18.39	51.42

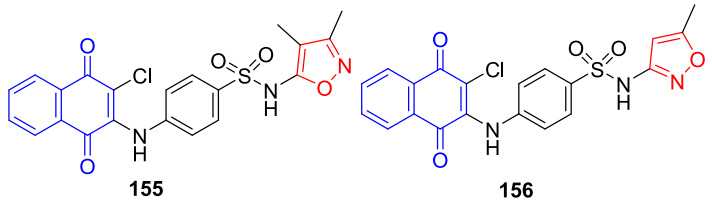

Comp.	*In vitro* IC$_{50}$ (μM)		
	CT-L activity	T-L activity	PGPH activity
Bortezomib	0.009	7.0	0.48
PI-083	1.0	4.5	4.5
155	3.9	9.2	21.2
156	11.2	13.2	16.7

Fig. 37. Naphthoquinone-isoxazole derivatives **149**–**156**.

Tyrosyl-DNA phosphodiesterase 2 (TDP2) is an enzyme that specifically repairs DNA damage mediated by topoisomerase II (TOP2). Yu *et al.* (Yu et al., 2018) report the synthesis of furoquinolinedione structure as a potential selective TDP2 inhibitor. Pharmacological experiments showed that compounds **159** and **160** were selective TDP2 inhibitors. The IC$_{50}$ of the recombinant TDP2 and TDP2 whole cell extract (WCE) was 1.9 and 2.1 μM, respectively.

Yang *et al.* (Yang et al., 2021) synthesized a series of isoxazolinequinolinedione derivatives based on the TDP2 inhibitors of furanoquinolinedione and isoxazolinedione, and conducted enzyme inhibition tests. Enzymatic analysis showed that compounds **161**–**170** exhibited high TDP2 inhibitory activity with IC$_{50}$ values ranging from 0.46 to 5.4 μM. The most potent compound **169**, showed the strongest inhibitory activity with an IC$_{50}$ of 0.46 μM (Fig. 39).

Combrink *et al.* (Combrink et al., 2007) designed and synthesized a series of 3-morpholino rifamycins and evaluated their antimicrobial activity. Compounds **171** and **172** containing isoxazole showed significant inhibitory activity against the *M. smegmatis* strain 43756Km1 with MIC values of 0.12 and 0.5 μM. It also showed significant inhibitory activity in *M. smegmatis* DSM 43756 with MIC values of 0.12 and 0.5 μM.

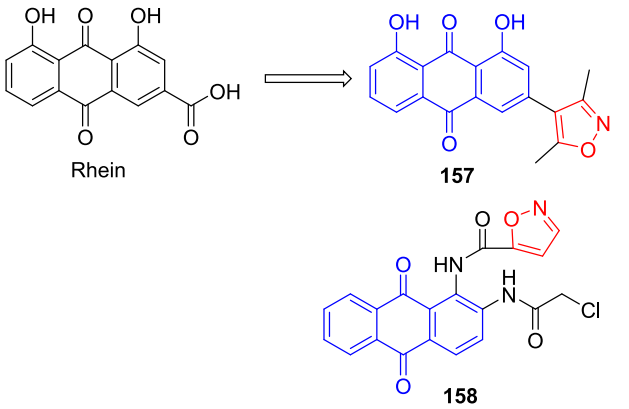

Comp.	Cytotoxicity IC_{50} (μM)	
	HeLa	MOLT4
Rhein	>100	37
157	16	14

Comp.	Cytotoxicity IC_{50} (μM)
	PC3
158	3.78
Mitoxantrone	0.29
Doxorubicin	0.25

Fig. 38. Anthraquinone-isoxazole derivatives **157**–**158**.

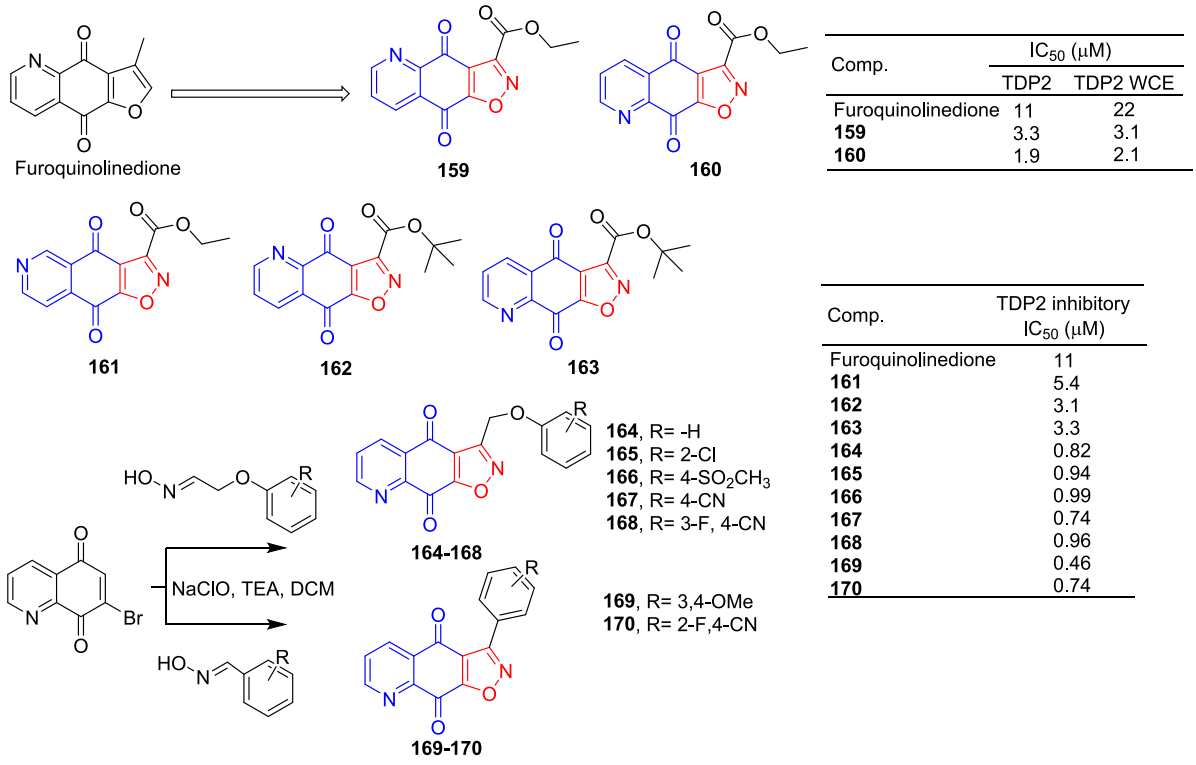

Comp.	IC_{50} (μM)	
	TDP2	TDP2 WCE
Furoquinolinedione	11	22
159	3.3	3.1
160	1.9	2.1

Comp.	TDP2 inhibitory IC_{50} (μM)
Furoquinolinedione	11
161	5.4
162	3.1
163	3.3
164	0.82
165	0.94
166	0.99
167	0.74
168	0.96
169	0.46
170	0.74

Fig. 39. Naphthoquinone-isoxazole derivatives **159**–**170**.

Compound **172** pairs of wild-type *E. coli* (DH5) pCTF104 (Arr-2^{+}), *E. coli* wild-type (DH5α) pCTF104 (Arr-2^{-}), *E. coli*-CGSC$^{\#}$ 5163 lpxC101 'leaky' strain (Arr-2^{+}), and *E. coli*-CGSC$^{\#}$ 5163 lpxC101 'leaky' strain (Arr-2^{-}) showed significant inhibitory activity, MIC values are 4, 4, 2 and 2 μM. Compound **171** for the *E. coli*-CGSC$^{\#}$ 5163 lpxC101 'leaky' strain (Arr-2^{+}), and the *E. coli*-CGSC$^{\#}$ 5163 lpxC101 'leaky' strain (Arr-2^{-}) showed significant inhibitory activity with MIC values of 2 and 1 μM.

Bargiotti *et al.* (Bargiotti et al., 2012) synthesized a series of 3-aryl-naphthalene (El-Garhy, 2015; Zhu et al., 2018)isoxazoles. Compounds were synthesized by reacting various naphthoquinones with in situ generated nitrile oxides, obtained through the treatment of corresponding oximes with triethylamine and aqueous NaClO in dichloromethane. These compounds were subsequently evaluated for their binding affinity to heat shock protein 90 and their antiproliferative activity against multiple human tumor cell lines (NCI-H460, A431, and STO). Compounds **173**–**184** have strong binding to Hsp90, with IC_{50} ranging from 0.031 to 0.77 μM. Compound **185**, which contains a polar hydrophilic compound, exhibits the strongest affinity for Hsp90 with $IC_{50} < 0.005$ μM. Complexes **182** and **185** down-regulated the Hsp90 client proteins EGFR, Akt, Cdk4, Raf-1, survivin, and up-regulated Hsp70. Furthermore, the combination of **173**–**185** showed significant inhibitory effects on a variety of cancer cells (Fig. 40).

Summary: In this section, the hybrid natural products of benzoquinone-isoxazole, naphthoquinone-isoxazole, and anthraquinone-isoxazole were reviewed. These compounds mainly have anti-tumor, anti-inflammatory, and antimicrobial activities. The biological activities of benzoquinone and anthraquinone natural products after hybridization with isoxazole were not significantly improved compared to their lead compounds or positive control drugs.

TDP2 has the potential to be a new target for the development of anti-viral drugs. Among the naphthoquinone-isoxazole derivatives, furanoquinolinedione deserves to be developed. After replacing furan with isoxazole as bioisosteres, the inhibitory activity of these compounds (**159**–**170**) against TDP2 was significantly improved. Similarly, compounds **173**–**185** showed strong anti-tumor activity *in vitro* as a novel series of Hsp90 inhibitors. The inhibitory effect of **182** on the

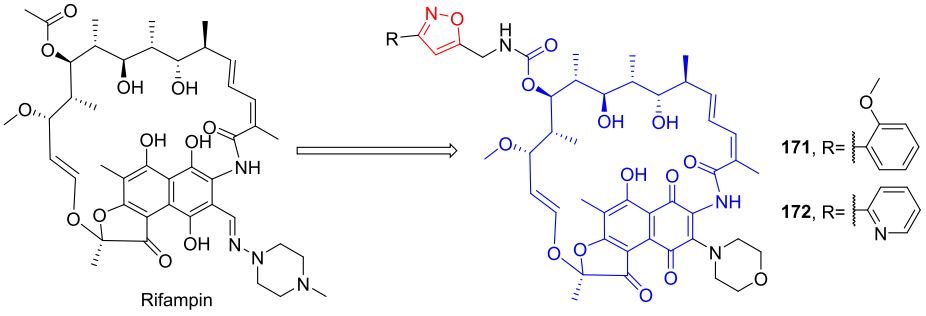

Comp.	MIC in μg/mL or ratio of MICs (Ribosylase$^+$/Ribosylase$^-$) for:										
	S. aureu		*Mycobacterium smegmatis*			*Escherichia coli* wild-type (DH5α)			*E. coli-CGSC*# 5163 *lpxC101 'leaky' strain*		
	ATCC# 29213 Wt (Rif-sensitive)	ATCC# 29213 *rpoB*^{H481Y} (Rif-resistant)	DSM 43756 (Arr-1$^+$)	43756Km1 (Arr$^-$)	Ratio of MICs	pCTF104 (Arr-2$^+$)	pCTF104 (Arr-2$^-$)	Ratio of MICs	pCTF104 (Arr-2$^+$)	pCTF104 (Arr-2$^-$)	Ratio of MICs
Rifampin	0.008	>63	32	0.5	64	>250	8	>32	8	0.24	32
171	0.06	NTb	0.12	0.12	1	>250	> 250	-	2	1	2
172	0.008	>63	0.5	0.5	1	4	4	1	2	2	1

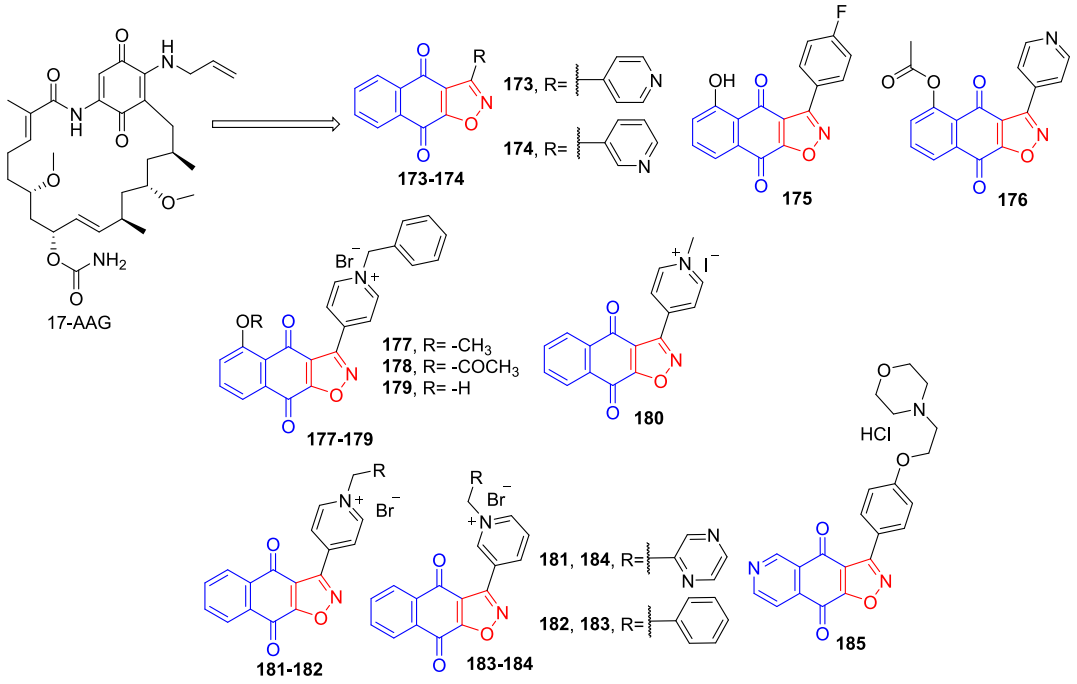

Comp.	IC_{50} (μM)			
	Binding Hsp90 (FP)	NCI-H460	STO	A431
17-AAG	1.095	0.010	-	0.069
173	0.39	0.14	0.011	0.056
174	0.54	0.062	0.04	0.043
175	0.29	0.124	0.61	0.29
176	0.084	0.15	0.150	0.06
177	0.34	0.18	0.168	0.168
178	0.031	>1	3.96	3.96
179	0.098	0.88	21.56	21.6
180	0.63	0.33	1.20	0.48
181	0.68	0.017	0.22	0.052
182	0.034	0.018	0.0022	0.0016
183	0.77	0.021	0.01	0.020
184	0.51	0.046	0.11	0.042
185	<0.005	0.041	0.054	0.02

Fig. 40. Naphthoquinone-isoxazole derivatives **171**–**185**.

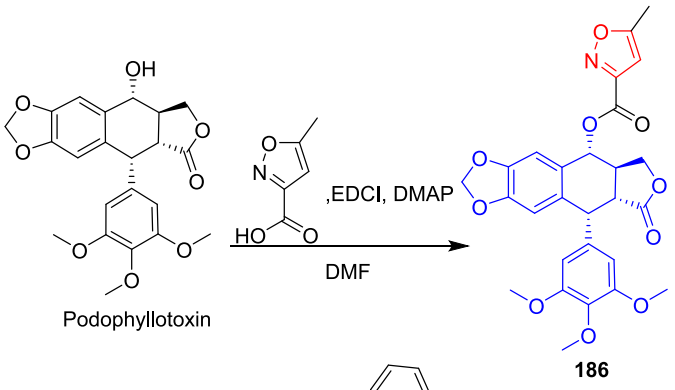

Anti-tumor activity

Comp.	IC_{50} (μM)		
	K562/ADR	K562	RF
186	0.052	0.025	2.080
Etoposide	2.211	0.345	6.408
Doxorubicin	18.779	0.220	85.359

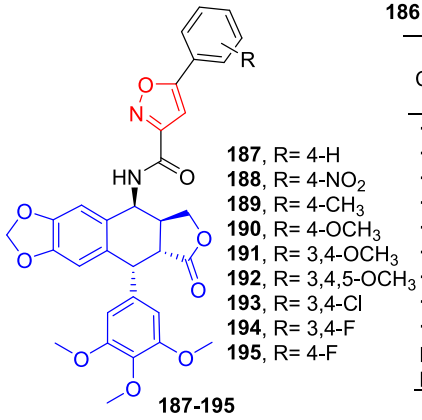

187, R= 4-H
188, R= 4-NO_2
189, R= 4-CH_3
190, R= 4-OCH_3
191, R= 3,4-OCH_3
192, R= 3,4,5-OCH_3
193, R= 3,4-Cl
194, R= 3,4-F
195, R= 4-F

Anti-tumor activity

Comp.	IC_{50} (μM)				
	A549	HT-29	ACHN	B-16	HeLa
187	13.6	19.5	17.5	16.3	5.9
188	17.9	22.6	26.4	16.8	7.5
189	24.7	27.9	28.5	20.3	5.26
190	38.1	32.1	30.3	22.5	11.2
191	23.1	38.4	23.1	12.7	13.3
192	19.8	25.1	34.2	23.4	18.4
193	31.07	11.2	16.8	22.7	12.6
194	12.7	14.1	16.4	27.5	21.2
195	20.6	19.9	15.6	23.5	16.6
Etoposide	2.8	1.81	7.61	1.39	1.52
Podophyllotoxin	3.6	1.02	2.3	2.5	2.8

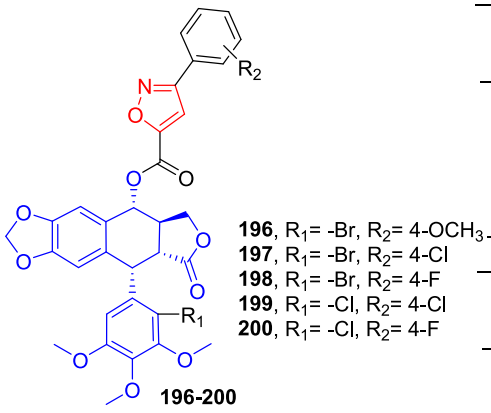

196, R_1= -Br, R_2= 4-OCH_3
197, R_1= -Br, R_2= 4-Cl
198, R_1= -Br, R_2= 4-F
199, R_1= -Cl, R_2= 4-Cl
200, R_1= -Cl, R_2= 4-F

Against the pre-third-instar larvae of *M. separata*

Comp.	1 mg/mL Corrected mortality rate (%)		
	15 days	25 days	35 days
Podophyllotoxin	16.7	27.6	34.5
196	33.3	41.4	48.3
197	36.7	48.3	55.2
199	36.7	44.8	69.0
200	46.7	55.2	62.1
Toosendanin	23.3	41.4	51.7

Against the female adults of *T. cinnabarinus*

Comp.	0.5 mg/mL Corrected mortality rate (%)	
	15 days	35 days
Podophyllotoxin	2.3	4.8
196	9.8	35.4
197	12.4	38.0
199	17.5	41.1
200	9.7	32.8
Spirodiclofen	27.2	65.4

Fig. 41. Lignin-isoxazole derivatives **186**–**200**.

A431 cell line was the most obvious, with an IC_{50} value of 1.6 nM.

2.7. Lignin-isoxazole hybridization

Multidrug resistance (MDR) of anti-tumor drugs is a major obstacle to successful tumor treatment. Finding new drugs with anti-MDR activity is an effective way to overcome tumor resistance. Zhang *et al.* (Zhang et al., 2016) designed and synthesized a series of aromatic heterocyclic ester compounds of podophyllotoxin to evaluate their anticancer activity against two human chronic myeloid leukemia cell lines K562 and K562/ADR. Compound **186** with isoxazole showed significant inhibitory activity in K562 and K562/ADR cells with IC_{50} values of 0.052 and 0.025 μM, respectively. Anti-tumor activity was better than doxorubicin (K562: IC_{50} = 18.779 μM; K562/ADR: IC_{50} = 0.220 μM). The resistance factor (RF) value of compound **186** was 2.080, which was also better than doxorubicin (RF = 85.359).

Kamal *et al.* (Kamal et al., 2013) designed and synthesized a series of different hetero-aromatic linked 4β-aminopodophyllotoxin derivatives and evaluated their anti-tumor activity. Among them, the isoxazole-linked compound **187**–**195** showed inhibitory effects on A549, HT-29, ACHN, B-16, and HeLa cell lines, with IC_{50} values ranging from 5.26 to 38.4 μM. Among them, **187**–**189** showed obvious anti-proliferation activity against HeLa cell lines with IC_{50} values of 5.9, 7.5, and 5.26 μM.

Yang *et al.* (Yang et al., 2021) designed and synthesized a series of podophyllotoxin derivatives containing isoxazole and evaluated their insecticidal activity. Compounds **196**–**198** showed significant growth inhibition effects on *Mythimna separata* (*M. separata*), with final fatality rates of 65.5 %, 69.0 %, and 62.1 %, respectively. Toosendanin and podophyllotoxin were superior to positive controls (34.5 %). Podophyllotoxin has acaricidal activity that is close to zero for *Tetranychus cinnabarinus* (*T. cinnabarinus*), while its isoxazole derivative has acaricidal activity higher than podophyllotoxin. The MRS values of **197**–**200**

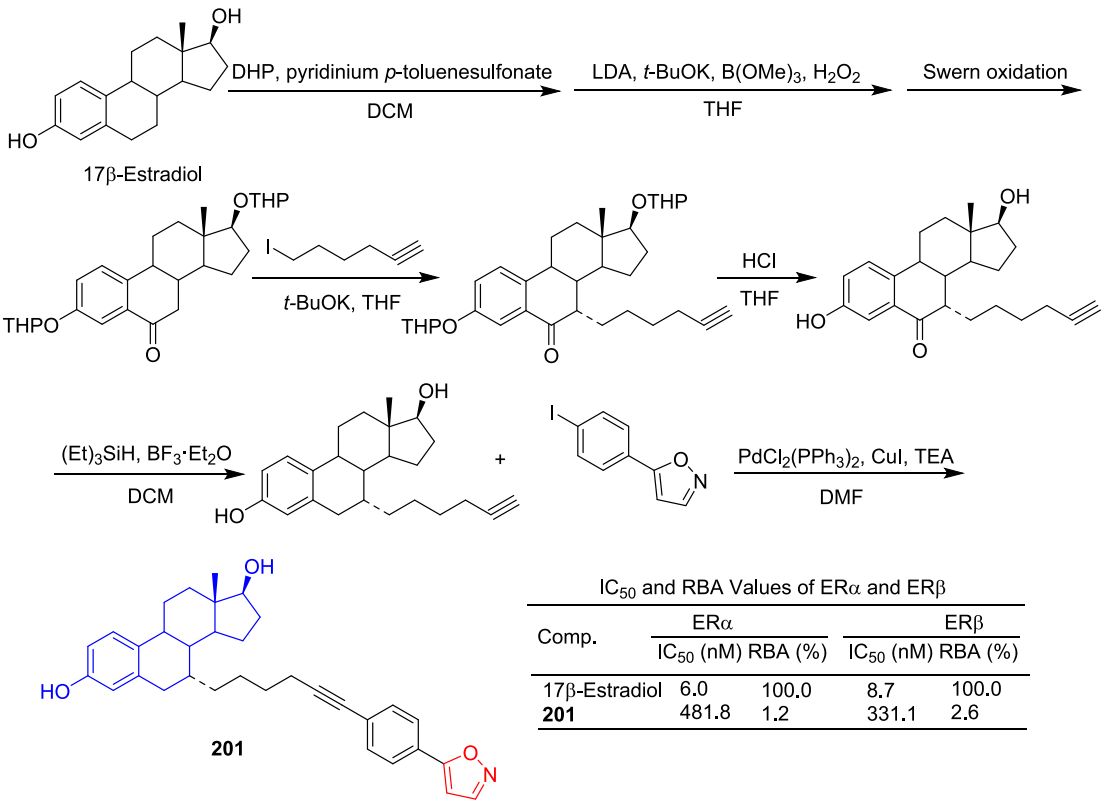

IC_{50} and RBA Values of ERα and ERβ

Comp.	ERα		ERβ	
	IC_{50} (nM)	RBA (%)	IC_{50} (nM)	RBA (%)
17β-Estradiol	6.0	100.0	8.7	100.0
201	481.8	1.2	331.1	2.6

Fig. 42. Steroidal-isoxazole derivative **201**.

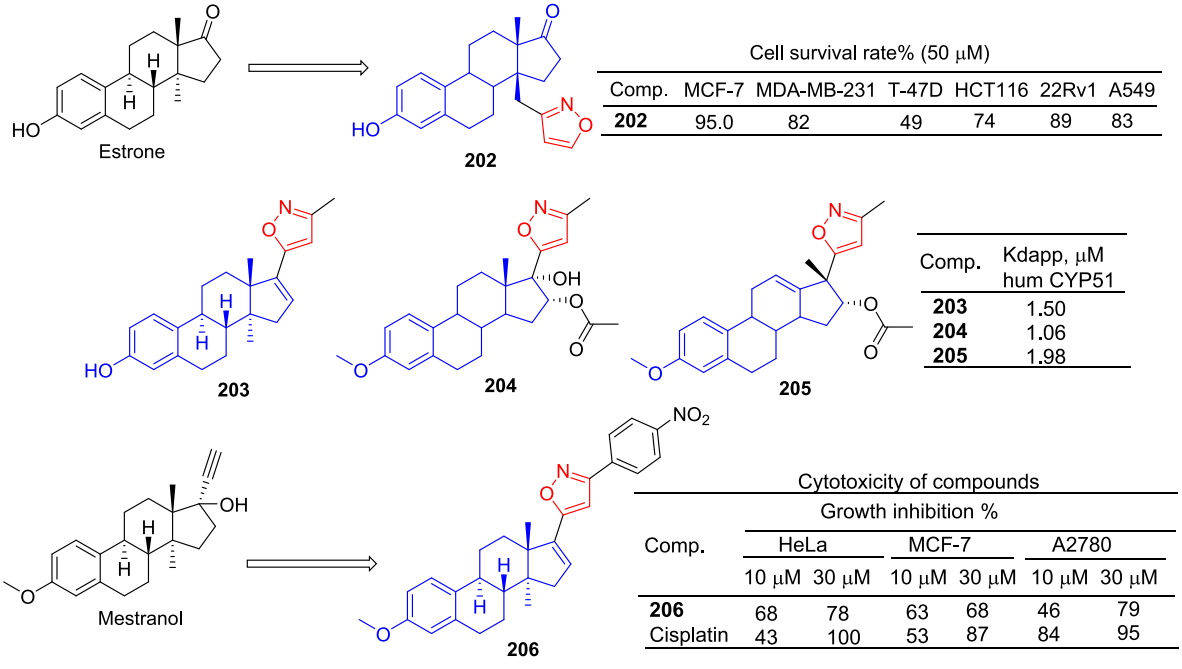

Cell survival rate% (50 μM)

Comp.	MCF-7	MDA-MB-231	T-47D	HCT116	22Rv1	A549
202	95.0	82	49	74	89	83

Comp.	Kdapp, μM hum CYP51
203	1.50
204	1.06
205	1.98

Cytotoxicity of compounds

Comp.	Growth inhibition %					
	HeLa		MCF-7		A2780	
	10 μM	30 μM	10 μM	30 μM	10 μM	30 μM
206	68	78	63	68	46	79
Cisplatin	43	100	53	87	84	95

Fig. 43. Steroidal-isoxazole derivatives **202**–**206**.

at 72 h were 35.4 %, 38.0 %, 41.1 %, and 32.8 %, respectively. Therefore, compounds **199** and **200** showed the strongest insecticidal activity against *Mythimna separata Walker* and *Tetranychus cinnabarinus Boisduval* (Fig. 41).

Summary: There are few natural products of lignin-isoxazole hybridization. Only podophyllotoxin derivatives have been reported, which have anti-tumor and insecticidal activities. The introduction of 5-methylisoxazole to the hydroxyl group of podophyllotoxin can significantly improve its anti-tumor activity *in vitro*, but the introduction of 5-phenylisoxazole can reduce its anti-tumor activity. Interestingly, the introduction of 5-phenylisoxazole increased the insecticidal activity of podophyllotoxin.

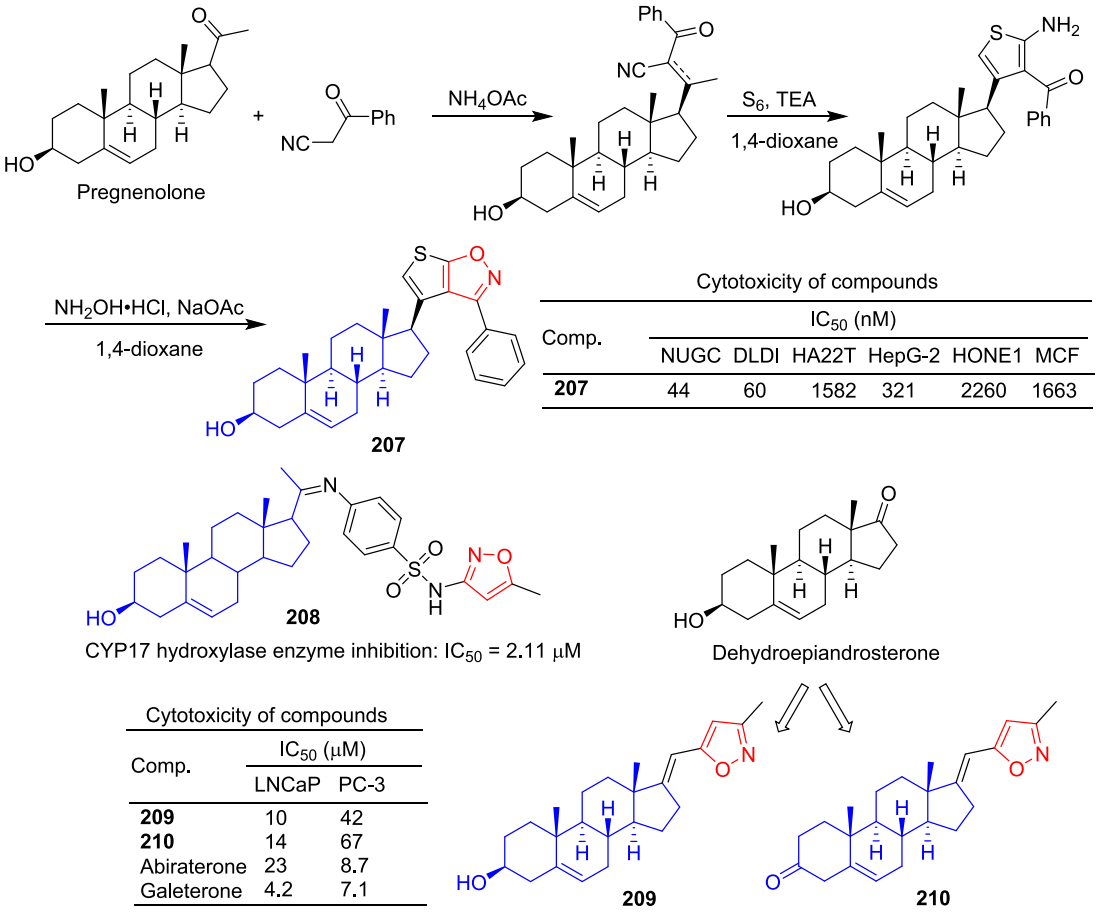

Cytotoxicity of compounds

Comp.	IC50 (nM)					
	NUGC	DLDI	HA22T	HepG-2	HONE1	MCF
207	44	60	1582	321	2260	1663

Cytotoxicity of compounds

Comp.	IC50 (μM)	
	LNCaP	PC-3
209	10	42
210	14	67
Abiraterone	23	8.7
Galeterone	4.2	7.1

Fig. 44. Steroidal-isoxazole derivatives **207**–**210**.

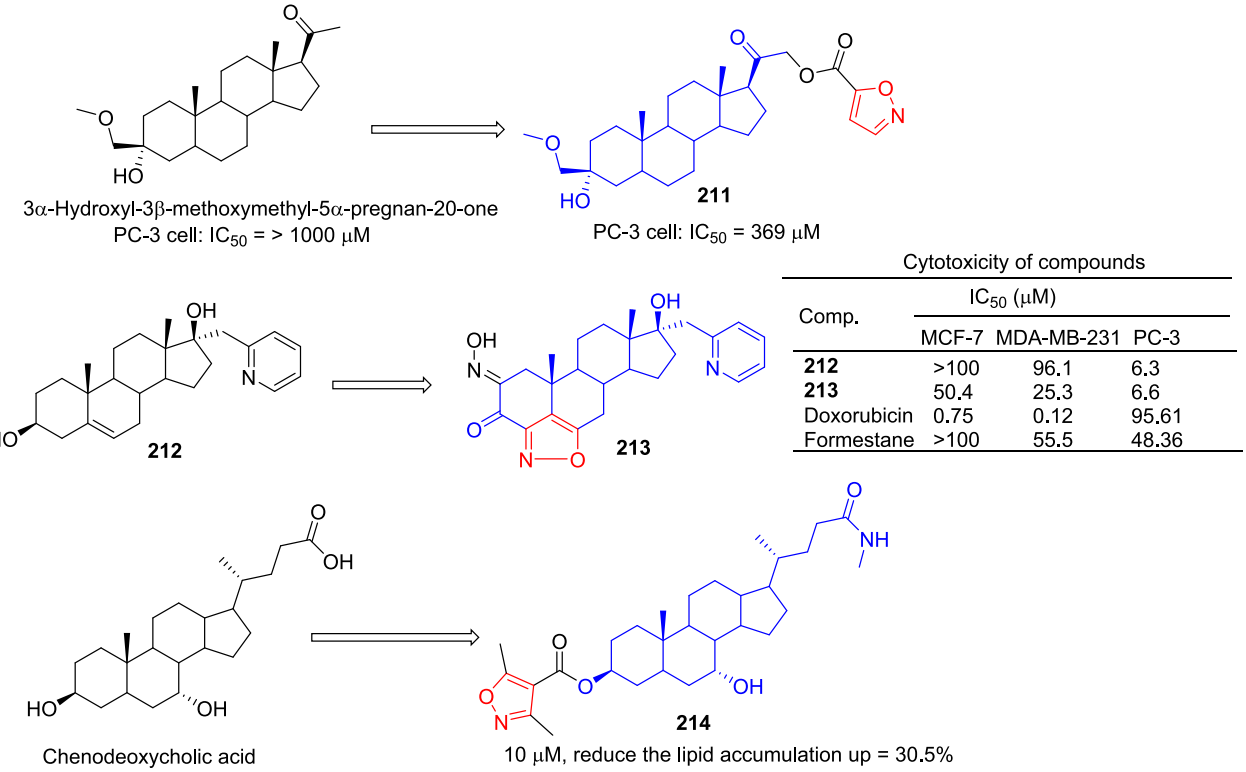

Cytotoxicity of compounds

Comp.	IC50 (μM)		
	MCF-7	MDA-MB-231	PC-3
212	>100	96.1	6.3
213	50.4	25.3	6.6
Doxorubicin	0.75	0.12	95.61
Formestane	>100	55.5	48.36

Fig. 45. Steroidal-isoxazole derivatives **211** and **213**–**214**.

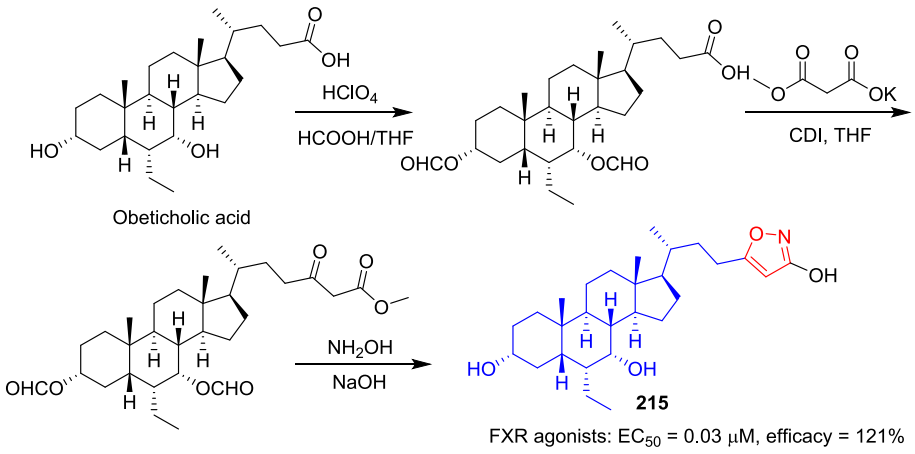

Fig. 46. Steroidal-isoxazole derivative **215**.

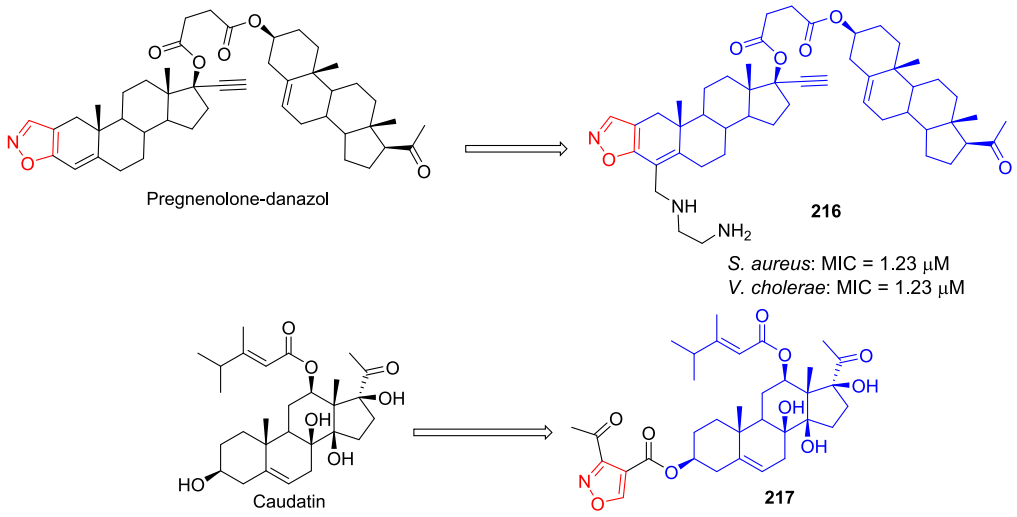

Comp.	HepG 2.2.15 cells CC_{50} (μM)	IC_{50} (μM)	
		HBsAg	DNA replication
Caudatin	244.58	142.67	40.62
217	132.72	201.23	16.97
Tenofovir	>1820.42	1446.35	0.77

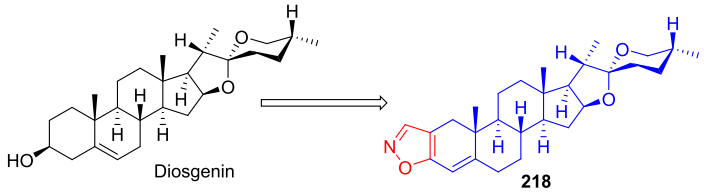

Comp.	IC_{50} (μM)		
	MCF-7	A549	MRC-5
218	9.15	14.92	>100
Diosgenin	26.91	36.21	100.7
Doxorubicin	9.78	16.90	0.12

Fig. 47. Steroidal-isoxazole derivatives **216**–**218**.

2.8. Steroidal-isoxazole hybridization

Jiang *et al.* (Jiang et al., 2013) designed and synthesized a series of 17β-estradiol derivatives that are linked to a large side chain at the C-7α position and determined their antagonistic activity of the endoplasmic reticulum by *in vitro* bioassays. Isoxazole-containing derivative **201** showed certain inhibition of ERα transfer activation activity in luciferase reporting experiments (ERα: IC_{50} = 481.8 nM, RBA = 1.2 %; and ERβ: IC_{50} = 331.1 nM, RBA = 2.6 %), and blocked the interaction between ERα and co-activators. Similarly, derivative **201** inhibited the growth of ERα-positive human breast cancer cells (Fig. 42).

Baranovsky *et al.* (Baranovsky et al., 2019) designed and synthesized

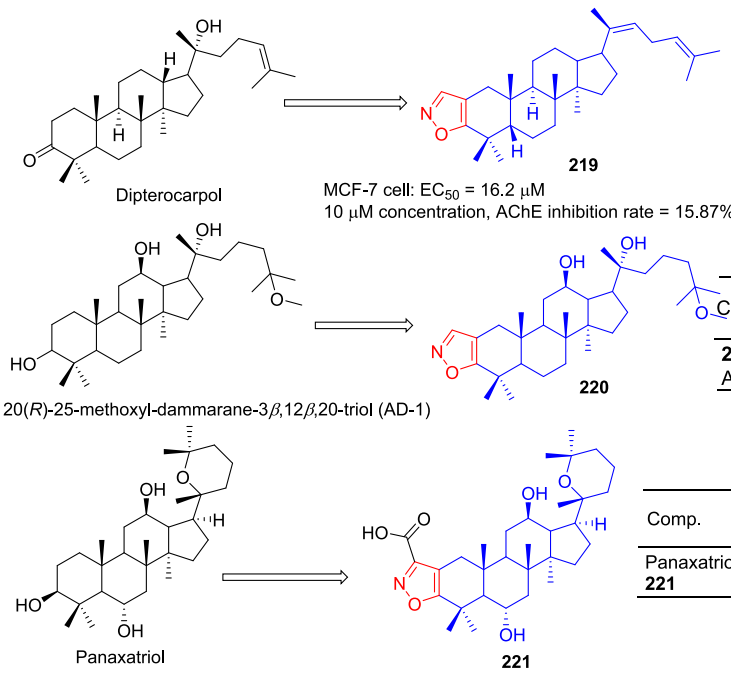

Comp.	IC$_{50}$ (μM)		
	RM-1	HCT116	GES-1
220	14.38	19.55	>100
AD-1	24.37	19.46	92.23

Comp.	Cell viability (% of control)			
	0 μM	0.1 μM	1.0 μM	10 μM
Panaxatriol	45.0	47.8	52.3	61.9
221	44.4	68.2	79.2	89.2

Fig. 48. Steroidal-isoxazole derivatives **219**–**221**.

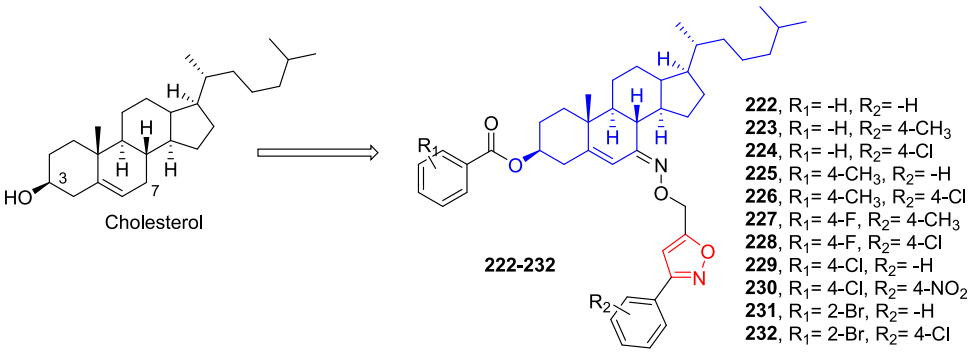

Against *M. separata* at a Concentration of 1 mg/mL

Comp.	corrected mortality rate (%)		
	10 days	25 days	35 days
223	40.7	48.1	51.8
224	44.4	59.2	66.6
225	25.9	44.4	55.5
229	33.3	40.7	48.1
231	37.0	48.1	55.5
232	14.8	37.0	48.1
Toosendanin	22.2	29.6	40.7

Against *P. xylostella* Treated at 20 μg/larva

Comp.	corrected mortality rate (%)	
	24 h	48 h
222	24.4	33.3
223	13.3	26.6
224	17.7	42.2
226	26.6	31.1
228	24.4	26.6
229	15.5	28.8
Toosendanin	15.5	53.3

Against Apterous Adults of *A. citricola* Treated at 0.04 μg/nymph

Comp.	corrected mortality rate (%)	
	24 h	48 h
223	13.8	40.3
224	18.4	41.4
227	13.8	38.0
230	4.6	55.2

LD$_{50}$ Values of Compounds at 48 h against *A. citricola*

Comp.	LD$_{50}$ (μg/nymph)
Cholesterol	0.237
230	0.041

Control Efficiency of Compounds against *A. citricola* in the Greenhouse Tests at 1.0 mg/mL

Comp.	control efficiency (%)			
	first day	third day	fifth day	seventh day
Cholesterol	3.9	9.5	14.5	18.1
230	8.3	40.3	54.5	59.8

Fig. 49. Steroidal-isoxazole derivatives **222**–**232**.

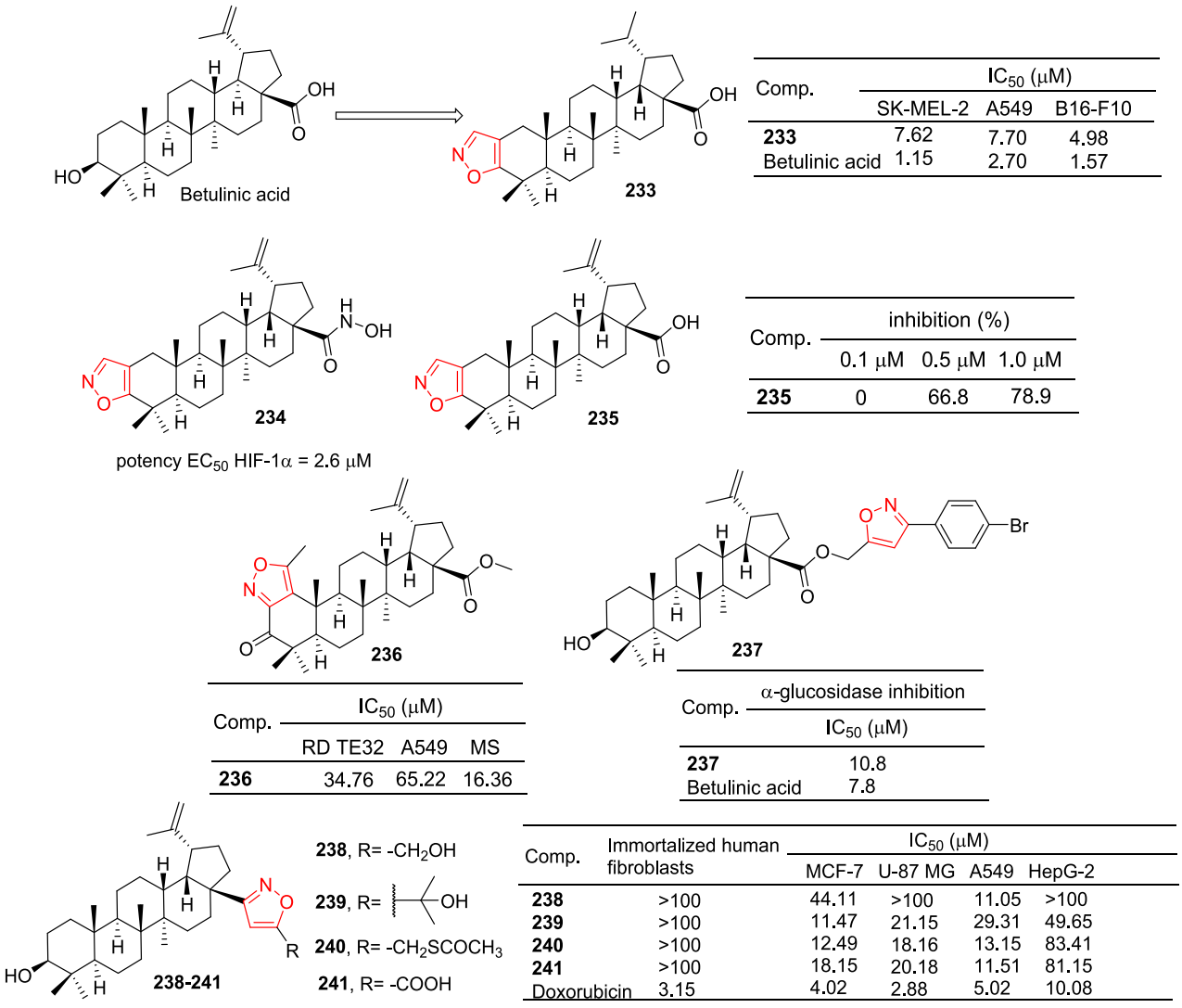

Comp.	IC50 (μM)		
	SK-MEL-2	A549	B16-F10
233	7.62	7.70	4.98
Betulinic acid	1.15	2.70	1.57

Comp.	inhibition (%)		
	0.1 μM	0.5 μM	1.0 μM
235	0	66.8	78.9

Comp.	IC50 (μM)		
	RD TE32	A549	MS
236	34.76	65.22	16.36

Comp.	α-glucosidase inhibition
	IC50 (μM)
237	10.8
Betulinic acid	7.8

Comp.	Immortalized human fibroblasts	IC50 (μM)			
		MCF-7	U-87 MG	A549	HepG-2
238	>100	44.11	>100	11.05	>100
239	>100	11.47	21.15	29.31	49.65
240	>100	12.49	18.16	13.15	83.41
241	>100	18.15	20.18	11.51	81.15
Doxorubicin	3.15	4.02	2.88	5.02	10.08

Fig. 50. Pentacyclic triterpenoids-isoxazole derivatives **233**–**241**.

a steroid derivative containing isoxazole at site C-14. Compound **202** showed a certain inhibitory effect on the T-47D cell line, and the cell survival rate decreased to 49 % at a concentration of 50 μM.

A series of isoxazolyl steroid derivatives synthesized by Baranovsky *et al.* (Baranovsky et al., 2021). Compounds **203**–**205** were found to have strong binding ligands to human CYP51 in the micromolar range, with Kdapp of 1.50, 1.06, and 1.98 μM, respectively.

Kovacs *et al.* (Kovacs et al., 2012) prepared novel 17-*exo*-isoxazolyl derivatives by a "click" chemical method. The derivatives were screened *in vitro* to detect their anti-proliferative activity against three human cancer cell lines (HeLa, MCF-7, and A2780). Compound **206** showed a certain inhibitory effect on HeLa, MCF-7, and A2780 at a concentration of 10 μM, with inhibition rates of 68 %, 63 %, and 46 %, respectively (Fig. 43).

Mohareb *et al.* (Mohareb et al., 2013) introduced various heterocycles in the C-17 position of the pregnenolone skeleton to obtain a series of derivatives and evaluated the cytotoxicity of some cancer cells. Compound **207**, which introduced isoxazole, had the strongest killing effect on NUGC and DLDI cell lines with IC_{50} values of 44 and 60 nM, respectively, and there was no toxicity against normal fibroblast cells. The synthesis route is depicted in Fig. 44. Firstly, the reaction between pregnenolone and 3-oxo-3-phenylpropanenitrile in the presence of ammonium acetate yielded the Knoevenagel condensation intermediate. Then, this intermediate was reacted with elemental sulfur and a catalytic amount of triethylamine to afford the thiophene derivative. Finally, the compound **207** was obtained by reacting the thiophene derivative with hydroxylamine hydrochloride in 1,4-dioxane containing sodium acetate.

Al-Masoudi *et al.* (Al-Masoudi et al., 2015) synthesized a series of pregnenolone analogues having aryl-imino groups at C-20 and evaluated the inhibitory activity of human CYP17 hydroxylase expressed in *E. coli*. Compound **208** was the most potent in the series with an IC_{50} of 2.11 μM. However, the activity was inferior to that of abiraterone acetate (IC_{50} = 0.072 μM).

Dalidovich *et al.* (Dalidovich et al., 2019) prepared isoxazole derivatives of [17(20)*E*]-21-norpregnene. The ability of the synthesized compound to inhibit the growth of prostate cancer cells was investigated. Among them, compounds **209** and **210** showed high inhibitory effects on LNCaP and PC-3 cell lines, with IC_{50} values ranging from 10–67 μM. The results also indicated that oxidation of the C_3 hydroxyl group did not enhance the antiproliferative activity of prostate cancer cells.

Tsai *et al.* (Tsai et al., 2017) designed and synthesized a series of steroid derivatives with C-21 hydrophilic substituents. Isoxazol-containing derivative **211** showed a weak inhibitory effect on PC-3 cells with an IC_{50} of 369 μM.

Ajdukoviic *et al.* (Ajdukovic et al., 2015) evaluated the potential antitumor activity of different a-modified 17α-picolyl and 17(*E*)-

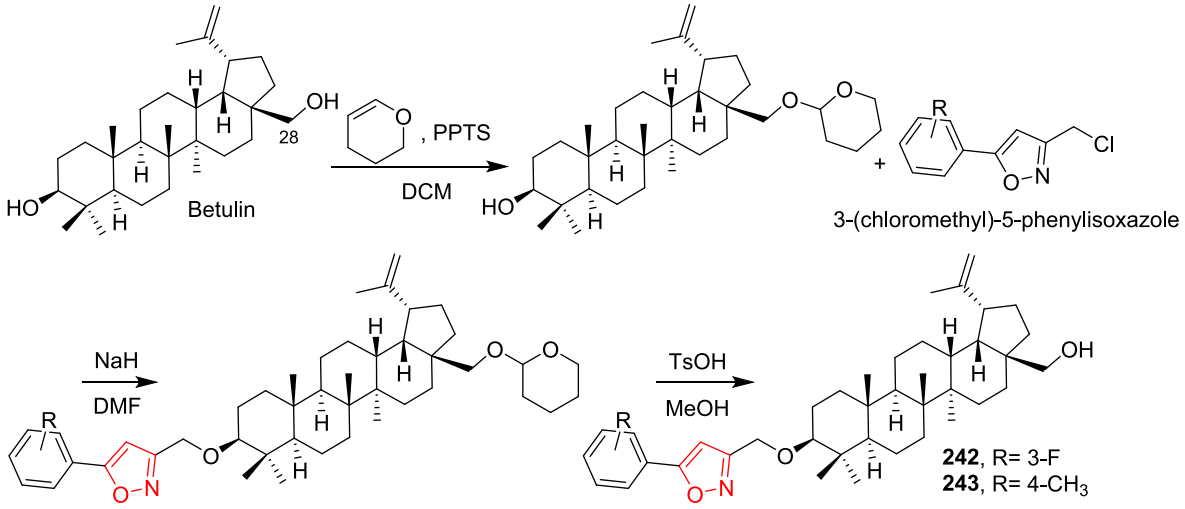

Comp.	IC50 (μM)		PTP1B/TCPTP
	PTP1B	TCPTP	
242	1.62	8.51	5.25
243	0.98	3.88	3.95
Betulin	11.72	-	-
Oleanolic acid	2.67	5.98	2.2

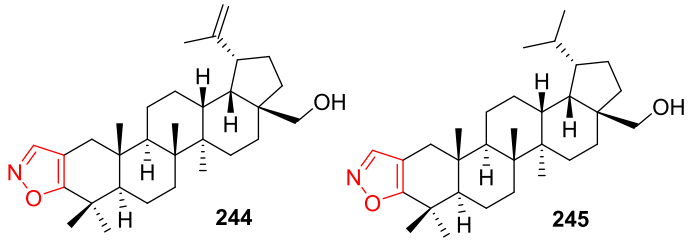

Comp.	IC50 (μM)						
	SK-MEL-2	A-375	DAOY	LN-229	OVCAR-3	HT-29	MCF-7
Betulinic acid	33	51	31	61	59	37	50
244	8	-	8	>75	60	10	25
245	8	10	7	75	75	75	>75

Fig. 51. Pentacyclic triterpenoids-isoxazole derivatives **242**–**245**.

picolinylidene androstane derivatives. The results of the 48 h *in vitro* experiment showed that compound **213** had the strongest inhibitory effect on PC-3 (IC_{50} = 6.6 μM).

Qiu *et al.* (Qiu et al., 2018) designed and synthesized a series of isoxazole-chenodeoxycholic acid hybrids and evaluated the lipid-lowering ability of the compounds using a 3T3-L1 adipocyte model. Compound **214** showed a significant lipid-lowering effect, reducing fat accumulation by 30.5 % at 10 μM. Pharmacological mechanism studies have shown that **214** blocks lipid accumulation by activating the FXR-SHP signaling pathway and effectively down-regulates the expression of the key lipogenesis regulator SREBP-1c (Fig. 45).

Obticholic acid is a Farnesoid X receptor (FXR) agonist that has entered a Phase III clinical trial in patients with nonalcoholic steatohepatitis (NASH). Xiao et al. obtained a series of derivatives based on obeticholic acid modified at C_{24}, in hopes of developing FXR agonists with higher selectivity. The derivative **215** (EC_{50} = 0.03 μM, efficacy = 121 %) linked to C_3-OH isoxazole shows a strong affinity for FXR (Xiao et al., 2017). The synthesis route is depicted in Fig. 46. The starting material, obticholic acid, was subjected to oxidation, condensation, decarboxylation, and cyclization reactions to yield compound **215**.

Figueroa-Valverde *et al.* (Figueroa-Valverde et al., 2011) synthesized the pregnenolone-danazol-ethylenediamine conjugate, and the antibacterial activity against *S. aureus* and *Vibrio cholerae* was tested. The bioactivity results showed that compound **216** inhibited the growth of both bacteria in a dose-dependent manner, with MIC values of 1.23 μM for *S. aureus* and *V. cholerae*.

Wang *et al.* (Wang et al., 2012) designed and synthesized a series of caudatin derivatives and detected their anti-hepatitis B virus (HBV) activity in HepG-2.2.15 cells. Compound **217** containing isoxazole showed inhibitory activity against HBV DNA replication with IC_{50} of 16.97 μM. Additionally, compound **217** inhibited HBsAg secretion to some extent (IC_{50} = 201.23 μM).

Yildiz *et al.* (Erdagi and Yildiz, 2022) modified diosgenin to obtain a series of derivatives and evaluated the cytotoxicity of these compounds in MCF-7 and A549. Compound **218** containing isoxazole showed stronger anti-tumor activity against MCF-7 and A549 cell lines with IC_{50} values of 9.15 μM and 14.92 μM, respectively, than diosgenin (IC_{50} values of 26.91 and 36.21 μM, respectively) (Fig. 47).

Smirnova *et al.* (Smirnova et al., 2020) designed and synthesized a series of dipterocarpus alatus derivatives and evaluated their cholinesterase inhibitory activity and cytotoxicity. Compound **219** containing isoxazole showed some cytotoxicity to the MCF-7 cell line (EC_{50} = 16.2 μM), and slightly inhibited AChE (15.87 %). There was no inhibitory effect on butyrylcholinesterase.

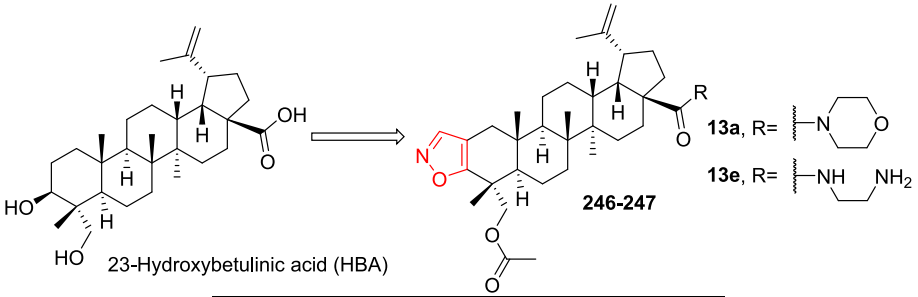

Comp.	IC$_{50}$ (μM)				
	HL-60	BEL-7402	SF-763	HeLa	B16
HBA	45.15	39.67	43.40	52.39	29.87
246	10.04	9.13	6.08	9.22	7.83
247	9.74	9.01	6.94	9.23	7.90
Doxorubicin	0.17	0.22	0.16	0.21	0.18

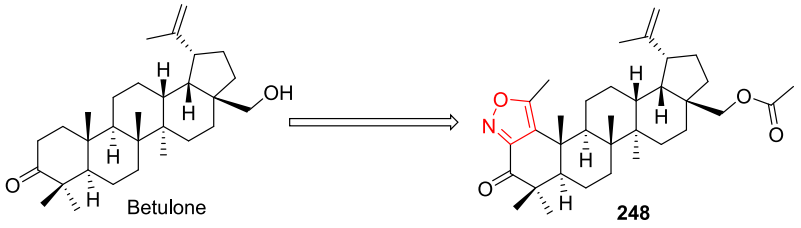

Comp.	IC$_{50}$ (μM)				
	RD TE32	A549	MS	HEp-2	HCT116
Betulone	13.25	32.94	18.22	22.48	34.03
248	14.77	7.85	14.00	22.07	19.01
Campthotecine	1.24	5.93	1.84	3.04	6.7

Fig. 52. Pentacyclic triterpenoids-isoxazole derivatives **246**–**248**.

20(*R*)-25-methoxyl-dammarane-3β,12β,20-triol (AD-1) is a newly discovered ginsenoside that induces G0/G1 cell cycle arrest, apoptosis, and ROS production. Ma *et al.* (Ma et al., 2021) obtained a series of AD-1 derivatives by introducing heterocyclic rings at the positions C-2 and C-3. The IC$_{50}$ values of the **220** isoxazole-containing derivative for the RM-1 and HCT116 cell lines were 14.38 and 19.55 μM. Compound **220** did not show obvious cytotoxicity to normal GES-1 cells (IC$_{50}$ > 100 μM).

To develop more effective anti-myocardial ischemia/reperfusion (MI/R) injury drugs, Wu *et al.* (Wu et al., 2020) designed and synthesized a series of heterocyclic panaxatriol fusion derivatives, and evaluated the cardiovascular activity of heterocyclic derivatives of panaxatriol. Compound **221** increased cell viability to approximately 88 % and 89.2 % at 10 μM. *In vivo*, captopril (20 mg/kg) and panaxatriol (40 mg/kg) reduced the size of the infarct by 34.0 % and 30.6 %, respectively. At a dose of 40 mg /kg, compound **221** reduced the size of the infarct to 20.5 %. Therefore, compound **221** can significantly reduce the size of the myocardial infarction, reduce the leakage of circulating cardiac troponin I (cTnI), and alleviate myocardial tissue injury (Fig. 48).

Xu *et al.* (Xu et al., 2021) designed and synthesized a series of cholesterol oxime ether derivatives containing isoxazole, and determined the agricultural activity of these compounds against *A. citricola*, *M. separata*, and *P. xylostella*. The control effect was tested in the greenhouse. Compounds **223**–**225** and **231**–**232** showed significant inhibitory effects on *M. separata*, with mortality rates (MRs) ranging from 48.1 % to 66.6 % after 35 days at a concentration of 1 mg/mL. Among them, compound **224** has the highest MRs against *M. separata*, reaching 66.6 %. The third instar larvae of *P. xylostella* were treated with 20 μg/larva compounds **222**–**224**, **226**, and **228**–**229** for 48 h. These compounds showed good insecticidal activity, with MRs ranging from 26.6 % to 42.2 %. Among them, compound **224** had the highest MR against *P. xylostella*, reaching 42.2 %. The insecticidal activity of *A. citricola* treated with 0.04 μg/larva for 48 h showed that the MR of compounds **223**, **224**, **227**, and **230** ranged from 38.0 % to 55.2 %. Among them, compound **230** had the highest MRs against *A. citricola*, reaching 55.2 %. The 48 h LD$_{50}$ value of compound **230** for *A. citricola* was 0.041 μg/nymph, while the cholesterol 48 h LD$_{50}$ value was 0.237 μg/nymph. Therefore, the aphid-killing activity of compound **230** is 5.8 times that of cholesterol. The control effect of compound **230** on *A. citricola* was tested in a greenhouse. The results showed that the control effects of **230** at 3, 5, and 7 days after treatment were 40.3 %, 54.5 %, and 59.8 %, respectively, while the corresponding cholesterol results were 9.5, 14.5 and 18.1 %, respectively. The results showed that the prophylactic effect of compound **230** was 3.3–4.2 times that of cholesterol (Fig. 49). Structure-activity relationships suggest that the C$_3$ hydroxyl group and the C$_7$ position of cholesterol are two important sites for modification.

Summary: In this section, the biological activities of various terpenoid natural products after hybridization with isoxazole molecules were reviewed, including estradiol, estrone, mestranol, pregnenolone, dehydroepiandrosterone, chenodeoxycholic acid, obeticholic acid, caudatin, diosgenin, dipterocarpol, panaxatriol, and cholesterol. Their semi-synthetic derivatives mainly have anti-tumor, antibacterial, anti-viral, lipid-lowering, anti-myocardial ischemia/reperfusion injury, and even agricultural activities. In anti-tumor activity, compound **207** showed good selectivity between tumor cells and normal cells. Compound **214** is valuable for further study in the treatment of hyperlipidemia. In addition, compared with panaxatriol, compound **221** can greatly improve the protective activity towards cardiomyocytes. The preliminary structure–activity relationship study suggested that fusing isoxazole can improve the activity of the parent compound.

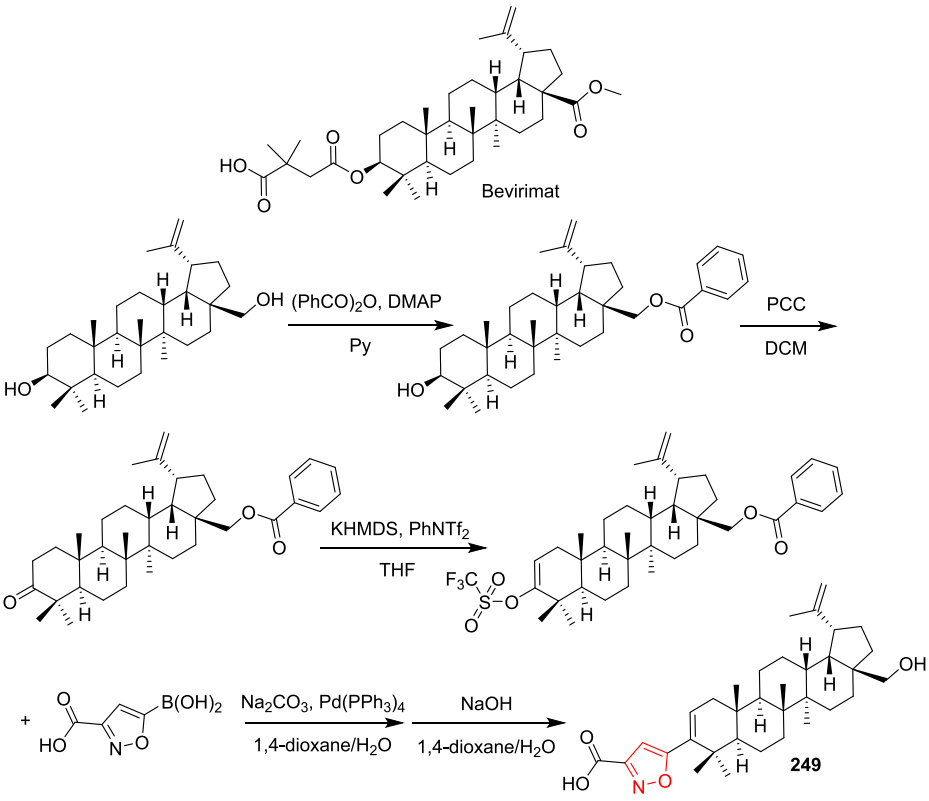

Comp.	WT HIV-1 inhibition EC_{50} (μM)	inhibition in the presence of 15 mg/mL HSA EC_{50} (μM)	Fold change EC_{50}WT(HSA) /EC_{50}WT	V370A HIV-1 inhibition EC_{50} (μM)	CC_{50} (μM)
Bevirimat	0.010	0.974	97.4	0.553	16.8
249	0.039	0.295	7.5	>2	12.1

Fig. 53. Pentacyclic triterpenoid-isoxazole derivative **249**.

2.9. Terpene-isoxazole hybridization

You *et al.* (You et al., 2003) designed and synthesized modified betulinic acid derivatives with A rings and evaluated the anti-tumor activity of three cancer cells. The derivative **233** containing isoxazole showed significant inhibitory effects on SK-MEL-2, A549, and B16-F10 cell lines with IC_{50} values of 1.15, 2.70, and 1.57 μM, respectively. On the activity of betulinic acid (SK-MEL-2: IC_{50} = 7.62 μM; A549: IC_{50} = 7.70 μM; B16-F10: IC_{50} = 4.98 μM). The findings also demonstrated that the introduction of isoxazole into the A ring of betulinic acid resulted in unfavorable anti-tumor activity.

Minassi *et al.* (Minassi et al., 2018) designed and synthesized betulate-isoxazole derivatives. Among them, compound **234** was found to be an inhibitor of HIF prolyl hydrolases (PHDs) with good biological activity (EC_{50} = 2.6 μM).

Xu *et al.* (Xu et al., 2012) designed and synthesized a series of betulinic acid derivatives by introducing different fused heterocycles into the A ring, and evaluated their inhibitory effects on the formation of osteoclasts induced by RANKL. At a concentration of 0.5 μM, the inhibition rate of compound **235** containing isoxazole was 66.8 %. The activity was much higher than that of betulinic acid ($IC_{50} \approx$ 20 μM).

Galaiko *et al.* (Galaiko et al., 2014) obtained a derivative from the methyl ester of betulonic acid and tested the cytotoxicity of compound **236** in RD TE32, A549 and MS cells. Compound **236** showed an obvious inhibitory effect on MS cells with an IC_{50} value of 16.36 μM.

Gundoju *et al.* (Gundoju et al., 2019) modified the C_{28} site of betulinic acid to obtain a series of derivatives and evaluated their inhibitory effects on α-glucosidase in RAW 264.7 cells. Compound **237** linked to isoxazole showed strong α-glucosidase inhibitory activity with an IC_{50} value of 10.8 μM. However, inhibitory activity was not as good as that of betulinic acid (IC_{50} = 7.8 μM).

Luginina *et al.* (Luginina et al., 2021) designed and synthesized betulinic acid-isoxazole conjugates and tested the anti-tumor activity of these compounds *in vitro*. Compounds **238** and **241** showed significant inhibitory effects on the A549 cell line with GI_{50} values of 11.05 and 11.51 μM, respectively. Compounds **239** and **240** showed significant inhibitory effects on the MCF-7 cell line with GI_{50} values of 11.47 and 12.49 μM, respectively. These compounds did not show significant cytotoxicity to immortalized human fibroblasts hTERT (GI_{50} > 100 μM) (Fig. 50).

He *et al.* (He et al., 2016) synthesized a series of derivatives by introducing 5-substituted phenyl-3-isoxazole at position C_3 of betulin. The PTP1B inhibitory activity of the target compounds was significantly improved than that of betulin. The IC_{50} of the compounds at **243** was 0.98 μM, which was 12 times that of betulin. The selectivity of the compound to the homologous enzyme TCPTP reached 3.95 times. The inhibitory activity of compound **242** on PTP1B was slightly weaker than that of **243**, with IC_{50} of 1.62 μM. However, the selectivity of the homologous enzyme TCPTP was the highest, and the selectivity coefficient reached 5.25 times. The synthesis route is depicted in Fig. 51. As a protective group, 3,4-dihydro-2*H*-pyran selectively protected the hydroxyl group at C_{28} of betulin, followed by reaction with various substituted 3-(chloromethyl)-5-phenylisoxazoles. Finally, the protective group was removed in a methanol solution containing *p*-toluenesulfonic acid to obtain the target compounds.

Koohang *et al.* (Koohang et al., 2009) reported that compound **244**

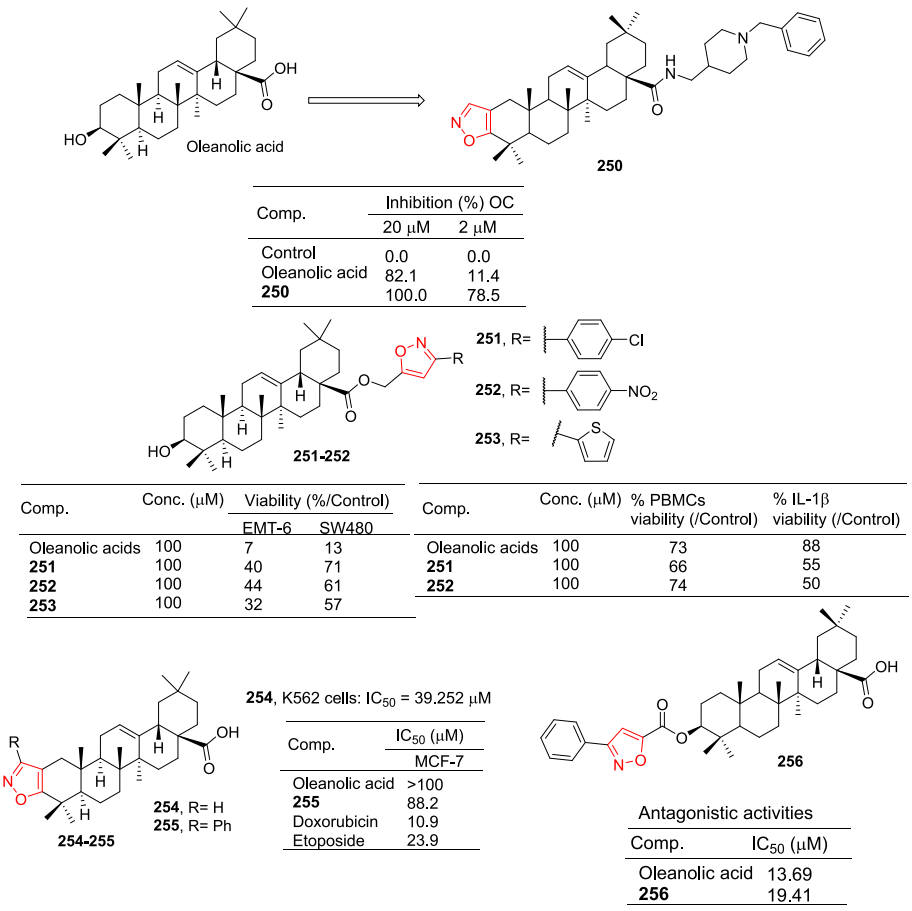

Comp.	Inhibition (%) OC	
	20 μM	2 μM
Control	0.0	0.0
Oleanolic acid	82.1	11.4
250	100.0	78.5

Comp.	Conc. (μM)	Viability (%/Control)	
		EMT-6	SW480
Oleanolic acids	100	7	13
251	100	40	71
252	100	44	61
253	100	32	57

Comp.	Conc. (μM)	% PBMCs viability (/Control)	% IL-1β viability (/Control)
Oleanolic acids	100	73	88
251	100	66	55
252	100	74	50

Comp.	IC_{50} (μM)
	MCF-7
Oleanolic acid	>100
255	88.2
Doxorubicin	10.9
Etoposide	23.9

Antagonistic activities

Comp.	IC_{50} (μM)
Oleanolic acid	13.69
256	19.41

Fig. 54. Pentacyclic triterpenoids-isoxazole derivatives **250**–**256**.

showed a significant inhibitory effect on SK-MEL-2 and DAOY cell lines with an IC_{50} of 8 μM. The IC_{50} values of compound **245** for these two cancer cells were 8 and 7 μM, respectively.

Zhang *et al.* (Zhang et al., 2015) designed and synthesized 23-hydroxybetulinic acid (HBA) derivatives substituted with isoxazole and evaluated their anti-tumor activity. Compounds **246** and **247** showed inhibitory effects on various cancer cells, especially on the SF-763 cell line with IC_{50} values of 6.08 and 6.94 μM. More than 3-hydroxybetulinic acid activity (IC_{50} = 43.40 μM).

Grishko *et al.* (Grishko et al., 2017) reported a method of synthesis of novel ring-A fused heterocyclic derivatives. Derivatives **248** containing isoxazole showed significant inhibitory effects on RD-TE32, A549, MS, HEp-2, and HCT116 cell lines with IC_{50} values of 14.77, 7.85, 14.00, 22.07, and 19.01 μM, respectively (Fig. 52).

Liu *et al.* (Liu et al., 2016) designed and synthesized a series of heterocyclic substituted derivatives of bevirimat as HIV-1 inhibitors. Cell culture efficacy of compound **249** against wild-type (wt) virus was weaker than that of bevirimat (EC_{50} = 10 nM). However, in the presence of human serum, the EC_{50} value at **249** was 0.295 μM, reflecting a much-reduced degree of serum-binding (7.5 times at 12 h versus 97.4 times for bevirimat). The synthesis route is depicted in Fig. 53. Betulin was used as the starting material, and the C_{28} primary hydroxyl group was protected using benzoic anhydride to form the corresponding ester. The triflate intermediate was prepared, followed by Suzuki coupling with aryl carboxylic acid. Finally, the benzoyl protecting group at the C_{28} position was removed, and the aryl ester was hydrolyzed.

Wu *et al.* (Wu et al., 2016) synthesized oleanolic acid derivatives containing isoxazole and evaluated their anti-bone resorption activities. The results showed that the isoxazole derivative **250** inhibited the osteoclast formation of rank-induced RAW264.7 cells at a concentration of 2 μM with an inhibitory rate of 78.5 %. The inhibitory rate of oleanolic acid was more than 11.4 %.

Chouaib *et al.* (Chouaib et al., 2016) reported the synthesis of oleanolic acid derivatives coupled with isoxazole and evaluated their anti-inflammatory activity. *In vitro* anti-inflammatory tests showed that compounds **251**–**252** had a greater inhibitory effect on the production of pro-inflammatory IL-1β cytokines in LPS-stimulated human peripheral blood mononuclear cells (PBMC) than oleanolic acid. The compounds **251**–**252** produced 55 % and 50 % IL-1β (/control) at a concentration of 100 μM, respectively, which was less than 88 % of oleanolic acid. They also reported the synthesis of the oleanol-isoxazole conjugate and evaluated the anti-proliferation of the cancer cell lines EMT-6 and SW480. The results of the *in vitro* cytotoxicity test showed that **251**–**253** had stronger anti-proliferative activity, and the survival rate of EMT-6 cells decreased to 40 %, 44 %, and 32 %. The survival rate of SW480 cells decreased to 71 %, 61 %, and 57 %. The introduction of heterocyclic rings at the C_3 position of isoxazole indicates, to some extent, that it exhibits superior anti-tumor activity compared to substituted phenyl.

Compound **254** has a strong inhibitory effect on leukemia cancer cells and inhibits the proliferation of K562 cells in a dose-dependent manner. After K562 cells were exposed to the compound **254** for 72 h, the IC_{50} value reached 39.252 μM. Compound **253** induces apoptosis and arrest of the G1 phase cell cycle, possibly due to decreased levels of pAkt (Pan et al., 2015).

Compound **255** has an additional benzene ring based on **254**, which has inhibitory activity on MCF-7 cells with an IC_{50} value of 88.2 μM (Mallavadhani et al., 2014).

Wang *et al.* (Wang et al., 2017) modified oleanolic acid at position C_3 to search for new interacting agents of FXR. The **256** isoxazole-modified oleanolic acid derivative showed an antagonistic effect on FXR with an

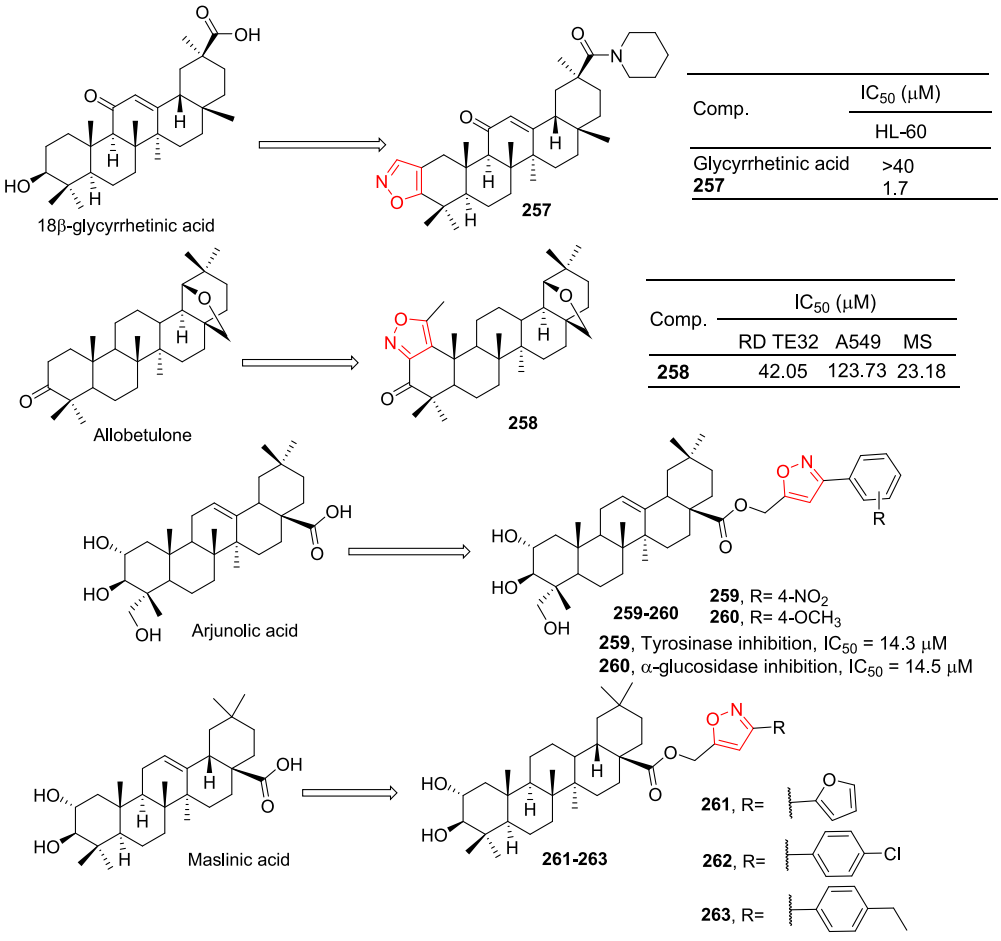

Comp.	IC_{50} (μM)
	HL-60
Glycyrrhetinic acid	>40
257	1.7

Comp.	IC_{50} (μM)		
	RD TE32	A549	MS
258	42.05	123.73	23.18

Comp.	Conc. (μM)	Viability (%/Control)	
		EMT-6	SW480
Maslinic acid	100	5	9
	30	5	11
	10	100	123
261	100	11	16
	30	6	10
	10	5	9

Comp.	Conc. (μM)	% PBMCs viability (/Control)	% IL-1β viability (/Control)
Maslinic acid	100	14	-
	30	53	109
261	100	78	4
	30	31	-
262	100	23	-
	30	57	33
263	100	58	-
	30	42	44

Fig. 55. Pentacyclic triterpenoids-isoxazole derivatives **257**–**263**.

IC_{50} value of 19.41 μM. The inhibitory effect did not exceed oleanolic acid (IC_{50} = 13.69 μM) (Fig. 54).

You *et al.* (Gao et al., 2010) designed and synthesized A-ring modified glycyrrhetinic acid derivatives. All of these derivatives improved the anti-proliferation effect of human HL-60 leukemia cells. The derivative **257** containing isoxazole showed a significant inhibitory effect on HL-60 cells with an IC_{50} value of 1.7 μM. It exceeded the activity of glycyrrhetinic acid (IC_{50} > 40 μM).

Galaiko *et al.* (Galaiko et al., 2014) synthesis triterpene A-condensed isoxazoles and tested the cytotoxicity of compound **258** against RTE32, A549, and MS cells. Compound **258** showed the strongest inhibitory effect on MS cells with an IC_{50} value of 23.18 μM.

Olanipekun *et al.* (Olanipekun et al., 2023) designed and synthesized a series of isoxazole-arjunolic acid derivatives and evaluated their inhibitory potentials for tyrosinase and α-glucosidase. Compound **259** had the strongest inhibitory effect on tyrosinase (IC_{50} = 14.3 μM), about three times that of the standard drug kojic acid (IC_{50} = 41.5 μM). Compound **260** had strong inhibition of α-glucosidase (IC_{50} = 14.5 μM), and the value of IC_{50} was comparable to that of standard acarbose (IC_{50} = 10.4 μM).

Compound **261**, a derivative of maslinic acid containing isoxazole, has a higher anti-carcinogenic effect than crataegic acid. In the breast cancer cell line EMT-6, the survival rate (percentage of live cells/control) of **261** and crataegic acid at 10 μM was 5 % and 100 %, respectively. In colon cancer SW480, survival rates (percentage of live cells/controls) for **261** and cratonic acid at 10 μM were 9 % and 123 %, respectively (Chouaib et al., 2016). Carboxyl-linked isoxazole compounds **261**–**263** of maslinic acid were found to have anti-inflammatory activity. The derivative **261** was the most anti-inflammatory (100 μM: IL-1β production rate = 4 %). The derivative **262**–**263** also has anti-inflammatory effects (IL-1β production rate = 33 % and 44 %, 30 μM) (Fig. 55).

Foskolin is a diterpene isolated from the roots of *Coleus forskohlii*. Burra *et al.* (Burra et al., 2017) performed a 1,3-dipolar cycloaddition reaction to introduce an isoxazole fragment onto the C_1-OH of forskolin. The anti-cancer activity of these compounds was evaluated against MCF-7 and BT-474 cell lines (Fig. 56). The IC_{50} value of compounds **264**–**272** against MCF-7 cells was 0.5 μM. The IC_{50} value of compound **267** against BT-474 cells was 0.5 μM. The activity of both compounds was higher than that of forskolin (MCF-7: IC_{50} = 63.3 μM; BT-474: IC_{50} >

Comp.	R_1	R_2	R_3	IC_{50} (μM)	
				MCF-7	BT-474
Forskolin	-	-	-	63.3	>100
264	H	acetyl	4-OCH_3	0.5	2.1
265	H	acetyl	3,4,5-OCH_3	0.5	29.3
266	H	acetyl	4-OCH_3	0.5	4
267	H	acetyl	4-OCH_2Ph	0.5	0.5
268	H	acetyl	2,4,6-OCH_3	0.5	>100
269	H	acetyl	H	0.5	5
270	acetyl	H	2,4,6-OCH_3	0.5	>100
271	H	acetyl	3,4-OCH_3	0.5	>100
272	acetyl	H	3,4-OCH_3	0.5	>100

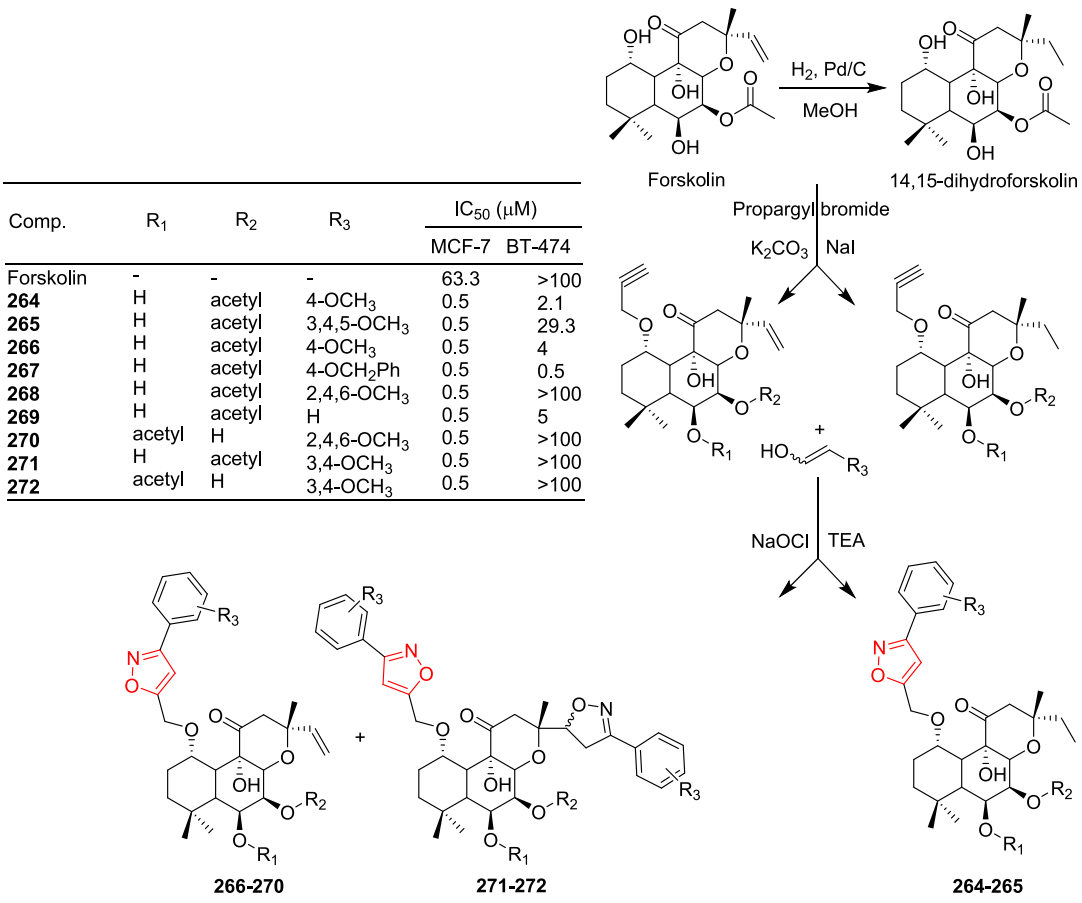

Fig. 56. Terpene-isoxazole derivatives **264**–**272**.

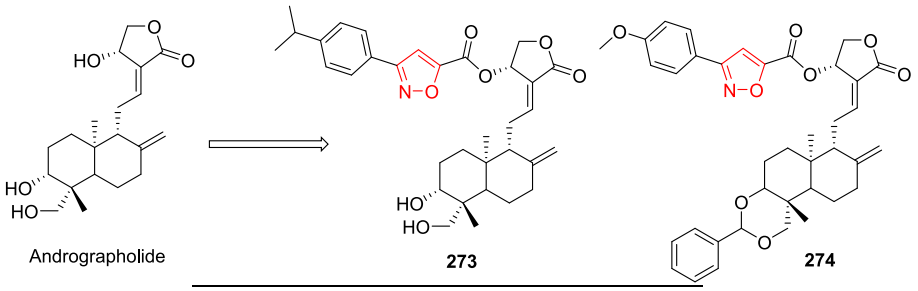

Comp.	IC_{50} (μM)			
	HCT-15	DU145	HeLa	VERO
Andrographolide	189.18	253.10	213.72	117.27
273	62.44	48.60	73.09	67.23
274	67.84	42.98	70.02	49.55

Fig. 57. Terpene-isoxazole derivatives **273**–**274**.

100 μM).

Mokenapelli *et al.* (Mokenapelli et al., 2021) synthesized a series of isoxazole-containing derivatives using andrographolide as the skeleton and evaluated the cytotoxicity of HCT15, HeLa, and DU145 cell lines. Compounds **273** and **274** showed significant cytotoxic activity against DU145 cell lines with IC_{50} values of 48.60 and 42.98 μM (Fig. 57).

Zhang *et al.* (Zhang et al., 2018) studied the *in vitro* anti-*S. aureus* activity of *N*-sulfonaminoethyloxime derivatives of dehydroabietic acid. The derivative **275** showed the highest inhibitory activity against the *S. aureus* Newman strain and multidrug-resistant strains (NRS-1, NRS-70, NRS-100, NRS-108, and NRS-271), with a MIC of 1.56–3.13 μg/mL.

Alwaseem *et al.* (Alwaseem et al., 2018) modified C_9 and C_{14} of parthenolide using P450-mediated chemical enzymes to obtain a series of parthenolide derivatives. Derivative **276** showed a significant inhibitory effect on the HCT116 cell line with an IC_{50} value of 8.3 μM. Anticancer activity was significantly higher than parthenolide (IC_{50} = 18.0 μM).

Modification of parthenolide C_9 or C_{14} sites by Tyagi *et al.* (Tyagi et al., 2016) could effectively enhance the anti-leukemia activity of parthenolide. Derivatives **276** and **277** significantly inhibited M9-ENL1 cells with IC_{50} values of 2.6 and 13.7 μM, respectively.

Chen *et al.* (Chen et al., 2019) reported an anti-thrombotic derivative based on isosteviol with anticoagulant and anti-platelet activities. Compound **278** selectively inhibited FXa (Ki = 9.786 μM) containing an

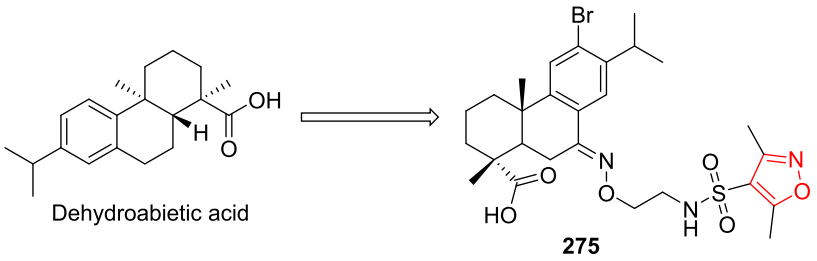

Comp.	MIC (μg/mL)					
	Newman	NRS-1	NRS-70	NRS-100	NRS-108	NRS-271
Vancomycin	0.78-1.56	1.56-3.13	0.2-0.39	0.39-0.78	0.39-0.78	0.39-0.78
Tetracycline	<0.2	>25	<0.2	<0.2	<0.2	<0.2
Dehydroabietic acid	12.5-20	12.5-25	12.5-25	12.5-20	12.5-20	12.5-20
275	1.56-3.13	1.56-3.13	1.56-3.13	1.56-3.13	1.56-3.13	1.56-3.13

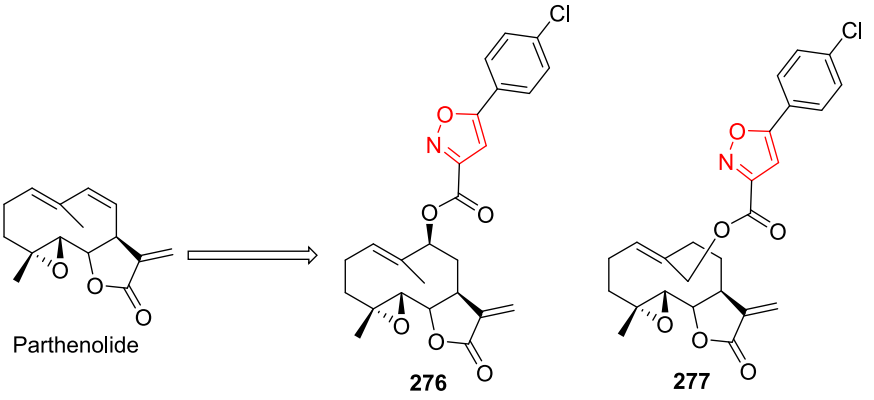

Comp.	IC_{50} (μM)
	HCT116
Parthenolide	18.0
276	8.3

Comp.	IC_{50} (μM)
	M9-ENL1
Parthenolide	5.4
276	2.6
277	23.7

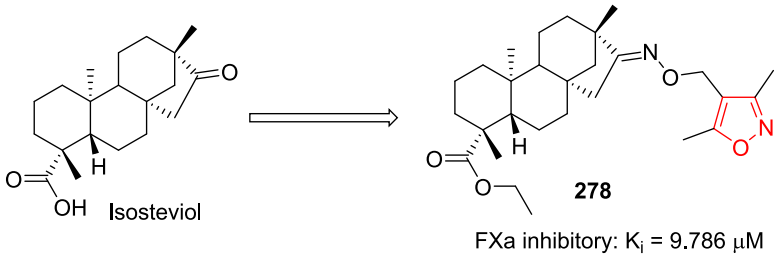

Fig. 58. Terpene-isoxazole derivatives **275**–**278**.

isoxazole structure against a panel of serine proteases, and it has certain anticoagulant activity (Fig. 58).

Summary: Terpene-isoxazole hybridization natural products mainly have anti-tumor, anti-inflammatory, anti-HIV, antibacterial, and anti-bone resorption activities. Moreover, PTP1B is recognized as a target for the therapy of diabetes. The inhibitory activity of compounds **242** and **243** on PTP1B was significantly better than that of the parent compound, and the preliminary structural-activity relationship showed that the introduction of electron-withdrawing groups to the *meta* position of the benzene ring or electron-donating groups to the *para* position of the benzene ring was beneficial to the activity.

Pentacyclic triterpenoids exist widely in many plants and have many pharmacological activities, including anti-tumor activity. Unfortunately, the anti-tumor activity of these pentacyclic triterpenoids-isoxazole derivatives was not satisfactory, the IC_{50} values of these derivatives on cancer cells did not reach the nanomolar level. Interestingly, forskolin, a labdane diterpene natural product, its C_1-isoxazole derivatives (**264**–**272**) exhibited significant anti-cancer activity against the MCF-7 breast cancer cells with $IC_{50} < 1$ μM. Furthermore, the preliminary structure–activity relationship showed that the introduction of electron-donating groups to the benzene ring at the C_3 position of isoxazole was beneficial to the activity.

2.10. Alkaloid-isoxazole hybridization

Camptothecin prevents the breakdown of the topoisomerase-I (Topo I)/DNA cleavable complex. Derivatives **279** and **280** showed significant inhibitory activity against A549, MCF-7, MDA-MBq231, HepG-2, KB, BEL-7402, MGC80-3, and SK-N-SH cell lines, with IC_{50} values ranging from 0.064–10.54 μM. Compound **279** had the strongest inhibitory effect on the HepG-2 cell line with an IC_{50} value of 0.064 μM (Pan et al., 2018). The synthetic routes for these two compounds are illustrated in Fig. 59. 10-Hydroxycamptothecin was used as the starting material, and the Duff reaction was first employed to introduce the aldehyde group at

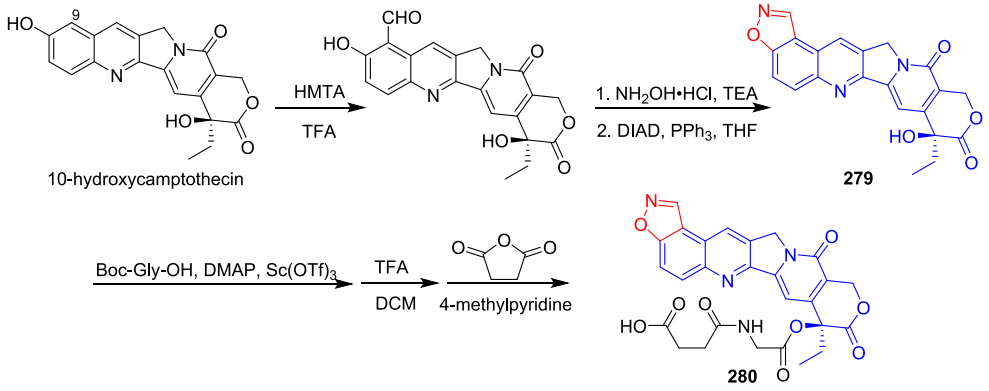

Comp.	IC50 (μM)							
	A549	MCF-7	MDA-MB-231	HepG-2	KB	BEL-7402	MGC80-3	SK-N-SH
Topotecan	1.424	2.135	1.898	0.237	2.610	7.118	0.190	0.093
279	1.028	1.157	0.488	0.064	3.342	10.54	0.514	0.463
280	1.832	>10	0.641	0.348	7.143	2.015	0.275	0.549

Fig. 59. Alkaloid-isoxazole derivatives **279**–**280**.

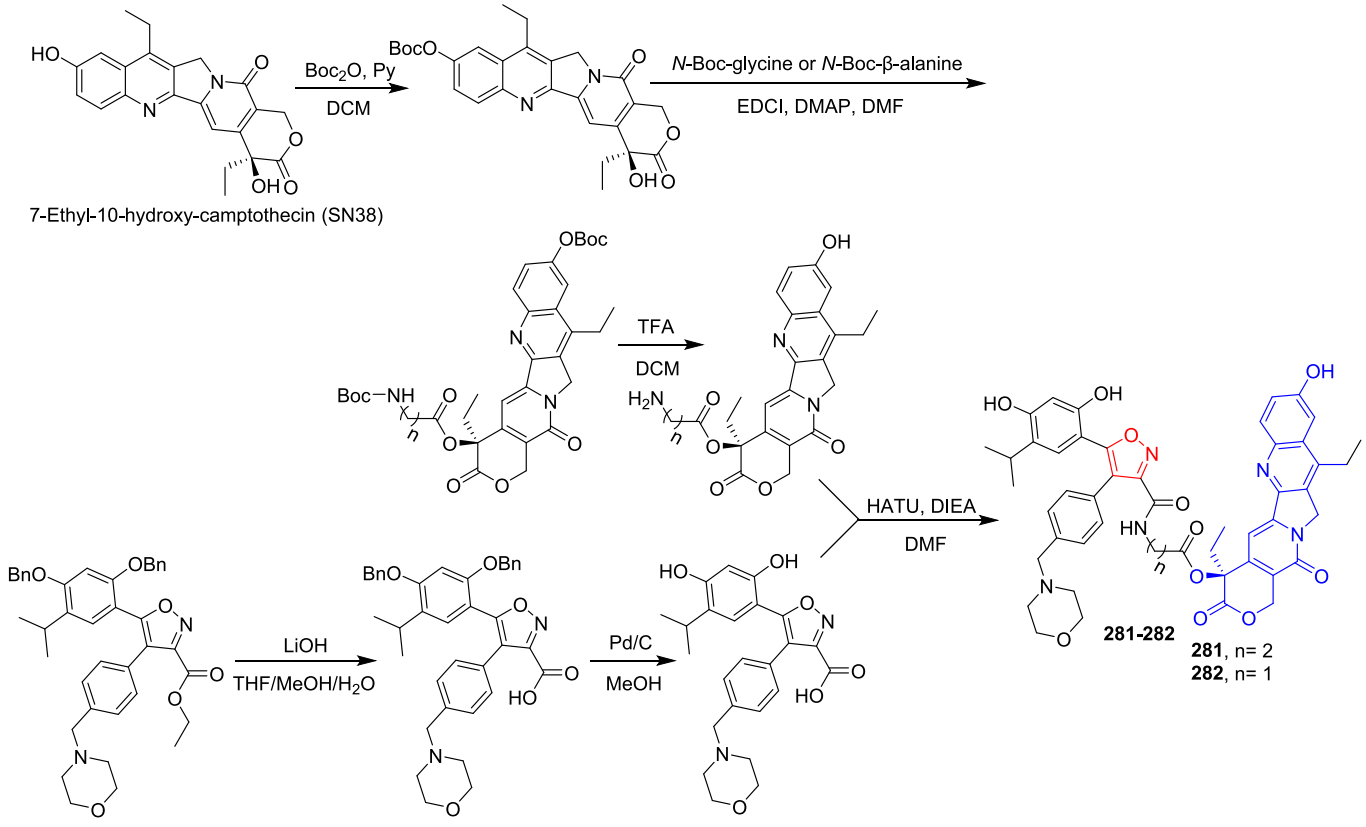

Comp.	HSP90	IC50 (nM)				
		A549	HCT116	MIA-PACA-2	Capan-1	HL7702
281	70	324	83	205	206	7893
282	72	56	22	46	36	6872
SNX5422	38	-	-	-	-	-
NVP-AUY922	12	39	121	38	657	1364
Irinotecan	-	1557	498	1329	1121	1305
SN38	-	11	4	13	8	18

Fig. 60. Alkaloid-isoxazole derivatives **281**–**282**.

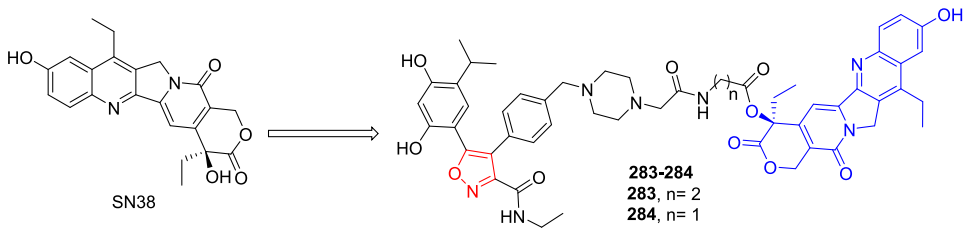

Comp.	HSP90	IC_{50} (nM)						
		A549	BGC823	HCT116	PSN-1	Capan-1	MCF-7	HL7702
283	70	106	17	302	14	14	20	6171
284	72	82	9	295	8	10	15	6722
NVP-AUY922	14	42	26	45	21	428	40	1285
AT13387	7	45	29	35	26	228	70	773
SN38	-	11	17	8	25	11	47	18
CPT-11	-	1390	728	945	945	1190	634	1387

Fig. 61. Alkaloid-isoxazole derivatives **283**–**284**.

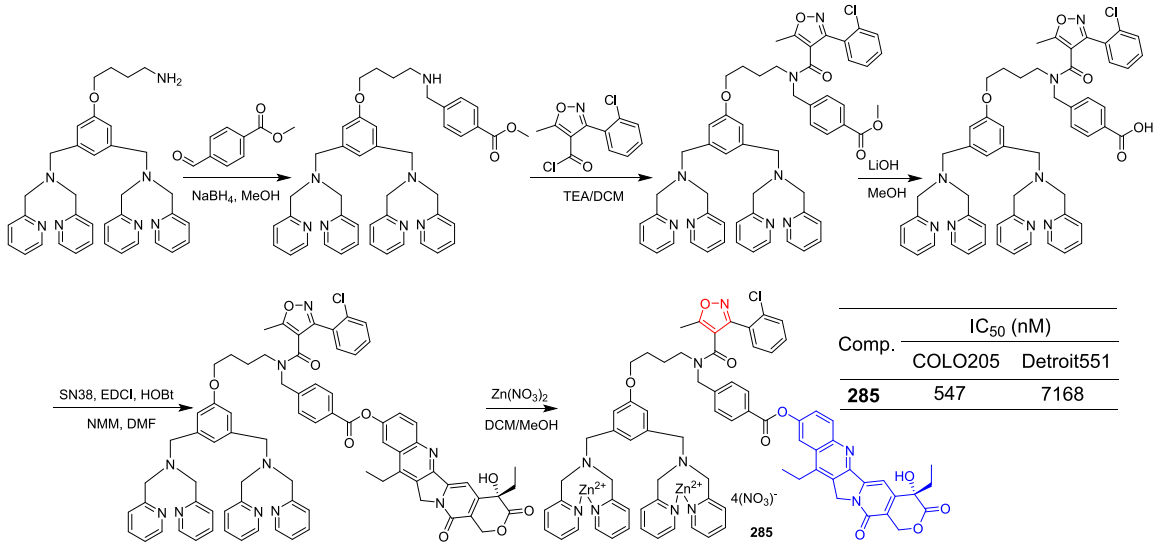

Comp.	IC_{50} (nM)	
	COLO205	Detroit551
285	547	7168

Fig. 62. Alkaloid-isoxazole derivative **285**.

the C_9 position. Subsequently, cyclization produced derivative **279** containing an isoxazole fragment. The compound **280** was synthesized by introducing *N*-succinylglycine to compound **279** using a one-pot method.

Zhu *et al.* (Zhu et al., 2020) developed a series of HSP90 inhibitor SN38 couplings at the 20-OH and 10-OH sites of ester and carbamate linkage of SN38. Among them, compounds **281** and **282** exhibit good HSP90α affinity with IC_{50} values of 72 and 70 nM. Compounds **281** and **282** showed significant inhibitory effects on A549, HCT116, MIA-PACA-2, Capan-1, and HL7702 cell lines with IC_{50} values ranging from 22–7893 nM. Furthermore, compound **282** showed excellent anti-tumor activity and low toxicity in HCT116 and Capan-1 xenograft tumor models. The pharmacokinetic analysis of the HCT116 and Capan-1 xenografts further confirmed that treatment with compound **282** led to effective cutting of tumor sites and prolonged exposure to SN38. The initial structure–activity relationship analysis suggested that the elongation of the carbon chain conferred enhanced antitumor activity. The synthetic routes for these two compounds are illustrated in Fig. 60.

Compounds **283** and **284** were designed and synthesized by the same research group using similar synthesis methods as compounds **281** and **282** (Fig. 61) (Cao et al., 2023). *In vitro* experiments showed that these exhibited acceptable stability in PBS and plasma, with significant HSP90 binding affinity and strong cytotoxic capacity. Compounds **283** and **284** have a strong binding affinity for HSP90 with IC_{50} values of 70 and 72 nM. It showed significant inhibitory effects on A549, BGC823, HCT116, PSN-1, Capan-1, and MCF-7 cell lines, with IC_{50} values ranging from 8 to 302 nM.

Liu *et al.* (Liu et al., 2019) reported a new conjugate of phosphatidylserine-targeted zinc (II) dipicolylamine drug and evaluated the *in vitro* cytotoxicity of these compounds against the COLO-205 cell line and the normal fibroblast Detroit 551. Cytotoxic compound **285** inhibited COLO-205 cells at 547 nM. Compound **285** is less toxic to normal cells (Detroit 551: IC_{50} = 7168 nM). As shown in Fig. 62, reductive amination of starting material with methyl 4-formylbenzoate and $NaBH_4$. Then, the ester intermediate was treated with an acyl chloride containing an isoxazole group under basic conditions in CH_2Cl_2. Subsequently, the SN38-conjugated intermediate was obtained through hydrolysis and esterification. Incubation with 2 equivalences of zinc nitrate with SN38-conjugated intermediate then afforded the compound **285**.

Filali *et al.* (Filali et al., 2016) obtained a novel derivative of isoxazole by linking Harmine and evaluated its anti-proliferative activity against OCVAR-3, MCF-7, and HCT116 cell lines by MTT assay. Of the synthesized derivatives, compounds **286** and **287** showed the best activity, with IC_{50} values ranging from 5.0–73.08 μM for the three cancer cells. The above results suggest that the introduction of electron-

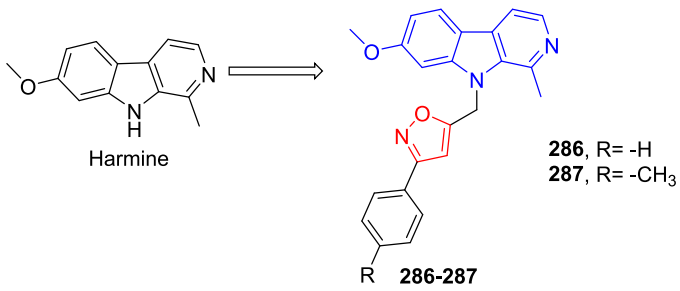

Comp.	AChE Inhibition	IC50 (μM)		
		OCVAR-3	MCF-7	HCT-116
Harmine	10.4	0.70	18.0	1.3
286	22.9	5.0	16.0	65.0
287	17.8	6.3	25.0	73.08
Galantamine	4.1	-	-	-
Tamoxifen	-	0.36	0.52	0.38

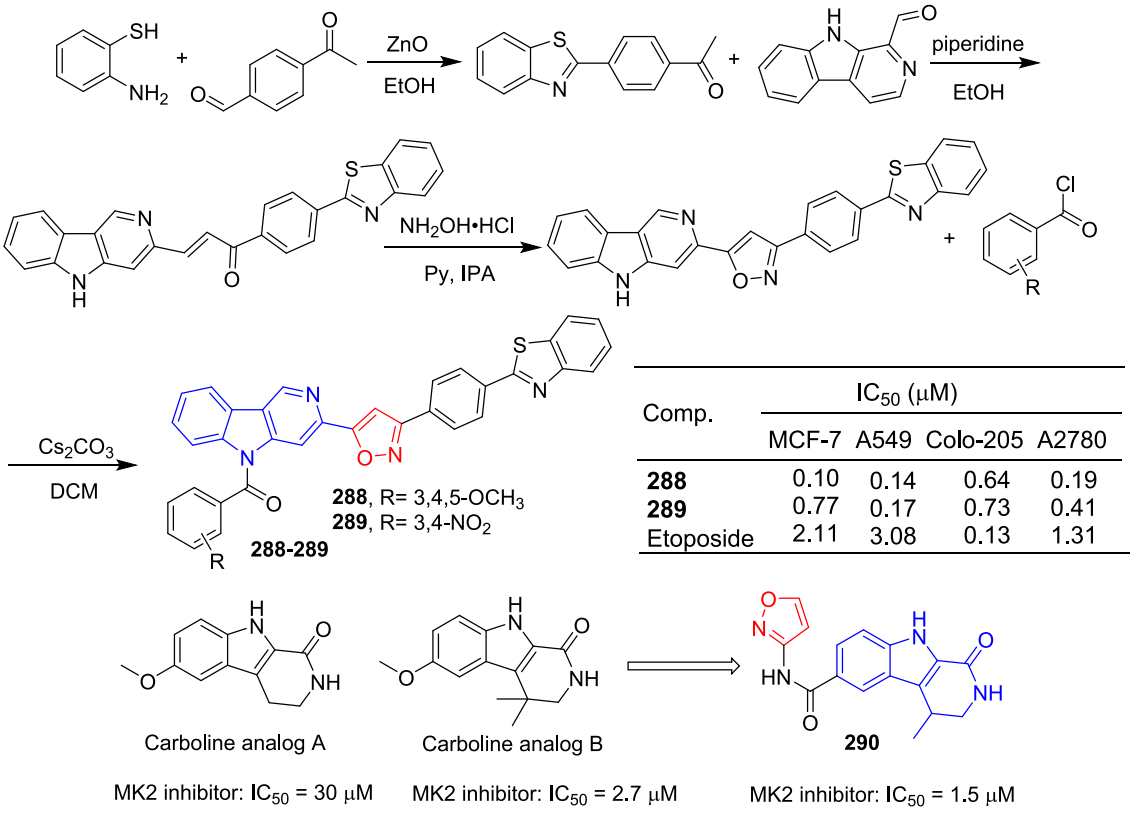

Comp.	IC50 (μM)			
	MCF-7	A549	Colo-205	A2780
288	0.10	0.14	0.64	0.19
289	0.77	0.17	0.73	0.41
Etoposide	2.11	3.08	0.13	1.31

Fig. 63. Alkaloid-isoxazole derivatives **286**–**290**.

donating groups at the *para*-position of the phenyl group may lead to a reduction in antiproliferative activity. Compounds **286** and **287** showed antiacetylcholinesterase activity with IC_{50} values of 22.9 and 17.9 μM.

Ravinaik *et al.* (Ravinaik et al., 2019) reported the synthesis of linked amide derivatives based on β-carboline and the evaluation of their antitumor activity. The synthetic approach to the targeted compounds **288**–**289** began with the cyclization of 2-aminobenzenethiol and 4-acetylbenzaldehyde in the presence of ZnO nanoparticles, resulting in the formation of 1-{4-(benzo[*d*]thiazol-2-yl)phenyl}ethanone. Subsequent reaction with 9*H*-pyrido[3,4-*b*]indole-1-carbaldehyde through Claisen-Schmidt condensation led to an α,β-unsaturated chalcone intermediate. The chalcone intermediate was then reacted with hydroxylamine hydrochloride and pyridine, leading to the formation of an isoxazole intermediate. Finally, coupling reactions between the isoxazole intermediate and various substituted benzoyl chlorides in the presence of Cs_2CO_3 afforded the target compounds **288**–**289**. Compounds **288** and **289** showed significant inhibitory effects on MCF-7, A549, Colo-205, and A2780 cell lines with IC_{50} values ranging from 0.10–0.77 μM, respectively.

Wu *et al.* (Wu et al., 2007) reported carboline-based MK2 inhibitors. Compound **290** containing isoxazole inhibited MK2; IC_{50} as low as 1.50 μM, as measured in a DELFIA assay (Fig. 63).

Indirubin has been shown to inhibit cyclin-dependent kinase (CDK) activity, leading to cell cycle arrest (Hoessel et al., 1999; Damiens et al., 2001). Furthermore, long-term animal studies have shown that indirubin does not have the toxicity of conventional anticancer drugs and does not affect bone marrow or hematopoietic stem cell production (Moon et al., 2006). Tang *et al.* (Chiou et al., 2015) synthesized a series

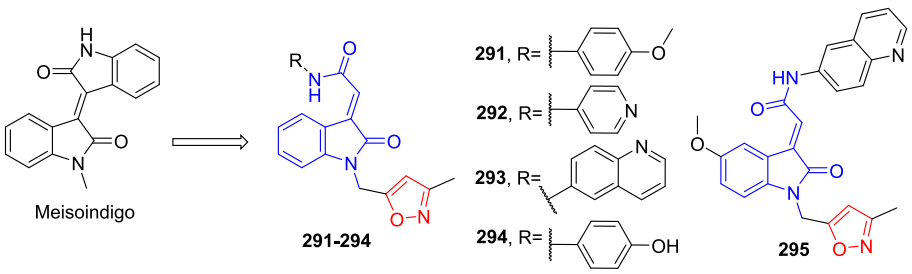

Comp.	IC$_{50}$ (μM)					
	NCI-H460	MCF-7	Hep3B	KB	SF-268	MKN-48
291	4.3	4.0	8.6	5.0	3.3	7.1
292	4.5	3.6	3.2	3.1	3.4	3.3
293	3.3	3.2	3.5	3.5	3.3	3.8
294	4.6	-	-	-	-	-
295	2.2	2.3	2.7	2.2	3.6	3.6
Indirubin-3'-oxime	32.6	25.5	9.0	19.2	37.0	36.7
Roscovitine	11.6	19.6	9.0	24.6	8.8	7.6

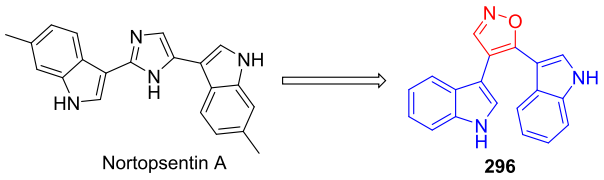

Comp.	IC$_{50}$ (μM)				
	GXF 251L	A549	LXFA 629L	PANC1	UXF 1138L
296	5.1	4.2	8.8	8.8	4.8

Fig. 64. Alkaloid-isoxazole derivatives **291**–**296**.

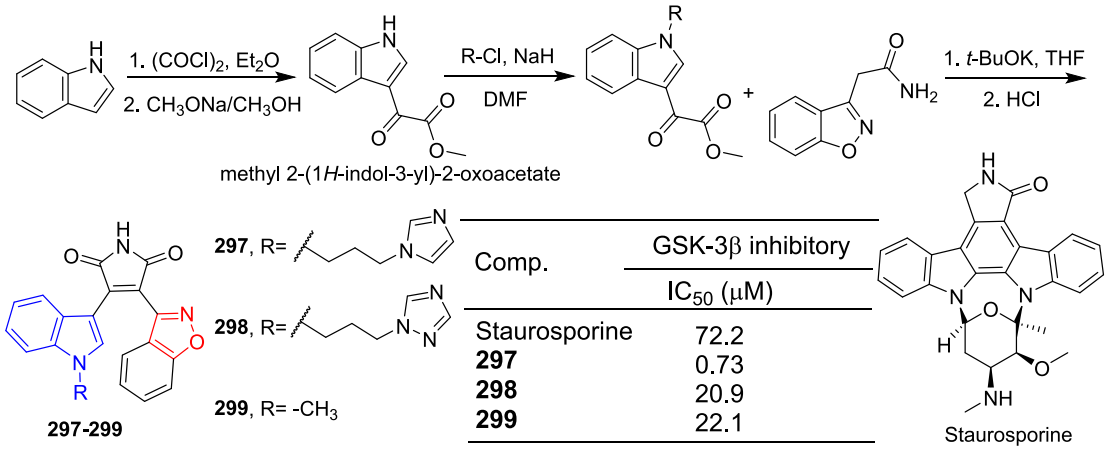

Comp.	GSK-3β inhibitory IC$_{50}$ (μM)
Staurosporine	72.2
297	0.73
298	20.9
299	22.1

Fig. 65. Alkaloid-isoxazole derivatives **297**–**299**.

of derivatives of 3-ylideneoxindole acetamides. Compounds **291**–**295** showed significant inhibitory activity against NCI-H460, MCF-7, Hep3B, KB, SF-268, and MKN-48 cell lines with IC$_{50}$ ranging from 2.2–8.6 μM. Compound **295** inhibits cells in the G1 phase, increasing the number of cells in the sub-G1 phase, suggesting that compound **295** exerts its anti-tumor activity through the apoptosis-inducing pathway. Furthermore, compound **295** causes up-regulation of the cell cycle regulator cyclin D1, which is maintained at high levels. Compound **295** in CT26-xenografted BALB/c mice treated by the i.p. route showed a reduction in tumor volume comparable to cisplatin.

Bisindole alkaloids, which are metabolites of deep-sea sponges, have been widely concerned for their antiviral, antibacterial, anti-inflammatory, and anti-tumor activities (Shin et al., 1999; Casapullo et al., 2000; Bao et al., 2005; Gul and Hamann, 2005). Diana *et al.* (Diana et al., 2010) synthesized a series of bisindolyl isoxazole derivatives and evaluated them in a variety of human tumor cell lines. Among them, compound **296** had a strong inhibitory effect on the GXF 251L, A549, LXFA 629L, PANC1, and UXF 1138L cell lines with IC$_{50}$ value < 10 μM (Fig. 64).

Staurosporine, an alkaloid, is a potent but non-selective inhibitor of GSK-3β. Ye *et al.* (Ye et al., 2013) synthesized a series of 3-benzoisoxazol-4-indolyl maleimide and evaluated their GSK-3β inhibitory activity. The reaction of indole with oxalyl chloride in diethyl ether, followed by treatment with sodium methoxide, afforded methyl 2-(1*H*-indol-3-yl)-2-oxoacetate. Subsequent *N*-alkylation reactions were performed using various alkyl chlorides. Finally, the target compounds were synthesized

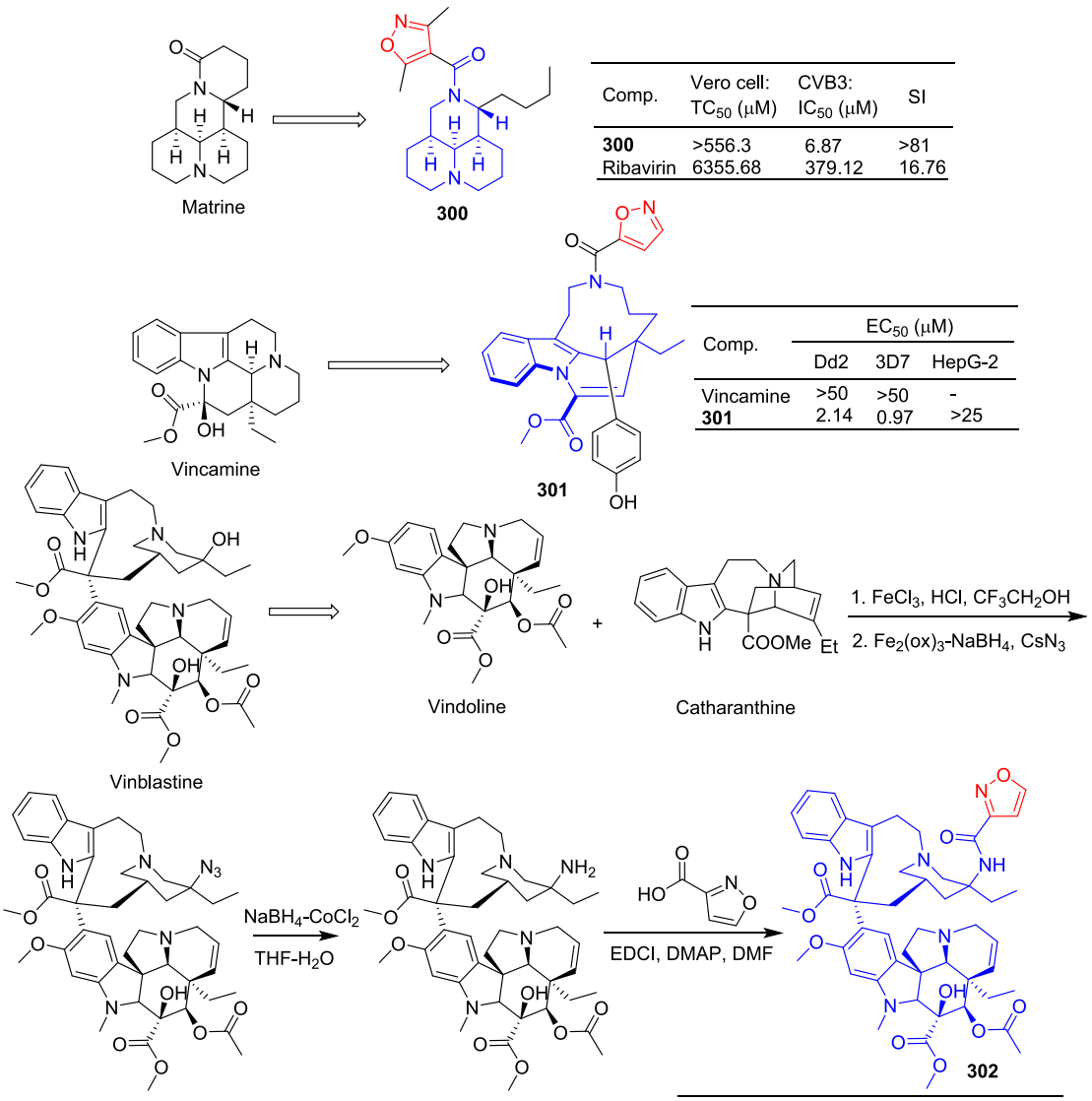

Comp.	Vero cell: TC_{50} (μM)	CVB3: IC_{50} (μM)	SI
300	>556.3	6.87	>81
Ribavirin	6355.68	379.12	16.76

Comp.	EC_{50} (μM)		
	Dd2	3D7	HepG-2
Vincamine	>50	>50	-
301	2.14	0.97	>25

Comp.	IC_{50} (nM)		
	L1210	HCT116	HCT116/VM46
Vinblastine	6.0	6.8	600
302	4.5	7	90

Fig. 66. Alkaloid-isoxazole derivatives **300**–**302**.

through a condensation reaction with 2-(benzo[*d*]isoxazol-3-yl)acetamide. Compounds **297**–**299** showed significant inhibitory effects on GSK-3β with IC_{50} values ranging from 0.73 to 22.1 μM. In cell function experiments, compounds **297**–**299** significantly reduced Aβ-induced Tau hyperphosphorylation by inhibiting GSK-3β (Fig. 65).

Li *et al.* (Li et al., 2017) synthesized a series of 12 *N*-substituted derivatives using matrine as the lead compound and evaluated their activity against the Coxsackie B3 virus (CVB3). The isoxazole-linked derivative **300** showed a significant inhibitory effect on the CVB3 virus with an IC_{50} value of 6.87 μM. There was no toxicity to normal Vero cells (IC_{50} > 556.3 μM).

Norwood *et al.* (Norwood et al., 2021) synthesized a series of vincamine compounds. Compound **301** showed strong inhibition of chloroquine-resistant *P. falciparum* Dd2, EC_{50} = 2.14 μM. For wild-type *P. falciparum* 3D7 cells, EC_{50} = 0.97 μM; HepG-2 cell: EC_{50} > 25 μM.

Lukesh *et al.* (Lukesh et al., 2017) synthesized vinblastine-amides derivatives and tested their anti-tumor activity. As depicted in Fig. 66, the azide intermediate was available directly in a single step from commercially available vindoline and catharanthine by enlisting first their Fe(III)-promoted coupling. Subsequent in situ Fe(III)-mediated free radical hydrogen atom transfer hydroazidation of anhydrovinblastine. The target compound was then obtained through a reduction reaction followed by a condensation reaction. Isoxazol-linked derivative **302** showed significant inhibitory effects on L1210, HCT116, and HCT116/VM46 cell lines with IC_{50} values of 4.5, 7.0, and 90 nM, respectively. Activity exceeding or approaching that of vinblastine (L1210: IC_{50} = 6.0 nM; HCT116: IC_{50} = 6.8 nM; HCT116/VM46: IC_{50} = 600 nM).

Summary: Alkaloid-isoxazole hybridization natural products mainly have anti-tumor, anti-viral, and anti-parasitic activities. Among these derivatives, camptothecin hybrid isoxazole derivatives showed the strongest anti-tumor activity *in vitro*, compound **284** was the most sensitive to the PSN-1 cell line with an IC_{50} value of 8 nM. Preliminary structure–activity relationships indicate that shortening carbon chains increases anti-tumor activity and reduces toxicity to normal cells (NL7702). Compound **300**, a matrine hybrid isoxazole derivative, showed significantly better anti-viral activity than ribavirin. Besides,

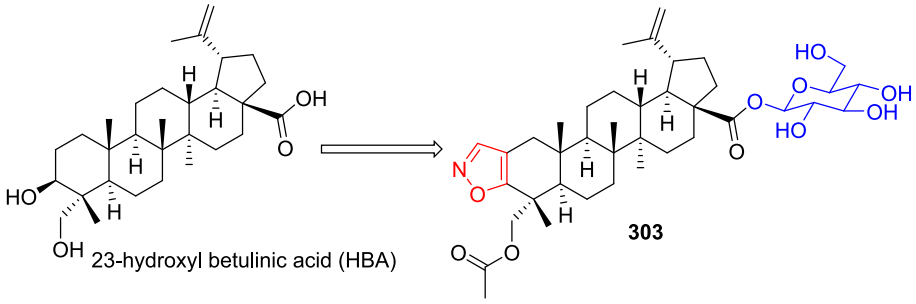

Comp.	IC_{50} (μM)				
	HL-60	BEL-7402	SF-763	HeLa	B16
HBA	45.15	39.67	43.40	52.39	29.87
303	16.71	17.02	15.10	18.43	15.16
Doxorubicin	0.17	0.22	0.16	0.21	0.18

Fig. 67. Carbohydrate-isoxazole derivative **303**.

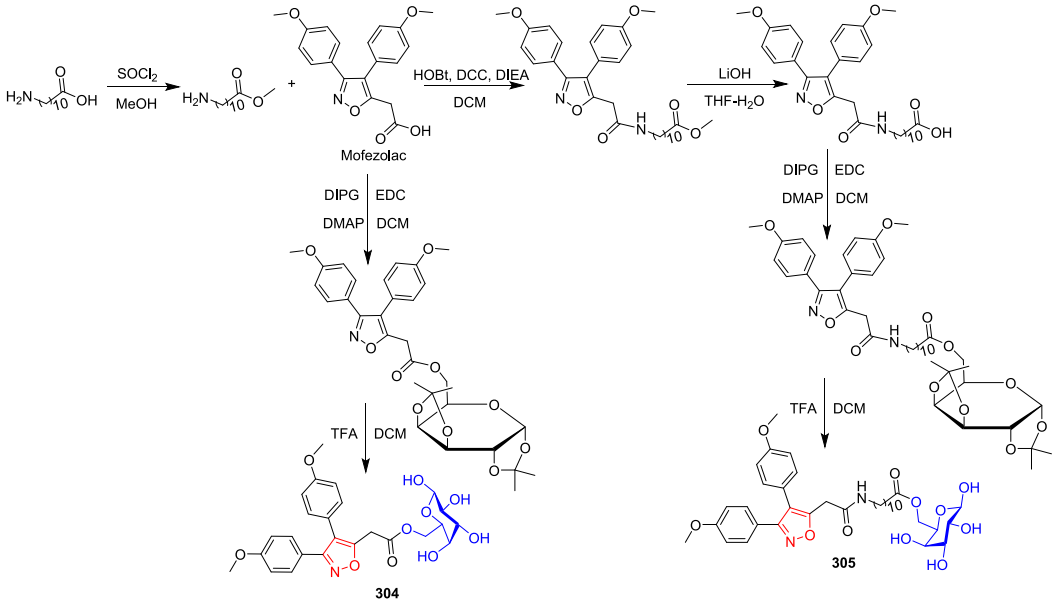

Comp.	COX-1		COX-2	
	IC_{50} (μM)	50 μM inhibition (%)	IC_{50} (μM)	50 μM inhibition (%)
Mofezolac	0.0079	100	>50	38
304	0.27	100	3.1	87
305	0.40	90	0.27	64

Fig. 68. Carbohydrate-isoxazole derivatives **304**–**305**.

compound **301** significantly enhanced the anti-parasitic activity compared to its parent compound vincamine.

2.11. *Carbohydrate-isoxazole hybridization*

Zhang *et al.* (Zhang et al., 2015) designed and synthesized 23-hydroxybetulinic acid (HBA) derivatives substituted with isoxazole and evaluated their anti-tumor activity. The glycosylated derivative **303** showed strong inhibitory effects on HL-60, BEL-7402, SF-763, HeLa, and B16 cell lines with IC_{50} ranging from 15.10–26.71 μM (Fig. 67).

Neuroinflammation is an early stage of several neurological and neurodegenerative diseases. Constitutive microglia COX-1 is one of the pro-inflammatory factors in neuroinflammation. Mofezolac (a highly selective COX-1 inhibitor) is linked to galactose via an ester or amide bond to obtain a substance that can cross the blood–brain barrier (BBB) and control the inflammatory response of the central nervous system. Compound **304** is a selective COX-1 inhibitor (COX-1: IC_{50} = 0.27 μM; COX-2: IC_{50} = 3.1 μM, SI = 11.5). Compound **305** is a COX-2 inhibitor (COX-1: IC_{50} = 0.40 μM; COX-2: IC_{50} = 0.27 μM). Compound **304** is chemically and metabolically stable, able to cross the monolayer of Caco-2 cells (similar to the blood–brain barrier), and its transport is detected mediated by GLUT-1. Additionally, compound **304** inhibited PGE2 release more effectively than mofezolac in LPS-stimulated mouse BV2 microglia cell lines (Perrone et al., 2017) (Fig. 68). The esterification of mofezolac with 1,2:3,4-di-O-isopropylidene-α-D-galactopyranose (DIPG) was initially conducted in the presence of EDC and DMAP to yield the corresponding intermediate. Subsequently, deprotection of the intermediate using trifluoroacetic acid resulted in the synthesis of compound **304**. Compound **305** was synthesized utilizing 11-aminoundecanoic acid as a linker following the same procedure as compound **304**.

Thiamethoxazole (HYM) is a broad-spectrum fungicide. When HYM

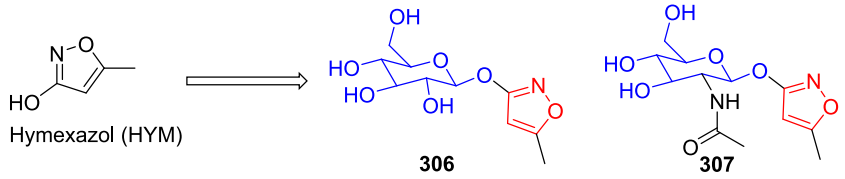

Comp.	Antifungal activity (%)					
	Concentration (μg/mL)	*Phytophthora capsica*	*Fusarium oxysporum*	*Rhizoctonia solani*	*Alternaria alternata*	*Sclerotinia sclerotiorum*
306	100	0.00	22.95	20.00	24.18	57.65
	200	1.37	18.84	35.56	72.53	71.76
	400	10.96	21.92	51.11	93.41	81.18
307	100	4.79	50.68	25.19	100.00	60.00
	200	20.55	59.93	45.19	100.00	83.53
	400	26.03	78.42	65.19	100.00	100.00
HYM	100	0.00	69.18	50.00	100.00	100.00
	200	10.96	79.45	77.78	100.00	100.00
	400	52.05	91.78	100.00	100.00	100.00

Comp.	*A. alternata*			*S. sclerotiorum*		
	EC_{50} (μg/mL)	EC_{90} (μg/mL)	Hillslope	EC_{50} (μg/mL)	EC_{90} (μg/mL)	Hillslope
306	15.57	86.31	1.283	117.10	519.40	1.475
307	1.58	34.84	0.7097	64.04	255.70	1.587
HYM	0.78	16.91	0.71533	50.30	166.67	1.834

Fig. 69. Carbohydrate-isoxazole derivatives **306**–**307**.

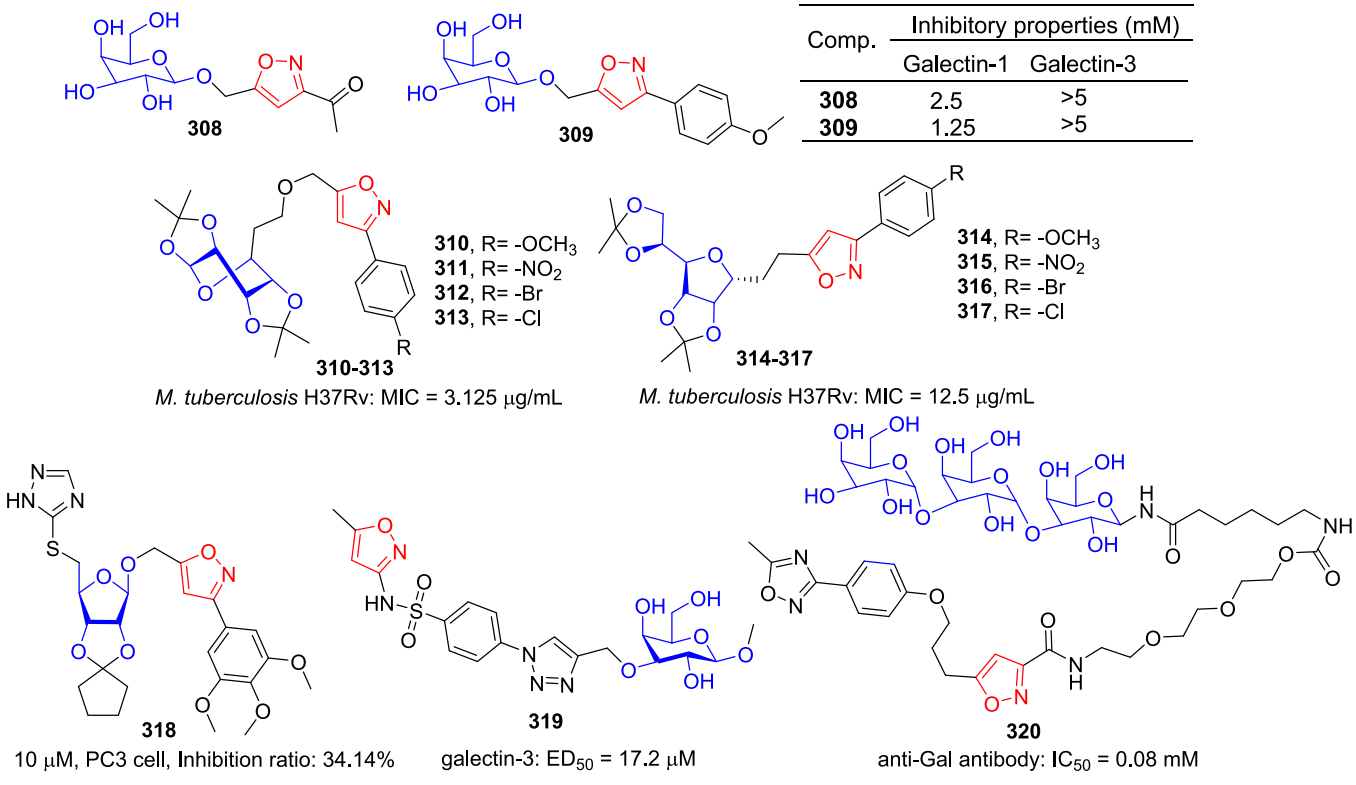

Comp.	Inhibitory properties (mM)	
	Galectin-1	Galectin-3
308	2.5	>5
309	1.25	>5

Fig. 70. Carbohydrate-isoxazole derivatives **308**–**320**.

is absorbed by plants, it is rapidly converted into two glucoside metabolites, which have less anti-fungal activity than HYM. To maintain strong anti-fungal activity *in vitro* and *in vivo*, HYM performs glycosylation with amino sugars, simulating plant glycosylation. The anti-fungal activity of glycosides **306** and **307** was the highest. *N*-acetylglucosamine had an obvious synergistic effect with HYM. Furthermore, glucoside **307** can significantly promote plant growth and induce an increase in plant defense enzyme activity. In addition, electron microscopy and proteomic results showed that glycoside **307** had a unique anti-fungal mechanism compared to HYM (Gao et al., 2022) (Fig. 69).

Giguere *et al.* (Giguère et al., 2006) synthesized galactosides containing isoxazole and discovered specific galactin-1 and −3 inhibitors. Compounds **308** and **309** showed inhibitory effects on galectin-1 with inhibitory properties of 2.5 and 1.25 mM.

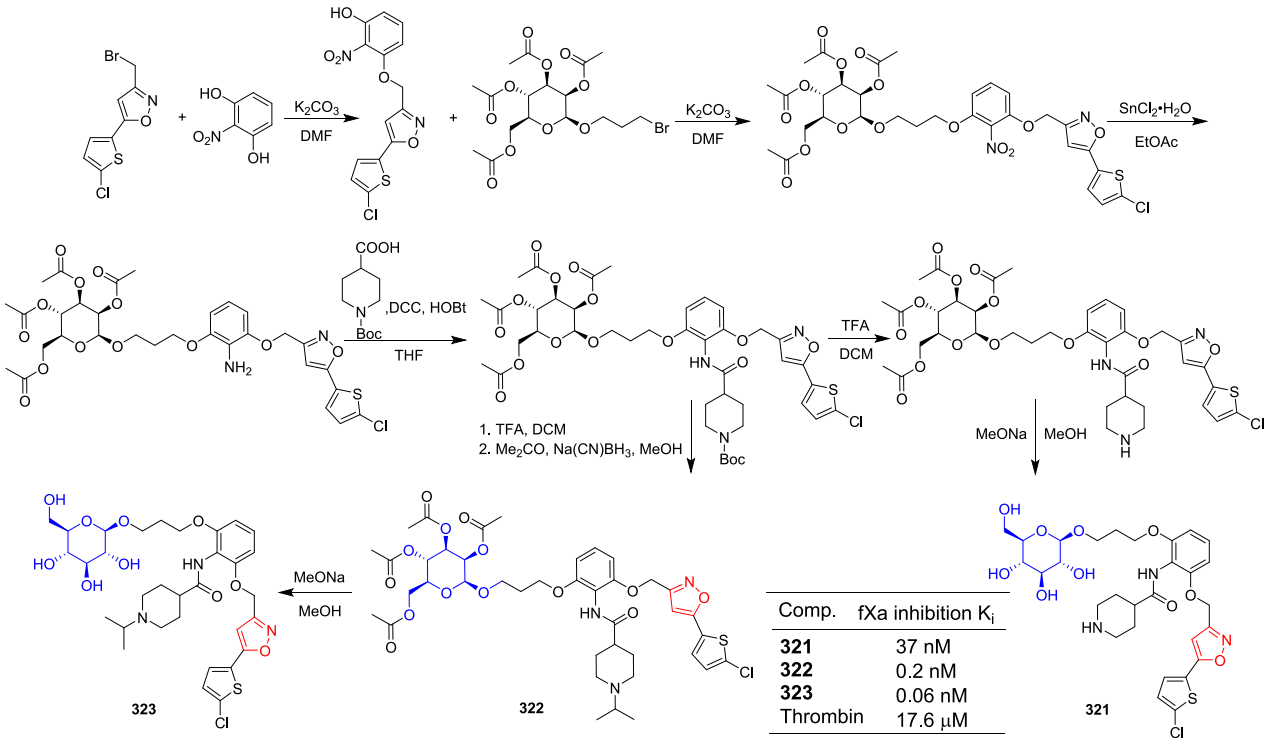

Fig. 71. Carbohydrate-isoxazole derivatives **321**–**323**.

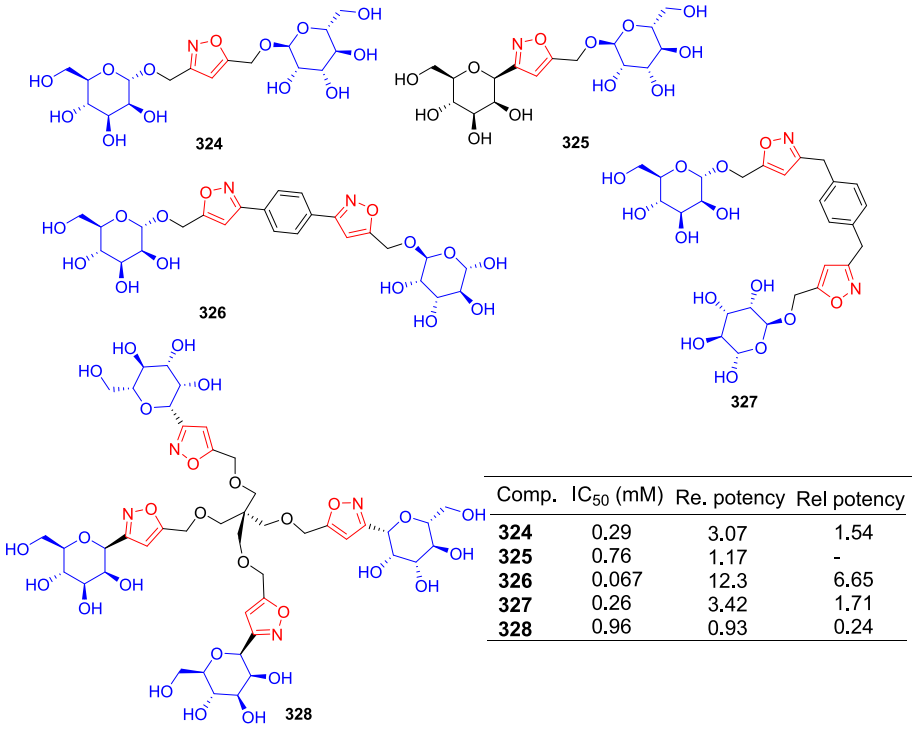

Fig. 72. Carbohydrate-isoxazole derivatives **324**–**328**.

Hajlaoui *et al.* (Hajlaoui et al., 2017) designed and synthesized new glycosubstituted isoxazole and screened these compounds for antibacterial activity against the *Mtb* H37Rv strain. Compounds **310**–**313** showed potent anti-tuberculosis activity with a MIC of 3.125 μg/mL. Compounds **314**–**317** showed moderate inhibitory activity with a MIC of 12.5 μg/mL.

Gueron *et al.* (Gueron et al., 2014) synthesized a series of *D*-nuclear furanoside derivatives containing isoxazole and tested their anti-tumor activity. Compound **318** can inhibit PC3 cell growth, and the inhibition rate is 34.14 % at 10 μM concentration. After treatment with compound **318** for 24 h, PC3 cells remained in the G0/G1 phase (54.5 %). Under the treatment of compound **318**, the increase in the population of G0/G1 cells was mainly at the expense of S phase cells, while the decrease in the population of G2/M cells was minimal.

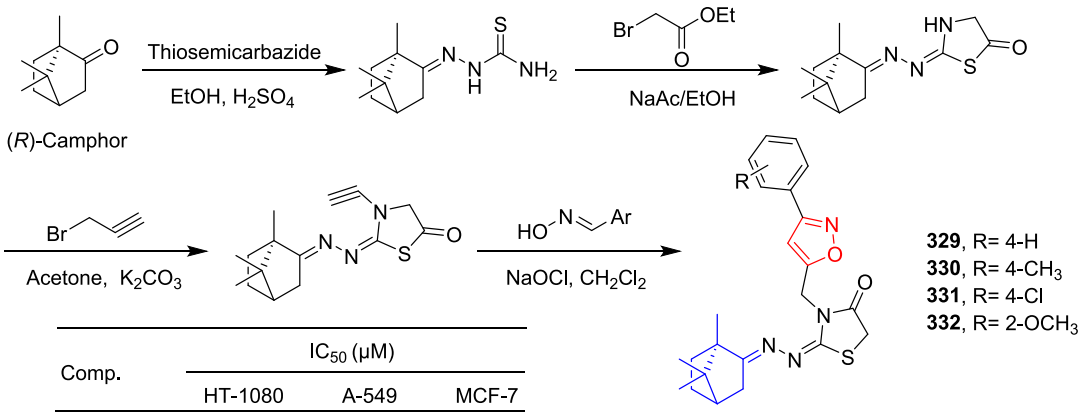

Comp.	IC$_{50}$ (μM)		
	HT-1080	A-549	MCF-7
329	17.27	22.85	24.23
330	13.81	17.29	19.21
331	12.76	11.62	16.92
332	19.67	25.02	31.76
Doxorubicin	5.76	7.54	6.23

Fig. 73. Camphor-isoxazole derivatives **329**–**332**.

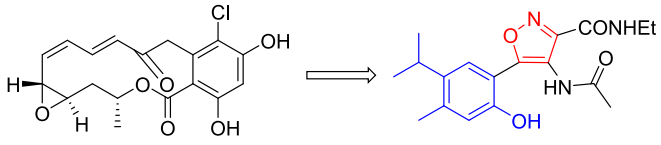

Comp.	Concentration (nM)	HbF%
Blank group	-	17.57
HU	100	19.42
333	85	30.26
333	120	34.65
333	127	39.19
333	200	40.80

Fig. 74. Radicicol-isoxazole derivative **333**.

Marchiori *et al.* (da Rosa et al., 2017) reported the synthesis of *O*-3-triazole-linked galactosyl arylsulfonamides as a potential inhibitor of *Trypanosoma Cruzi* cell invasion. The infection index of compound **319** was reduced (~20), and in corning Epic label-free assays, compound **319** had a high binding affinity to galactin-3 (EC$_{50}$ = 17.2 μM).

Chen *et al.* (Chen et al., 2001) describe the synthesis of compound **320** and its ability to inhibit αGal binding to human anti-Gal antibodies. With two known αGal trisaccharide standards, Galα1-3Galβ1-4GlcNAcβ-Allyl (IC$_{50}$ = 0.03 mM) and Galα1-3Galβ1-4Glcβ-NHAc (IC$_{50}$ = 0.07 mM) were compared. Compound **320** showed an anti-Gal binding affinity comparable to the two αGal standards, with an IC$_{50}$ value of 0.08 mM (Fig. 70).

Lopopolo *et al.* (Lopopolo et al., 2012) reported a series of potent serine protease factor Xa (fXa) inhibitors containing *O*-glucoside. Compounds **321**–**323** showed good anti-coagulant activity *in vitro* with K$_i$ values of 37, 0.2, and 0.06 nM, respectively (Fig. 71).

Pérez-Balderas *et al.* (Pérez-Balderas et al., 2005) designed and synthesized a series of isoxazole-glycoconjugates and evaluated the binding affinity of these conjugates with concanavalin A using an enzyme-linked lectin essay (ELLA). Conjugates **324**–**328** showed inhibitory effects on HRP-labeled concanavalin A binding with IC$_{50}$ ranging from 0.067 to 0.96 mM (Fig. 72).

Summary: Natural products often have the shortcomings of low bioavailability and poor water solubility. Therefore, the introduction of carbohydrates into their structures can often improve their physical properties. Carbohydrate-isoxazole hybridization natural products mainly have anti-tumor, anti-inflammatory, anti-fungal, anti-coagulant, and anti-parasitic activities. To develop anti-coagulant drugs with better safety, fXa inhibitors have emerged as attractive options for venous thromboembolism treatment. Compound **323** achieved *in vitro* excellent inhibition potency against fXa, with a K$_i$ value of 60 pM. The other compounds in this section do not exhibit particularly desirable pharmacological activity. For instance, mofezolac is an anti-inflammatory drug bearing isoxazole moiety, unfortunately, the introduction of carbohydrate fragments into its structure did not increase its inhibitory activity against COX-1.

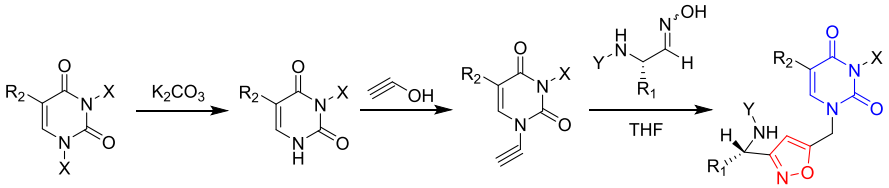

Comp.	EC$_{50}$ (μg/mL)		SI	
	Cox.B3	VSV	Cox.B3	VSV
334	2.46	3.29	10.608	7.9393
335	-	2.54	-	27.91
336	1.02	1.25	98.07	80.02
Ribabirin	9.69	40.58	30.96	7.3931

Fig. 75. Uracil-isoxazole derivatives **334**–**336**.

2.12. Other natural products-isoxazole hybridization

Ousidi *et al.* (Ousidi et al., 2023) synthesized the corresponding thiazolidin-4-one from natural (*R*)-camphor, followed by *N*-alkylation with propargyl bromide prior to subjecting the resulting product to 1,3-dipolar cycloaddition reactions with a series of nitrile oxides. Subsequently, *in vitro* cytotoxicity evaluation was performed on the four synthetic products containing camphor and isoxazole fragments. Unfortunately, their activity against three human cancer cells did not surpass that of the positive control drug Doxorubicin (Fig. 73). The preliminary structure–activity relationship revealed that introducing an electron-withdrawing group in the *para*-position of the phenyl group conferred beneficial effects on activity. Additionally, compound **311** exhibited significant inhibition potential against BCl-2 protein as confirmed by molecular docking studies. Furthermore, through hydrogen bonding interactions with ARG109 and SER105 residues, the nitrogen atom of isoxazole acted as a hydrogen bond acceptor indicating its crucial role.

β-thalassemia can be treated with fetal hemoglobin (HbF) inducers. Currently, hydroxyurea (HU) is the only approved drug capable of inducing HbF, and studies have found that HU treatment is associated with a down-regulation of the heat shock protein (HSP) HSP90AA1 gene. However, the side effects of HU treatment limit enthusiasm for its use. Radicicol is a natural antibiotic, a resorcylic acid lactone known as a natural inhibitor of HSP90 and therefore a potential inducer of HbF in erythroid cells from β-thalassemia patients (Fig. 74). Additionally, it has been discovered that the resorcinolic portion plays a crucial role as a pharmacophore. However, radicicol presents several challenges for therapeutic application including poor solubility, significant liver toxicity, intrinsic chemical instability or loss of activity *in vivo*. Therefore, to develop a novel inducer for HbF, the researchers introduced isoxazole fragments for structural modification. Compound **333** exhibited remarkable induction activity towards HbF and thus represents a strong candidate for ameliorating the phenotype associated with β-thalassemia (Ilaria et al., 2021; Zuccato et al., 2024).

The synthesis route of a series of nucleoside-isoxazole hybrid molecules, as illustrated in Fig. 75, was reported by Kim *et al.* (Kim et al., 2003). The amino groups at both the N_1 and N_3 positions were protected by starting with 5-substituted uracil before selective deprotection of the amino acid at the N_3 position through stirring in a weak base solution was performed. Subsequently, Mitsunobu and cyclization reactions were employed to synthesize the target compounds. Evaluation against poliovirus (Cox.B3) and vesicular stomatitis virus (VSV) revealed that compounds **334**–**336** exhibited superior antiviral activity compared to ribavirin. Among them, compound **336** demonstrated the highest activity with significantly higher selectivity index than ribavirin, indicating its ideal antiviral efficacy and low toxicity towards host cells.

3. Conclusions and perspectives

Natural products encompass all metabolites derived from animals, plants, and microorganisms. Over the past century, structurally diverse natural products have made significant contributions to drug research, including antibiotics, immunosuppressants, anti-tumor agents, cholesterol-lowering drugs, and other clinically utilized medications, most of which are closely associated with natural products. In comparison to synthetic compounds, natural products exhibit greater diversity in terms of structural scaffold and stereochemistry while also possessing a wider range of molecular weight and lipid-water partition coefficient. Furthermore, natural products can actively participate in regulating various aspects of biological processes. These distinctive characteristics and advantages position natural products at the forefront of drug research.

Optimizing the structure of lead compounds is the main task for the development of new drugs, and the structure combination principle has become a strategy for the optimization of lead compounds. With natural products as lead compounds, isoxazole is introduced into different positions of their structure through structural modification may obtain active molecules with high efficiency and low toxicity. As previously mentioned, natural products-isoxazole hybrids have made great progress in medicinal chemistry, but there are still some problems and directions for further development: (i) To obtain both more active compounds and novel chemical structures, researchers can hybridize three or more of the above fragments with the same pharmacological activity. For example, combining two or more natural products of chalcone, flavone, coumarin and naphthoquinone with isoxazole may obtain more powerful anti-tumor agents. (ii) The key to the development of new drugs is the discovery of drug targets. Even though most natural product-isoxazole derivatives have good pharmacological activity, the targets of these compounds are still unclear, making it difficult to enter clinical trials. Computer-aided drug design can be used to find the target of natural product-isoxazole derivatives. At the same time, by extracting pharmacophore features and combining them with scaffold hopping, novel inhibitors for various targets can be obtained to solve the structural disadvantages of natural products such as large molecular weight. (iii) Most natural products have the disadvantages of poor water solubility and low bioavailability. Given this, researchers can use rational drug design strategies or novel drug delivery systems to improve the water solubility, absorption, distribution, metabolism, excretion, and toxicity of these natural product-isoxazole derivatives. Moreover, substituted imidazole, triazole, pyrazole, thiazole, amide, etc. can be used as bioisosteres of isoxazole. If isoxazole is changed into other bioisosteres, more effective bioactive molecules may be developed. (iv) Although many natural product-isoxazole derivatives have better pharmacological activity compared with traditional clinical drugs. However, these compounds have not established complete structure–activity relationship studies. Besides, the mechanism of action of many natural product-isoxazole derivatives is not clear, and *in vivo* activity evaluation has not been carried out, so it is necessary to further study these derivatives.

In conclusion, with the increase of research and development of natural products-isoxazole derivatives, there will be more and more isoxazoles with good efficacy, low toxicity, and superior pharmacokinetic properties applied in clinical practice, and make outstanding contributions to the prevention and protection of human health.

CRediT authorship contribution statement

Jin Wang: Conceptualization, Data curation, Formal analysis, Funding acquisition, Writing – original draft, Writing – review & editing. **Dong-Bo Wang:** Conceptualization, Data curation, Writing – original draft. **Li-Li Sui:** Formal analysis, Investigation, Methodology. **Tian Luan:** Conceptualization, Data curation, Formal analysis, Funding acquisition, Investigation, Methodology, Project administration, Supervision, Validation, Writing – original draft, Writing – review & editing.

Declaration of competing interest

The authors declare that they have no known competing financial interests or personal relationships that could have appeared to influence the work reported in this paper.

Acknowledgements

This study received funding from the Scientific Research Project of the Department of Education of Liaoning Province, China (No. LJKMZ20221801; No. LJKQZ20222274), the PhD Start-up Foundation of Liaoning Province, China (No. 2022-BS-341), the Doctoral Research Foundation of Shenyang Medical College (No. 20205041).

References

Abu-Bakr, S.M., Khidre, M.D., Omar, M.A., Swelam, S.A., Awad, H.M., 2019. Synthesis of furo[3,2-g]chromones under microwave irradiation and their antitumor activity evaluation. J. Heterocycl. Chem. 57, 731–743.

Adachi, H., Nosaka, C., Atsumi, S., Nakae, K., Umezawa, Y., Sawa, R., Kubota, Y., Nakane, C., Shibuya, M., Nishimura, Y., 2021. Structure-activity relationships of natural quinone vegfrecine analogs with potent activity against VEGFR-1 and -2 tyrosine kinases. J. Antibiot. (tokyo) 74, 734–742.

Ahmed, M., Abdul Qadir, M., Hameed, A., Imran, M., Muddassar, M., 2018. Screening of curcumin-derived isoxazole, pyrazoles, and pyrimidines for their anti-inflammatory, antinociceptive, and cyclooxygenase-2 inhibition. Chem. Biol. Drug Des. 91, 338–343.

Ahmed, M., Qadir, M.A., Hameed, A., Arshad, M.N., Asiri, A.M., Muddassar, M., 2018. Sulfonamides containing curcumin scaffold: Synthesis, characterization, carbonic anhydrase inhibition and molecular docking studies. Bioorg. Chem. 76, 218–227.

Ajdukovic, J.J., Penov Gasi, K.M., Jakimov, D.S., Klisuric, O.R., Jovanovic-Santa, S.S., Sakac, M.N., Aleksic, L.D., Djurendic, E.A., 2015. Synthesis, structural analysis and antitumor activity of novel 17α-picolyl and 17(E)-picolinylidene A-modified androstane derivatives. Bioorg. Med. Chem. 23, 1557–1568.

Allen, T.A., Narayanan, N.S., Kholodar-Smith, D.B., Zhao, Y., Laubach, M., Brown, T.H., 2008. Imaging the spread of reversible brain inactivations using fluorescent muscimol. J. Neurosci. Methods 171, 30–38.

Al-Masoudi, N.A., Mahdi, K.M., Abdul-Rida, N.A., Saeed, B.A., Engel, M., 2015. A new pregnenolone analogues as privileged scaffolds in inhibition of CYP17 hydroxylase enzyme. Synthesis and in silico molecular docking study. Steroids 100, 52–59.

Alwaseem, H., Frisch, B.J., Fasan, R., 2018. Anticancer activity profiling of parthenolide analogs generated via P450-mediated chemoenzymatic synthesis. Bioorg. Med. Chem. 26, 1365–1373.

Amolins, M.W., Peterson, L.B., Blagg, B.S., 2009. Synthesis and evaluation of electron-rich curcumin analogues. Bioorg. Med. Chem. 17, 360–367.

Anand, P., Singh, B., 2014. Pyrrolo-isoxazole: a key molecule with diverse biological actions. Mini-Rev. Med. Chem. 14, 623–627.

Andrews, M.C., Wentz, A.C., 1975. Effects of Danazol on gonadotropins and steroid blood levels in normal and anovulatory women. Am. J. Obstet. Gynecol. 121, 817.

Arya, J.S., Joseph, M.M., Sherin, D.R., Nair, J.B., Manojkumar, T.K., Maiti, K.K., 2019. Exploring mitochondria-mediated intrinsic apoptosis by new phytochemical entities: an explicit observation of cytochrome c dynamics on lung and melanoma cancer cells. J. Med. Chem. 62, 8311–8329.

Asha Bhanu, P., China Raju, B., Jayavardhana Rao, Y., Narasimha, G., Kesava Rao, B., 2020. Facile synthesis and docking studies of 7-hydroxyflavanone isoxazoles and acrylates as potential anti-microbial agents. Med. Chem. Res. 29, 217–228.

Awadallah, F.M., El-Waei, T.A., Hanna, M.M., Abbas, S.E., Ceruso, M., Oz, B.E., Guler, O. O., Supuran, C.T., 2015. Synthesis, carbonic anhydrase inhibition and cytotoxic activity of novel chromone-based sulfonamide derivatives. Eur. J. Med. Chem. 96, 425–435.

Badadhe, P.V., Patil, L.R., Bhagat, S.S., Chate, A.V., Shinde, D.W., Nikam, M.D., Gill, C. H., 2013. Synthesis and antimicrobial screening of some novel chromones and pyrazoles with incorporated isoxazole moieties. J. Heterocycl. Chem. 50, 999–1004.

Balaji, N.V., HariBabu, B., Rao, V.U., Subbaraju, G.V., Nagasree, K.P., Kumar, M.M.K., 2019. Synthesis, screening and docking analysis of hispolon pyrazoles and isoxazoles as potential antitubercular agents. Curr. Top. Med. Chem. 19, 662–682.

Bao, B., Sun, Q., Yao, X., Hong, J., Lee, C.O., Sim, C.J., Im, K.S., Jung, J.H., 2005. Cytotoxic bisindole alkaloids from a marine sponge Spongosorites sp. J. Nat. Prod. 68, 711–715.

Baranovsky, A.V., Ladyko, A.S., Shatskaya, V.A., Scherbakov, A.M., 2019. 14β-(Isoxazol-3-yl)methylestrane steroids: chemoselective synthesis and transformations with heterocyclic ring opening. Russ. J. Org. Chem. 55, 202–214.

Baranovsky, A., Ladyko, A., Shkel, T., Sokolov, S., Strushkevich, N., Gilep, A., 2021. Transformations, NMR studies and biological testing of some 17β-isoxazolyl steroids and their heterocyclic ring cleavage derivatives. Steroids 166, 108768.

Bargiotti, A., Musso, L., Dallavalle, S., Merlini, L., Gallo, G., Ciacci, A., Giannini, G., Cabri, W., Penco, S., Vesci, L., Castorina, M., Milazzo, F.M., Cervoni, M.L., Barbarino, M., Pisano, C., Giommarelli, C., Zuco, V., De Cesare, M., Zunino, F., 2012. Isoxazolo(aza)naphthoquinones: A new class of cytotoxic Hsp90 inhibitors. Eur. J. Med. Chem. 53, 64–75.

Barmade, M.A., Murumkar, P.R., Sharma, M.K., Yadav, M.R., 2016. Medicinal chemistry perspective of fused isoxazole derivatives. Curr. Top. Med. Chem. (sharjah, United Arab Emirates) 16, 2863–2883.

Baumann, S., Fas, S.C., Giaisi, M., Müller, W.W., Merling, A., Gülow, K., Edler, L., Krammer, P.H., Li-Weber, M., 2008. Wogonin preferentially kills malignant lymphocytes and suppresses T-cell tumor growth by inducing PLCgamma1- and Ca2+-dependent apoptosis. Blood 111, 2354–2363.

Bian, J., Li, T., Weng, T., Wang, J., Chen, Y., Li, Z., 2017. Synthesis, evaluation and quantitative structure-activity relationship (QSAR) analysis of Wogonin derivatives as cytotoxic agents. Bioorg. Med. Chem. Lett. 27, 1012–1016.

Binford, S.L., Maldonado, F., Brothers, M.A., Weady, P.T., Zalman, L.S., Meador 3rd, J. W., Matthews, D.A., Patick, A.K., 2005. Conservation of amino acids in human rhinovirus 3C protease correlates with broad-spectrum antiviral activity of rupintrivir, a novel human rhinovirus 3C protease inhibitor. Antimicrob. Agents Chemother. 49, 619–626.

Bolden, J.E., Peart, M.J., Johnstone, R.W., 2006. Anticancer activities of histone deacetylase inhibitors. Nat. Rev. Drug Discov. 5, 769–784.

Brain, R.A., Ramirez, A.J., Fulton, B.A., Chambliss, C.K., Brooks, B.W., 2008. Herbicidal effects of sulfamethoxazole in Lemna gibba: using p-aminobenzoic acid as a biomarker of effect. Environ. Sci. Technol. 42, 8965–8970.

Burra, S., Voora, V., Rao, C.P., Vijay Kumar, P., Kancha, R.K., David Krupadanam, G.L., 2017. Synthesis of novel forskolin isoxazole derivatives with potent anti-cancer activity against breast cancer cell lines. Bioorg. Med. Chem. Lett. 27, 4314–4318.

Cao, Y., Shen, Q., Ding, M., Chen, Y., Lu, W., Zhu, S., 2023. Development of HSP90 inhibitors-SN38 conjugates for cancer treatment. Bioorg. Chem. 137, 106582.

Casapullo, A., Bifulco, G., Bruno, I., Riccio, R., 2000. New bisindole alkaloids of the topsentin and hamacanthin classes from the Mediterranean marine sponge Rhaphisia lacazei. J. Nat. Prod. 63, 447–451.

Chakraborti, S., Dhar, G., Dwivedi, V., Das, A., Poddar, A., Chakraborti, G., Basu, G., Chakrabarti, P., Surolia, A., Bhattacharyya, B., 2013. Stable and potent analogues derived from the modification of the dicarbonyl moiety of curcumin. Biochemistry 52, 7449–7460.

Changtam, C., Hongmanee, P., Suksamrarn, A., 2010. Isoxazole analogs of curcuminoids with highly potent multidrug-resistant antimycobacterial activity. Eur. J. Med. Chem. 45, 4446–4457.

Chen, Y., Zhang, W., Chen, X., Wang, J., Wang, P.G., 2001. αGal-conjugated anti-rhinovirus agents: chemo-enzymatic syntheses and testing of anti-Gal binding. J. Chem. Soc., Perkin Trans. 1, 1716–1722.

Chen, Y., Wang, S., Xu, X., Liu, X., Yu, M., Zhao, S., Liu, S., Qiu, Y., Zhang, T., Liu, B.F., Zhang, G., 2013. Synthesis and biological investigation of coumarin piperazine (piperidine) derivatives as potential multireceptor atypical antipsychotics. J. Med. Chem. 56, 4671–4690.

Chen, Y., Lan, Y., Wang, S., Zhang, H., Xu, X., Liu, X., Yu, M., Liu, B.F., Zhang, G., 2014. Synthesis and evaluation of new coumarin derivatives as potential atypical antipsychotics. Eur. J. Med. Chem. 74, 427–439.

Chen, P., Zhang, D., Li, M., Wu, Q., Lam, Y.P.Y., Guo, Y., Chen, C., Bai, N., Malhotra, S., Li, W., O'Connor, P.B., Fu, H., 2019. Discovery of novel, potent, isosteviol-based antithrombotic agents. Eur. J. Med. Chem. 183, 111722.

Cheng, J.F., Chen, M., Liu, B., Hou, Z., Arrhenius, T., Nadzan, A.M., 2006. Design and synthesis of heterocyclic malonyl-CoA decarboxylase inhibitors. Bioorg. Med. Chem. Lett. 16, 695–700.

Chiou, C.T., Lee, W.C., Liao, J.H., Cheng, J.J., Lin, L.C., Chen, C.Y., Song, J.S., Wu, M.H., Shia, K.S., Li, W.T., 2015. Synthesis and evaluation of 3-ylideneoxindole acetamides as potent anticancer agents. Eur. J. Med. Chem. 98, 1–12.

Chopra, B., Dhingra, A.K., 2021. Natural products: a lead for drug discovery and development. Phytother. Res. 35, 4660–4702.

Chouaib, K., Romdhane, A., Delemasure, S., Dutartre, P., Elie, N., Touboul, D., Ben Jannet, H., Ali Hamza, M.h., 2016. Regiospecific synthesis, anti-inflammatory and anticancer evaluation of novel 3,5-disubstituted isoxazoles from the natural maslinic and oleanolic acids. Ind. Crops Prod. 85, 287–299.

Cingolani, G., Panella, A., Perrone, M.G., Vitale, P., Di Mauro, G., Fortuna, C.G., Armen, R.S., Ferorelli, S., Smith, W.L., Scilimati, A., 2017. Structural basis for selective inhibition of Cyclooxygenase-1 (COX-1) by diarylisoxazoles mofezolac and 3-(5-chlorofuran-2-yl)-5-methyl-4-phenylisoxazole (P6). Eur. J. Med. Chem. 138, 661–668.

Collins, R.C., 1980. Anticonvulsant effect of muscimol. Neurology 30, 575.

Combrink, K.D., Denton, D.A., Harran, S., Ma, Z., Chapo, K., Yan, D., Bonventre, E., Roche, E.D., Doyle, T.B., Robertson, G.T., Lynch, A.S., 2007. New C25 carbamate rifamycin derivatives are resistant to inactivation by ADP-ribosyl transferases. Bioorg. Med. Chem. Lett. 17, 522–526.

da Rosa, R., Hoehr de Moraes, M., Zimmermann, L.A., Schenkel, E.P., Steindel, M., Bernardes, L.S.C., 2017. Design and synthesis of a new series of 3,5-disubstituted isoxazoles active against Trypanosoma cruzi and Leishmania amazonensis. Eur. J. Med. Chem. 128, 25–35.

Dalidovich, T.S., Hurski, A.L., Morozevich, G.E., Latysheva, A.S., Sushko, T.A., Strushkevich, N.V., Gilep, A.A., Misharin, A.Y., Zhabinskii, V.N., Khripach, V.A., 2019. New azole derivatives of [17(20)E]-21-norpregnene: Synthesis and inhibition of prostate carcinoma cell growth. Steroids 147, 10–18.

Damiens, E., Baratte, B., Marie, D., Eisenbrand, G., Meijer, L., 2001. Anti-mitotic properties of indirubin-3'-monoxime, a CDK/GSK-3 inhibitor: induction of endoreplication following prophase arrest. Oncogene 20, 3786–3797.

Darwish, E.S., Atia, K.A., Farag, A.M., 2014. Synthesis and antimicrobial evaluation of some isoxazole based heterocycles. Heterocycles 89, 1393–1411.

Das, J., Pany, S., Panchal, S., Majhi, A., Rahman, G.M., 2011. Binding of isoxazole and pyrazole derivatives of curcumin with the activator binding domain of novel protein kinase C. Bioorg. Med. Chem. 19, 6196–6202.

Defossa, E., Wagner, M., 2014. Recent developments in the discovery of FFA1 receptor agonists as novel oral treatment for type 2 diabetes mellitus. Bioorg. Med. Chem. Lett. 24, 2991–3000.

Dengale, S.G., Akolkar, H.N., Darekar, N.R., Shaikh, M.H., Deshmukh, K.K., Mhaske, S. D., Karale, B.K., Raut, D.N., Khedkar, V.M., 2022. Synthesis and biological evaluation of 2-(4,5,6,7-tetrahydrobenzo[c]Isoxazol-3-yl)-4H-chromen-4-ones. Polycyclic Aromat. Compd. 42, 6337–6351.

Dhar, G., Chakravarty, D., Hazra, J., Dhar, J., Poddar, A., Pal, M., Chakrabarti, P., Surolia, A., Bhattacharyya, B., 2015. Actin-curcumin interaction: insights into the mechanism of actin polymerization inhibition. Biochemistry 54, 1132–1143.

Diana, P., Carbone, A., Barraja, P., Kelter, G., Fiebig, H.H., Cirrincione, G., 2010. Synthesis and antitumor activity of 2,5-bis(3'-indolyl)-furans and 3,5-bis(3'-indolyl)-isoxazoles, nortopsentin analogues. Bioorg. Med. Chem. 18, 4524–4529.

Dixit, P., Tripathi, A.C., Saraf, S.K., 2013. Synthesis and characterization of some heteroaromatic derivatives of 3-but-2-enoyl-chromen-2-one and their potential as anti-inflammatory agents. J. Heterocycl. Chem. 50, 1431–1436.

Dolder, C., Nelson, M., Deyo, Z., 2008. Paliperidone for schizophrenia. Am. J. Health-Syst. Pharm. 65, 403–413.

Dong, H.H., Wang, Y.H., Peng, X.M., Zhou, H.Y., Zhao, F., Jiang, Y.Y., Zhang, D.Z., Jin, Y. S., 2021. Synergistic antifungal effects of curcumin derivatives as fungal biofilm inhibitors with fluconazole. Chem. Biol. Drug Des. 97, 1079–1088.
El-Garhy, O.H., 2015. An overview of the azoles of interest. Int. J. Curr. Pharm. Res. 7, 1–6.
Erdagi, S.I., Yildiz, U., 2022. Synthesis, structural analysis and antiproliferative activity of nitrogen-containing hetero spirostan derivatives: oximes, heterocyclic ring-fused and furostanes. ChemistrySelect 7.
Farooq, S., Ngaini, Z., 2022. Synthesis of Benzalacetophenone-based Isoxazoline and Isoxazole Derivatives. Curr. Org. Chem. 26, 679–692.
Figueroa-Valverde, L., Diaz-cedillo, F., Lopez Ramos, M., Garcia Cervera, E., 2011. Synthesis of pregnenolone-danazol-ethylenediamine conjugate. Relationship between descriptors log P, π, Rm, and Vm and its antibacterial activity in S. aureus and V. cholerae. Med. Chem. Res. 20, 847–853.
Filali, I., Romdhane, A., Znati, M., Jannet, H.B., Bouajila, J., 2016. Synthesis of new harmine isoxazoles and evaluation of their potential anti-alzheimer, anti-inflammatory, and anticancer activities. Med. Chem. 12, 184–190.
Galaiko, N.V., Nazarov, A.V., Tolmacheva, I.A., Slepukhin, P.A., Vikharev, Y.B., Maiorova, O.A., Grishko, V.V., 2014. Synthesis of triterpene A-condensed azoles. Chem. Heterocycl. Compd. 50, 65–75.
Gao, Y., Guo, X., Li, X., Liu, D., Song, D., Xu, Y., Sun, M., Jing, Y., Zhao, L., 2010. The Synthesis of glycyrrhetinic acid derivatives containing a nitrogen heterocycle and their antiproliferative effects in human leukemia cells. Molecules 15, 4439–4449.
Gao, Y., Cheng, H., Khan, S., Xiao, G., Rong, L., Bai, C., 2020. Development of coumarine derivatives as potent anti-filovirus entry inhibitors targeting viral glycoprotein. Eur. J. Med. Chem. 204, 112595.
Gao, K., Qin, Y., Wang, L., Li, X., Liu, S., Xing, R., Yu, H., Chen, X., Li, P., 2022. Design, synthesis, and antifungal activities of hymexazol glycosides based on a biomimetic strategy. J. Agric. Food Chem. 70, 9520–9535.
Ghorab, M.M., Alsaid, M.S., Al-Ansary, G.H., Abdel-Latif, G.A., Abou El Ella, D.A., 2016. Analogue based drug design, synthesis, molecular docking and anticancer evaluation of novel chromene sulfonamide hybrids as aromatase inhibitors and apoptosis enhancers. Eur. J. Med. Chem. 124, 946–958.
Giannini, G., Marzi, M., Pezzi, R., Brunetti, T., Battistuzzi, G., Marzo, M.D., Cabri, W., Vesci, L., Pisano, C., 2009. N-Hydroxy-(4-oxime)-cinnamide: a versatile scaffold for the synthesis of novel histone deacetylase [correction of deacetilase] (HDAC) inhibitors. Bioorg. Med. Chem. Lett. 19, 2346–2349.
Giguère, D., Patnam, R., Bellefleur, M.A., St-Pierre, C., Sato, S., Roy, R., 2006. Carbohydrate triazoles and isoxazoles as inhibitors of galectins-1 and -3. Chem. Commun. (camb.) 2379–2381.
Gomha, S.M., Zaki, Y.H., Abdelhamid, A.O., 2015. Utility of 3-acetyl-6-bromo-2H-chromen-2-one for the synthesis of new heterocycles as potential antiproliferative agents. Molecules 20, 21826–21839.
Greene, S., Watanabe, K., Braatz-Trulson, J., Lou, L., 1995. Inhibition of dihydroorotate dehydrogenase by the immunosuppressive agent leflunomide. Biochem. Pharmacol. 50, 861.
Grishko, V.V., Tolmacheva, I.A., Nebogatikov, V.O., Galaiko, N.V., Nazarov, A.V., Dmitriev, M.V., Ivshina, I.B., 2017. Preparation of novel ring-A fused azole derivatives of betulin and evaluation of their cytotoxicity. Eur. J. Med. Chem. 125, 629–639.
Gu, H.S., Chen, X., Zhang, J.W., Zhang, L., Li, L., 2017. Synthesis and biological evaluation of novel flavanone derivatives as potential antipsychotic agents. Chem. Biol. Drug Des. 89, 353–364.
Gueron, G., Avanzo, R.E., Schuster, F., Carabelos, M.N., Vazquez, E., Fascio, M.L., D'Accorso, N.B., 2014. Differential effect of heterocyclic D-ribofuranoside derivatives on human prostate cancer cell viability and cell cycle progression. Biomed. Pharmacother. 68, 847–854.
Gul, W., Hamann, M.T., 2005. Indole alkaloid marine natural products: an established source of cancer drug leads with considerable promise for the control of parasitic, neurological and other diseases. Life Sci. 78, 442–453.
Gundoju, N., Bokam, R., Yalavarthi, N.R., Azad, R., Ponnapalli, M.G., 2019. Betulinic acid derivatives: a new class of α-glucosidase inhibitors and LPS-stimulated nitric oxide production inhibition on mouse macrophage RAW 264.7 cells. Nat. Prod. Res. 33, 2618–2622.
Hajlaoui, K., Guesmi, A., Ben Hamadi, N., Msaddek, M., 2017. Synthesis of carbohydrate-substituted isoxazoles and evaluation of their antitubercular activity. Heterocycl. Commun. 23, 225–229.
Hamama, W.S., Ibrahim, M.E., Zoorob, H.H., 2017. Synthesis, DFT study, and antitumor activity of some new heterocyclic compounds incorporating isoxazole moiety. J. Chin. Chem. Soc. (weinheim, Ger.) 64, 1203–1212.
He, H., Ge, Y., Dai, H., Cui, S., Ye, F., Jin, J., Shi, Y., 2016. Design, synthesis and biological evaluation of stilbene derivatives as novel inhibitors of protein tyrosine phosphatase 1B. Molecules 21.
He, H., Dai, H., Ge, Y., Shi, L., Zou, Z., Ye, F., Jin, J., Shi, Y., 2016. Design, synthesis of betulin derivatives containing 5-phenyl-3-isoxazole and their inhibitory activities against protein tyrosine phosphatase 1B. Chinese J. Org. Chem. 36, 2888–2894.
Hoessel, R., Leclerc, S., Endicott, J.A., Nobel, M.E., Lawrie, A., Tunnah, P., Leost, M., Damiens, E., Marie, D., Marko, D., Niederberger, E., Tang, W., Eisenbrand, G., Meijer, L., 1999. Indirubin, the active constituent of a Chinese antileukaemia medicine, inhibits cyclin-dependent kinases. Nat. Cell Biol. 1, 60–67.
Huang, X., Deng, H., Shen, Q.K., Quan, Z.S., 2022. Tanshinone IIA: pharmacology, total synthesis, and progress in structure-modifications. Curr. Med. Chem. 29, 1959–1989.
Ibrahim, M.E., Hamama, W.S., Metwalli, A.E., Zoorob, H.H., 2016. Chemoselective synthesis of enamino-coumarin derivatives identified as potent antitumor agents. J. Heterocycl. Chem. 53, 1318–1323.
Ilaria, L., Roberto, G., Daniele, 2021. Isoxazole derivatives as inducers of fetal hemoglobin in erythroid precursor cells from beta-thalassemic patients, US11077116, 2021-08-03.
Jiang, X.R., Wang, P., Smith, C.L., Zhu, B.T., 2013. Synthesis of novel estrogen receptor antagonists using metal-catalyzed coupling reactions and characterization of their biological activity. J. Med. Chem. 56, 2779–2790.
Kamal, A., Tamboli, J.R., Vishnuvardhan, M.V.P.S., Adil, S.F., Nayak, V.L., Ramakrishna, S., 2013. Synthesis and anticancer activity of heteroaromatic linked 4β-amido podophyllotoxins as apoptotic inducing agents. Bioorg. Med. Chem. Lett. 23, 273–280.
Kamal, A., Shaik, A.B., Rao, B.B., Khan, I., Bharath Kumar, G., Jain, N., 2015. Design and synthesis of pyrazole/isoxazole linked arylcinnamides as tubulin polymerization inhibitors and potential antiproliferative agents. Org. Biomol. Chem. 13, 10162–10178.
Kaushik, S., Sanawar, R., Lekshmi, A., Chandrasekhar, L., Nair, M., Bhatnagar, S., Santhoshkumar, T.R., 2019. ER alpha selective chromone, isoxazolylchromones, induces ROS-mediated cell death without autophagy. Chem. Biol. Drug Des. 94, 1352–1367.
Kim, B., Lee, Y., Kim, B.H., Lee, Y.S., 2003. New pyrimidine nucleoside analogs containing an isoxazoline or isoxazole ring, useful as antiviral agents in the treatment of e.g. vesicular stomatitis virus (VSV) and Cox B3 virus, WO2003018577, 2003-03-06.
Koohang, A., Majewski, N.D., Szotek, E.L., Mar, A.A., Eiznhamer, D.A., Flavin, M.T., Xu, Z.-Q., 2009. Synthesis and cytotoxicity of 2-cyano-28-hydroxy-lup-1-en-3-ones. Bioorg. Med. Chem. Lett. 19, 2168–2171.
Kovacs, D., Kadar, Z., Motyan, G., Schneider, G., Wolfling, J., Zupko, I., Frank, E., 2012. Synthesis, characterization and biological evaluation of some novel 17-isoxazoles in the estrone series. Steroids 77, 1075–1085.
Krishna, C., Bhargavi, M.V., Rao, Y.J., Krupadanam, G.L.D., 2017. Synthesis of pyrano isoxazoline/isoxazole annulated coumarins via intramolecular nitrile oxide cycloaddition and their cytotoxicity. Russ. J. Gen. Chem. 87, 1857–1863.
Krogsgaard-Larsen, P., Honore, T., Hansen, J.J., Curtis, D.R., Lodge, D., 1980. New class of glutamate agonist structurally related to ibotenic acid. Nature (lond.) 284, 64.
Kumar, G.B., Bukhari, S.N.A., Qin, H.L., 2017. Synthesis of new arylisoxazole-oxindole conjugates as potent antiproliferative agents. Chem. Biol. Drug Des. 89, 634–638.
Kumboonma, P., Senawong, T., Saenglee, S., Senawong, G., Somsakeesit, L.-O., Yenjai, C., Phaosiri, C., 2019. New histone deacetylase inhibitors and anticancer agents from Curcuma longa. Med. Chem. Res. 28, 1773–1782.
Kuo, C.J., Shie, J.J., Fang, J.M., Yen, G.R., Hsu, J.T.A., Liu, H.G., Tseng, S.N., Chang, S.C., Lee, C.Y., Shih, S.R., Liang, P.H., 2008. Design, synthesis, and evaluation of 3C protease inhibitors as anti-enterovirus 71 agents. Bioorg. Med. Chem. 16, 7388–7398.
Lal, J., Gupta, S.K., Thavaselvam, D., Agarwal, D.D., 2013. Biological activity, design, synthesis and structure activity relationship of some novel derivatives of curcumin containing sulfonamides. Eur. J. Med. Chem. 64, 579–588.
Larsen, J.K., Krogh-Nielsen, L., Brøsen, K., 2015. The use of the monoamine oxidase inhibitor isocarboxazide in treatment-resistant depression. Ugeskr. Laeger 177, V06150499.
Lawrence, H.R., Kazi, A., Luo, Y., Kendig, R., Ge, Y., Jain, S., Daniel, K., Santiago, D., Guida, W.C., Sebti, S.M., 2010. Synthesis and biological evaluation of naphthoquinone analogs as a novel class of proteasome inhibitors. Bioorg. Med. Chem. 18, 5576–5592.
Lee, C.C., Huang, K.F., Lin, P.Y., Huang, F.C., Chen, C.L., Chen, T.C., Guh, J.H., Lin, J.J., Huang, H.S., 2012. Synthesis, antiproliferative activities and telomerase inhibition evaluation of novel asymmetrical 1,2-disubstituted amidoanthraquinone derivatives. Eur. J. Med. Chem. 47, 323–336.
Li, Z., Liu, N., Tu, J., Ji, C., Han, G., Wang, Y., Sheng, C., 2019. Discovery of novel simplified isoxazole derivatives of sampangine as potent anti-cryptococcal agents. Bioorg. Med. Chem. 27, 832–840.
Li, Y.H., Tang, S., Li, Y.H., Cheng, X.Y., Zhang, X., Wang, Y.X., Su, F., Song, D.Q., 2017. Novel 12N-substituted matrinanes as potential anti-coxsackievirus agents. Bioorg. Med. Chem. Lett. 27, 829–833.
Lima, L.M., Silva, B.N.M.D., Barbosa, G., Barreiro, E.J., 2020. β-lactam antibiotics: An overview from a medicinal chemistry perspective. Eur. J. Med. Chem. 208, 112829.
Liu, Y.W., Chen, Y.Y., Hsu, C.Y., Chiu, T.Y., Liu, K.L., Lo, C.F., Fang, M.Y., Huang, Y.C., Yeh, T.K., Pak, K.Y., Gray, B.D., Hsu, T.A., Huang, K.H., Shih, C., Shia, K.S., Chen, C. T., Tsou, L.K., 2019. Linker Optimization and therapeutic evaluation of phosphatidylserine-targeting zinc dipicolylamine-based drug conjugates. J. Med. Chem. 62, 6047–6062.
Liu, Z., Swidorski, J.J., Nowicka-Sans, B., Terry, B., Protack, T., Lin, Z., Samanta, H., Zhang, S., Li, Z., Parker, D.D., Rahematpura, S., Jenkins, S., Beno, B.R., Krystal, M., Meanwell, N.A., Dicker, I.B., Regueiro-Ren, A., 2016. C-3 benzoic acid derivatives of C-3 deoxybetulinic acid and deoxybetulin as HIV-1 maturation inhibitors. Bioorg. Med. Chem. 24, 1757–1770.
Li-Weber, M., 2009. New therapeutic aspects of flavones: the anticancer properties of Scutellaria and its main active constituents Wogonin, Baicalein and Baicalin. Cancer Treat. Rev. 35, 57–68.
Lopopolo, G., de Candia, M., Panza, L., Romano, M.R., Lograno, M.D., Campagna, F., Altomare, C., 2012. β-D-Glucosyl conjugates of highly potent inhibitors of blood coagulation factor Xa bearing 2-chorothiophene as a P1 Motif. ChemMedChem 7, 1669–1677.
Lu, Z.H., Liu, Q., Liu, L., Wu, H.Y., Zheng, L., Zhao, J.M., 2018. A novel synthesized sulfonamido-based gallate-JEZTC blocks cartilage degradation on rabbit model of osteoarthritis: an in vitro and in vivo study. Cell. Physiol. Biochem. 49, 2304–2319.
Luginina, J., Linden, M., Bazulis, M., Kumpins, V., Mishnev, A., Popov, S.A., Golubeva, T. S., Waldvogel, S.R., Shults, E.E., Turks, M., 2021. Electrosynthesis of stable betulin-

derived nitrile oxides and their application in synthesis of cytostatic lupane-type triterpenoid-isoxazole conjugates. Eur. J. Org. Chem. 2021, 2557–2577.
Lukesh 3rd, J.C., Carney, D.W., Dong, H., Cross, R.M., Shukla, V., Duncan, K.K., Yang, S., Brody, D.M., Brütsch, M.M., Radakovic, A., Boger, D.L., 2017. Vinblastine 20' amides: synthetic analogues that maintain or improve potency and simultaneously overcome pgp-derived efflux and resistance. J. Med. Chem. 60, 7591–7604.
Ma, L., Miao, D., Lee, J.J., Li, T., Chen, Y., Su, G., Zhao, Y., 2021. Synthesis and biological evaluation of heterocyclic ring-fused dammarane-type ginsenoside derivatives as potential anti-tumor agents. Bioorg. Chem. 116, 105365.
Mahapatra, M., Paidesetty, S.K., Bishoyi, A.K., Padhy, R.N., 2022. Design, molecular docking study of synthesised N-heteroaryl substituted gallamide derivatives and their antibacterial assessment. Nat. Prod. Res. 36, 5575–5583.
Mallavadhani, U.V., Vanga, N.R., Jeengar, M.K., Naidu, V.G.M., 2014. Synthesis of novel ring-A fused hybrids of oleanolic acid with capabilities to arrest cell cycle and induce apoptosis in breast cancer cells. Eur. J. Med. Chem. 74, 398–404.
Marwaha, S., Uvell, H., Salin, O., Lindgren, A.E.G., Silver, J., Elofsson, M., Gylfe, A., 2014. N-acylated derivatives of sulfamethoxazole and sulfafurazole inhibit intracellular growth of Chlamydia trachomatis. Antimicrob. Agents Chemother. 58, 2968.
Mayadevi, M., Sherin, D.R., Keerthi, V.S., Rajasekharan, K.N., Omkumar, R.V., 2012. Curcumin is an inhibitor of calcium/calmodulin dependent protein kinase II. Bioorg. Med. Chem. 20, 6040–6047.
McKinlay, M.A., 2001. Recent advances in the treatment of rhinovirus infections. Curr. Opin. Pharmacol. 1, 477–481.
Megens, A.A.H.P., Awouters, F.H.L., Schotte, A., Meert, T.F., Dugovic, C., Niemegeers, C. J.E., Leysen, J.E., 1994. Survey on the pharmacodynamics of the new antipsychotic risperidone. Psychopharmacology (Berlin) 114, 9–23.
Meng, T., Zhang, D., Xie, Z., Yu, T., Wu, S., Regenass, U., Hilpert, K., Huang, M., Geng, M., Shen, J., 2014. Discovery and optimization of 4,5-diarylisoxazoles as potent dual inhibitors of pyruvate dehydrogenase kinase and heat shock protein 90. J. Med. Chem. 57, 9832–9843.
Mimaki, T., 1998. Clinical pharmacology and therapeutic drug monitoring of zonisamide. Ther. Drug Monit. 20, 593–597.
Minassi, A., Rogati, F., Cruz, C., Prados, M.E., Galera, N., Jinenez, C., Appendino, G., Bellido, M.L., Calzado, M.A., Caprioglio, D., Munoz, E., 2018. Triterpenoid Hydroxamates as HIF Prolyl Hydrolase Inhibitors. J. Nat. Prod. 81, 2235–2243.
Mishra, S., Karmodiya, K., Surolia, N., Surolia, A., 2008. Synthesis and exploration of novel curcumin analogues as anti-malarial agents. Bioorg. Med. Chem. 16, 2894–2902.
Mohamed, M.F., Saddiq, A.A., Al-Shaikh, T.M., Ibrahim, N.S., Abdelhamid, I.A., 2021. Computational studies and sever apoptotic bioactivity of new heterocyclic cyanoacrylamide based p-fluorophenyl and p-phenolic compounds against liver carcinoma (Hepg2). Bioorg. Chem. 114, 105147.
Mohareb, R.M., El-Sayed, N.N.E., Abdelaziz, M.A., 2013. The Knoevenagel reactions of pregnenolone with cyanomethylene reagents: Synthesis of thiophene, thieno[2,3-b] pyridine, thieno[3,2-d]isoxazole derivatives of pregnenolone and their in vitro cytotoxicity towards tumor and normal cell lines. Steroids 78, 1209–1219.
Mokenapelli, S., Yerrabelli, J.R., Das, N., Roy, P., Chitneni, P.R., 2021. Synthesis and cytotoxicity of novel 14α-O-(andrographolide-3-subsitutedisoxazole-5-carboxylate) derivatives. Nat. Prod. Res. 35, 3738–3744.
Moon, M.J., Lee, S.K., Lee, J.W., Song, W.K., Kim, S.W., Kim, J.I., Cho, C., Choi, S.J., Kim, Y.C., 2006. Synthesis and structure-activity relationships of novel indirubin derivatives as potent anti-proliferative agents with CDK2 inhibitory activities. Bioorg. Med. Chem. 14, 237–246.
Narlawar, R., Pickhardt, M., Leuchtenberger, S., Baumann, K., Krause, S., Dyrks, T., Weggen, S., Mandelkow, E., Schmidt, B., 2008. Curcumin-derived pyrazoles and isoxazoles: swiss army knives or blunt tools for Alzheimer's disease? ChemMedChem 3, 165–172.
Nasr, T., Bondock, S., Rashed, H.M., Fayad, W., Youns, M., Sakr, T.M., 2018. Novel hydrazide-hydrazone and amide substituted coumarin derivatives: synthesis, cytotoxicity screening, microarray, radiolabeling and in vivo pharmacokinetic studies. Eur. J. Med. Chem. 151, 723–739.
Nie, J.P., Qu, Z.N., Chen, Y., Chen, J.H., Jiang, Y., Jin, M.N., Yu, Y., Niu, W.Y., Duan, H. Q., Qin, N., 2020. Discovery and anti-diabetic effects of novel isoxazole based flavonoid derivatives. Fitoterapia 142, 104499.
Nifantev, E.E., Koroteev, A.M., Pozdeev, A.O., Koroteev, M.P., Vasyanina, L.K., Kaziev, G. Z., Rogovskii, V.S., Knyazev, V.V., Shirokikh, K.E., Semeikin, A.V., Fedotcheva, T.A., Matyushin, A.I., Shimanovskii, N.L., 2015. Synthesis and cytotoxic activity of dihydroquercetin aryl derivatives. Pharm. Chem. J. 49, 78–81.
Niu, C., Yin, L., Nie, L.F., Dou, J., Zhao, J.Y., Li, G., Aisa, H.A., 2016. Synthesis and bioactivity of novel isoxazole chalcone derivatives on tyrosinase and melanin synthesis in murine B16 cells for the treatment of vitiligo. Bioorg. Med. Chem. 24, 5440–5448.
Norwood, V.M., Murillo-Solano, C., Goertzen, M.G., Brummel, B.R., Perry, D.L., Rocca, J. R., Chakrabarti, D., Huigens, R.W., 2021. Ring distortion of vincamine leads to the identification of re-engineered antiplasmodial agents. ACS Omega 6, 20455–20470.
Nussmeier, N.A., Whelton, A.A., Brown, M.T., Langford, R.M., Hoeft, A., Parlow, J.L., Boyce, S.W., Verburg, K.M., 2005. Complications of the COX-2 inhibitors parecoxib and valdecoxib after cardiac surgery. N. Engl. J. Med. 352, 1081–1091.
Ohnmacht, S.A., Neidle, S., 2014. Small-molecule quadruplex-targeted drug discovery. Bioorg. Med. Chem. Lett. 24, 2602–2612.
Olanipekun, B.E., Ponnapalli, M.G., Patel, H.K., Munipalle, K., Shaik, K., 2023. Design, synthesis of new phenyl acetylene and isoxazole analogues of arjunolic acid as potent tyrosinase and alpha glucosidase inhibitors. Nat. Prod. Res. 37, 1092–1097.
Ousidi, A.N., Bimoussa, A., Loubidi, M., Fawzi, M., Laamari, Y., Oubella, A., Maatallah, M., Berteina-Raboin, S., Auhmani, A., Taha, M.L., Morjani, H., Itto, M.Y. A., 2023. Design, synthesis, cytotoxic effect evaluation and molecular docking of (R)-camphor-based thiazolidinone isoxazole and thiazolidinone-1,2,3-triazole hybrids". ChemistrySelect 8, e202203349.
Pallett, K.E., Little, J.P., Veerasekaran, P., Viviani, F., 1997. Inhibition of 4-hydroxy-phenylpyruvate dioxygenase: the mode of action of the herbicide RPA 201772 (isoxaflutole). Pestic. Sci. 50, 83–84.
Pan, P., Chen, J., Li, X., Li, M., Yu, H., Zhao, J.J., Ni, J., Wang, X., Sun, H., Tian, S., Zhu, F., Liu, F., Huang, Y., Hou, T., 2018. Structure-based drug design and identification of H(2)O-soluble and low toxic hexacyclic camptothecin derivatives with improved efficacy in cancer and lethal inflammation models in vivo. J. Med. Chem. 61, 8613–8624.
Pan, S., Hu, J., Zheng, T., Liu, X., Ju, Y., Xu, C., 2015. Oleanolic acid derivatives induce apoptosis in human leukemia K562 cell involved in inhibition of both Akt1 translocation and pAkt1 expression. Cytotechnology 67, 821–829.
Park, J.Y., Shin, S., Park, K.C., Jeong, E., Park, J.H., 2016. Synthesis and in vitro assay of new triazole linked decursinol derivatives showing inhibitory activity against cholinesterase for Alzheimer's disease therapeutics. J. Korean Chem. Soc. 60, 125–130.
Pati, M.L., Vitale, P., Ferorelli, S., Iaselli, M., Miciaccia, M., Boccarelli, A., Davide Di Mauro, G., Fortuna, C.G., Souza Domingos, T.F., Rodrigues Pereira da Silva, L.C.D., de Padula, M., Cabral, L.M., Sathler, P.C., Vacca, A., Scilimati, A., Perrone, M.G., 2019. Translational impact of novel widely pharmacological characterized mofezolac-derived COX-1 inhibitors combined with bortezomib on human multiple myeloma cell lines viability. Eur. J. Med. Chem. 164, 59–76.
Peng, X., Wu, G., Zhao, A., Huang, K., Chai, L., Natarajan, B., Yang, S., Chen, H., Lin, C., 2020. Synthesis of novel caffeic acid derivatives and their protective effect against hydrogen peroxide induced oxidative stress via Nrf2 pathway. Life Sci. 247, 117439.
Pérez-Balderas, F., Hernández-Mateo, F., Santoyo-González, F., 2005. Synthesis of multivalent neoglycoconjugates by 1,3 dipolar cycloaddition of nitrile oxides and alkynes and evaluation of their lectin-binding affinities. Tetrahedron 61, 9338–9348.
Perrone, M.G., Vitale, P., Ferorelli, S., Boccarelli, A., Coluccia, M., Pannunzio, A., Campanella, F., Di Mauro, G., Bonaccorso, C., Fortuna, C.G., Scilimati, A., 2017. Effect of mofezolac-galactose distance in conjugates targeting cyclooxygenase (COX)-1 and CNS GLUT-1 carrier. Eur. J. Med. Chem. 141, 404–416.
Polier, G., Ding, J., Konkimalla, B.V., Eick, D., Ribeiro, N., Köhler, R., Giaisi, M., Efferth, T., Desaubry, L., Krammer, P.H., Li-Weber, M., 2011. Wogonin and related natural flavones are inhibitors of CDK9 that induce apoptosis in cancer cells by transcriptional suppression of Mcl-1. Cell Death Dis. 2, e182.
Poma, P., Notarbartolo, M., Labbozzetta, M., Maurici, A., Carina, V., Alaimo, A., Rizzi, M., Simoni, D., D'Alessandro, N., 2007. The antitumor activities of curcumin and of its isoxazole analogue are not affected by multiple gene expression changes in an MDR model of the MCF-7 breast cancer cell line: analysis of the possible molecular basis. Int. J. Mol. Med. 20, 329–335.
Pyrczak-Felczykowska, A., Narlawar, R., Pawlik, A., Guzow-Krzeminska, B., Artymiuk, D., Hac, A., Rys, K., Rendina, L.M., Reekie, T.A., Herman-Antosiewicz, A., Kassiou, M., 2019. Synthesis of usnic acid derivatives and evaluation of their antiproliferative activity against cancer cells. J. Nat. Prod. 82, 1768–1778.
Qiu, R., Luo, G., Li, X., Zheng, F., Li, H., Zhang, J., You, Q., Xiang, H., 2018. Lipid accumulation inhibitory activities of novel isoxazole-based chenodeoxycholic acids: Design, synthesis and preliminary mechanism study. Bioorg. Med. Chem. Lett. 28, 2879–2884.
Qiu, R., Luo, G., Cai, X., Liu, L., Chen, M., Chen, D., You, Q., Xiang, H., 2018. Structure-guided design and synthesis of isoflavone analogs of GW4064 with potent lipid accumulation inhibitory activities. Bioorg. Med. Chem. Lett. 28, 3726–3730.
Rajanarendar, E., Ramakrishna, S., Govardhan Reddy, K., Nagaraju, D., Reddy, Y.N., 2013. A facile synthesis, anti-inflammatory and analgesic activity of isoxazolyl-2,3-dihydrospiro[benzo[f]isoindole-1,3'-indoline]-2',4,9-triones. Bioorg. Med. Chem. Lett. 23, 3954–3958.
Rao, Y.J., Sowjanya, T., Thirupathi, G., Murthy, N.Y.S., Kotapalli, S.S., 2018. Synthesis and biological evaluation of novel flavone/triazole/benzimidazole hybrids and flavone/isoxazole-annulated heterocycles as antiproliferative and antimycobacterial agents. Mol. Diversity 22, 803–814.
Ravinaik, B., Ramachandran, D., Basaveswara Rao, M.V., 2019. Design and synthesis of novel β-carboline linked amide derivatives as anticancer agents. Russ. J. Gen. Chem. 89, 511–516.
Reddy, S.T., Mendonza, J.J., Makani, V.K.K., Bhadra, M.P., Uppuluri, V.M., 2020. Synthesis of some novel methyl β-orsellinate based 3, 5-disubstituted isoxazoles and their anti-proliferative activity: Identification of potent leads active against MCF-7 breast cancer cell. Bioorg. Chem. 105, 104374.
Rodrigues, F.C., Kumar, N.V.A., Hari, G., Pai, K.S.R., Thakur, G., 2021. The inhibitory potency of isoxazole-curcumin analogue for the management of breast cancer: A comparative in vitro and molecular modeling investigation. Chem. Pap. 75, 5995–6008.
Rotbart, H.A., Webster, A.D., Abzug, M., Adderson, E., Alberti, C., Ansevin, C., Aspalter, R., Belani, K., Bernadini, G., Bien, M., Blanche, S., Boucher, F.D., Cappello, M., Carbone, J., Chapel, H., Chataway, J., Cree, B., Davies, G., Dobbins, E., Elder, M., Fernandez-Cruz, E., Fowler, S., Gern, J., Gonzalez, H., Gottesman, G., Groothius, D., Gungor, T., Haron, E., Hartman, K., Hassin-Baer, S., Hedderwick, S., Herold, B., Huisoon, A., Jain, A., Jones, A., Johnston, A., Kennedy, C., Keyes, T., King, D., Kurachek, S., Kyriakides, T., Levy, J., Mellon, M., Mellor, D., Mudgal, R., O'Keefe, B., Obermiller, T., Boggs, S., Oleastro, M., Parker, T., Pawson, R., Pettett, G., Potter, M., Prentice, H., Raffi, F., Rahal, J., Rankin, P., Romero, J., Ross, S., Sanders, L., Schmalsteig, F., Seger, R., Sullivan, B., Tarafder, J., Thilo, E., Thompson, A., Turner, R., Waring, G., Williams, L., Zaia, J., 2001. Treatment of potentially life-threatening enterovirus infections with pleconaril. Clin. Infect. Dis. 32, 228–235.

Sahoo, S.K., Rani, B., Gaikwad, N.B., Ahmad, M.N., Kaul, G., Shukla, M., Nanduri, S., Dasgupta, A., Chopra, S., Yaddanapudi, V.M., 2021. Synthesis and structure-activity relationship of new chalcone linked 5-phenyl-3-isoxazolecarboxylic acid methyl esters potentially active against drug resistant Mycobacterium tuberculosis. Eur. J. Med. Chem. 222, 113580.
Saidi, I., Manachou, M., Znati, M., Bouajila, J., Ben Jannet, H., 2022. Synthesis of new halogenated flavonoid-based isoxazoles: in vitro and in silico evaluation of α-amylase inhibitory potential, a SAR analysis and DFT studies. J. Mol. Struct. 1247, 131379.
Salgia, N.J., Zengin, Z.B., Pal, S.K., 2020. Tivozanib in renal cell carcinoma: a new approach to previously treated disease. Ther. Adv. Med. Oncol. 12, 1758835920923818.
Santos, M.M., Faria, N., Iley, J., Coles, S.J., Hursthouse, M.B., Martins, M.L., Moreira, R., 2010. Reaction of naphthoquinones with substituted nitromethanes. Facile synthesis and antifungal activity of naphtho[2,3-d]isoxazole-4,9-diones. Bioorg. Med. Chem. Lett. 20, 193–195.
Scott, L.J., 2007. Sitaxentan: in pulmonary arterial hypertension. Drugs 67, 761–770.
Selvam, C., Jachak, S.M., Thilagavathi, R., Chakraborti, A.K., 2005. Design, synthesis, biological evaluation and molecular docking of curcumin analogues as antioxidant, cyclooxygenase inhibitory and anti-inflammatory agents. Bioorg. Med. Chem. Lett. 15, 1793–1797.
Shaik, A., Bhandare, R.R., Palleapati, K., Nissankararao, S., Kancharlapalli, V., Shaik, S., 2020. Antimicrobial, antioxidant, and anticancer activities of some novel isoxazole ring containing chalcone and dihydropyrazole derivatives. Molecules 25.
Shakeel, R., Masood ur, R., Tripathi, V.K., Singh, J., Ara, T., Koul, S., Farooq, S., Kaul, A., 2014. Synthesis and biological evaluation of novel isoxazoles and triazoles linked 6-hydroxycoumarin as potent cytotoxic agents. Bioorg. Med. Chem. Lett. 24, 4243–4246.
Sherin, D.R., Rajasekharan, K.N., 2015. Mechanochemical synthesis and antioxidant activity of curcumin-templated azoles. Arch. Pharm. (weinheim) 348, 908–914.
Shi, W., Hu, J., Bao, N., Li, D., Chen, L., Sun, J., 2017. Design, synthesis and cytotoxic activities of scopoletin-isoxazole and scopoletin-pyrazole hybrids. Bioorg. Med. Chem. Lett. 27, 147–151.
Shin, J., Seo, Y., Cho, K.W., Rho, J.R., Sim, C.J., 1999. New Bis(Indole) alkaloids of the topsentin class from the sponge spongosorites genitrix. J. Nat. Prod. 62, 647–649.
Shultz, M.D., Cao, X., Chen, C.H., Cho, Y.S., Davis, N.R., Eckman, J., Fan, J., Fekete, A., Firestone, B., Flynn, J., Green, J., Growney, J.D., Holmqvist, M., Hsu, M., Jansson, D., Jiang, L., Kwon, P., Liu, G., Lombardo, F., Lu, Q., Majumdar, D., Meta, C., Perez, L., Pu, M., Ramsey, T., Remiszewski, S., Skolnik, S., Traebert, M., Urban, L., Uttamsingh, V., Wang, P., Whitebread, S., Whitehead, L., Yan-Neale, Y., Yao, Y.-M., Zhou, L., Atadja, P., 2011. Optimization of the in vitro cardiac safety of hydroxamate-based Histone deacetylase inhibitors. J. Med. Chem. 54, 4752–4772.
Shultz, M., Fan, J., Chen, C., Cho, Y.S., Davis, N., Bickford, S., Buteau, K., Cao, X., Holmqvist, M., Hsu, M., Jiang, L., Liu, G., Lu, Q., Patel, C., Suresh, J.R., Selvaraj, M., Urban, L., Wang, P., Yan-Neale, Y., Whitehead, L., Zhang, H., Zhou, L., Atadja, P., 2011. The design, synthesis and structure-activity relationships of novel isoindoline-based histone deacetylase inhibitors. Bioorg. Med. Chem. Lett. 21, 4909–4912.
Simoni, D., Rizzi, M., Rondanin, R., Baruchello, R., Marchetti, P., Invidiata, F.P., Labbozzetta, M., Poma, P., Carina, V., Notarbartolo, M., Alaimo, A., D'Alessandro, N., 2008. Antitumor effects of curcumin and structurally beta-diketone modified analogs on multidrug resistant cancer cells. Bioorg. Med. Chem. Lett. 18, 845–849.
Singh, J., Zeller, W., Zhou, N., Hategan, G., Mishra, R.K., Polozov, A., Yu, P., Onua, E., Zhang, J., Ramírez, J.L., Sigthorsson, G., Thorsteinnsdottir, M., Kiselyov, A.S., Zembower, D.E., Andrésson, T., Gurney, M.E., 2010. Structure-activity relationship studies leading to the identification of (2E)-3-[l-[(2,4-dichlorophenyl)methyl]-5-fluoro-3-methyl-lH-indol-7-yl]-N-[(4,5-dichloro-2-thienyl)sulfonyl]-2-propenamide (DG-041), a potent and selective prostanoid EP3 receptor antagonist, as a novel antiplatelet agent that does not prolong bleeding. J. Med. Chem. 53, 18–36.
Smirnova, I.E., Kazakova, O.B., Loesche, A., Hoenke, S., Csuk, R., 2020. Evaluation of cholinesterase inhibitory activity and cytotoxicity of synthetic derivatives of di- and triterpene metabolites from Pinus silvestris and Dipterocarpus alatus resins. Med. Chem. Res. 29, 1478–1485.
Smith, G.R., Caglic, D., Capek, P., Zhang, Y., Godbole, S., Reitz, A.B., Dickerson, T.J., 2012. Reexamining hydroxamate inhibitors of botulinum neurotoxin serotype A: extending towards the β-exosite. Bioorg. Med. Chem. Lett. 22, 3754–3757.
Stebelska, K., 2013. Fungal hallucinogens psilocin, ibotenic acid, and muscimol: analytical methods and biologic activities. Ther. Drug Monit. 35, 420–442.
Sunduru, N., Salin, O., Gylfe, A., Elofsson, M., 2015. Design, synthesis and evaluation of novel polypharmacological antichlamydial agents. Eur. J. Med. Chem. 101, 595–603.
Sunitha, V., Kumar, A.K., Lincoln, C.A., Jalapathi, P., Reddy, V.G., 2018. Synthesis and antibacterial evaluation of benzofuran based 3,5-disubstituted isoxazoles. Russ. J. Gen. Chem. 88, 2669–2674.
Sunitha, V., Kumar, A.K., Mahesh, M., Shankaraiah, P., Jalapathi, P., Lincoln, C.A., 2018. Synthesis and antimicrobial evaluation of bis-3,5-disubstituted isoxazoles based chalcones. Russ. J. Gen. Chem. 88, 1904–1911.
Suresh, L., Kumar, P.S.V., Onkar, P., Srinivas, L., Pydisetty, Y., Chandramouli, G.V.P., 2017. Synthesis and in vitro evaluation of dihydro-6H-chromeno[4,3-b]isoxazolo [4,5-e]pyridine derivatives as potent antidiabetic agents. Res. Chem. Intermed. 43, 5433–5451.
Swapnaja, K.J., Yennam, S., Chavali, M., Poornachandra, Y., Kumar, C.G., Muthusamy, K., Jayaraman, V.B., Arumugam, P., Balasubramanian, S., Sriram, K.K., 2016. Design, synthesis and biological evaluation of diaziridinyl quinone isoxazole hybrids. Eur. J. Med. Chem. 117, 85–98.
Syed, H., Safa, R., Chidlow, G., Osborne, N.N., 2006. Sulfisoxazole, an endothelin receptor antagonist, protects retinal neurones from insults of ischemia/reperfusion or lipopolysaccharide. Neurochem. Int. 48, 708–717.
Sysak, A., Obminska-Mrukowicz, B., 2017. Isoxazole ring as a useful scaffold in a search for new therapeutic agents. Eur. J. Med. Chem. 137, 292–309.
Taka, T., Changtam, C., Thaichana, P., Kaewtunjai, N., Suksamrarn, A., Lee, T.R., Tuntiwechapikul, W., 2014. Curcuminoid derivatives enhance telomerase activity in an in vitro TRAP assay. Bioorg. Med. Chem. Lett. 24, 5242–5246.
Talley, J.J., Brown, D.L., Carter, J.S., Graneto, M.J., Koboldt, C.M., Masferrer, J.L., Perkins, W.E., Rogers, R.S., Shaffer, A.F., Zhang, Y.Y., Zweifel, B.S., Seibert, K., 2000. 4-[5-Methyl-3-phenylisoxazol-4-yl]- benzenesulfonamide, Valdecoxib: A Potent and Selective Inhibitor of COX-2. J. Med. Chem. 43, 775–777.
Thakur, A., Verma, M., Bharti, R., Sharma, R., 2022. Oxazole and isoxazole: From one-pot synthesis to medical applications. Tetrahedron 119, 132813.
Tsai, S.E., Lee, J.C., Uramaru, N., Takayama, H., Huang, G.J., Wong, F.F., 2017. Synthesis and antiproliferative activity of 3α-hydroxyl-3β-methoxymethyl-5α-pregnan-20-one with a C-21 hydrophilic substituent. Heteroat. Chem. 28.
Tyagi, V., Alwaseem, H., O'Dwyer, K.M., Ponder, J., Li, Q.Y., Jordan, C.T., Fasan, R., 2016. Chemoenzymatic synthesis and antileukemic activity of novel C9- and C14-functionalized parthenolide analogs. Bioorg. Med. Chem. 24, 3876–3886.
Uchino, T., Sanyal, S.N., Yamabe, M., Kaku, T., Takebayashi, S., Shimaoka, T., Shimada, T., Noguchi, T., Ono, K., 2008. Rescue of pulmonary hypertension with an oral sulfonamide antibiotic sulfisoxazole by endothelin receptor antagonistic actions. Hypertens. Res. 31, 1781–1790.
Urdaneta, A., Siso, A., Urdaneta, B., Cardenas, R., Quintero, L., Avila, R., Suarez-Roca, H., 2009. Lack of correlation between the central anti-nociceptive and peripheral anti-inflammatory effects of selective COX-2 inhibitor parecoxib. Brain Res. Bull. 80, 56–61.
Uysal, S., Soyer, Z., Saylam, M., Tarikogullari, A.H., Yilmaz, S., Kirmizibayrak, P.B., 2021. Design, synthesis and biological evaluation of novel naphthoquinone-4-aminobenzensulfonamide/carboxamide derivatives as proteasome inhibitors. Eur. J. Med. Chem. 209, 112890.
Viviani, F., Little, J.P., Pallett, K.E., 1998. The mode of action of isoxaflutole II. Characterization of the inhibition of carrot 4-hydroxyphenylpyruvate dioxygenase by the diketonitrile derivative of isoxaflutole. Pestic. Biochem. Physiol. 62, 125–134.
Wan, M., Xu, L., Hua, L., Li, A., Li, S., Lu, W., Pang, Y., Cao, C., Liu, X., Jiao, P., 2014. Synthesis and evaluation of novel isoxazolyl chalcones as potential anticancer agents. Bioorg. Chem. 54, 38–43.
Wang, L.J., Geng, C.A., Ma, Y.B., Huang, X.Y., Luo, J., Chen, H., Guo, R.H., Zhang, X.M., Chen, J.J., 2012. Synthesis, structure-activity relationships and biological evaluation of caudatin derivatives as novel anti-hepatitis B virus agents. Bioorg. Med. Chem. 20, 2877–2888.
Wang, X., Hu, Q., Tang, H., Pan, X., 2023. Isoxazole/isoxazoline skeleton in the structural modification of natural products: a review. Pharmaceuticals 16, 228.
Wang, Z.C., Qin, Y.J., Wang, P.F., Yang, Y.A., Wen, Q., Zhang, X., Qiu, H.Y., Duan, Y.T., Wang, Y.T., Sang, Y.L., Zhu, H.L., 2013. Sulfonamides containing coumarin moieties selectively and potently inhibit carbonic anhydrases II and IX: design, synthesis, inhibitory activity and 3D-QSAR analysis. Eur. J. Med. Chem. 66, 1–11.
Wang, S.R., Xu, T., Deng, K., Wong, C.W., Liu, J., Fang, W.S., 2017. Discovery of farnesoid X receptor antagonists based on a library of oleanolic acid 3-O-esters through diverse substituent design and molecular docking methods. Molecules 22, 690/691-690/613.
Wasmann, R.E., Muilwijk, E.W., Burger, D.M., Verweij, P.E., Knibbe, C.A., Brueggemann, R.J., 2018. Clinical pharmacokinetics and pharmacodynamics of micafungin. Clin. Pharmacokinet. 57, 267–286.
Witherell, G., 2000. AG-7088 Pfizer. Curr. Opin. Investig. Drugs 1, 297–302.
Wu, J., Bao, B.H., Shen, Q., Zhang, Y.C., Jiang, Q., Li, J.X., 2016. Novel heterocyclic ring-fused oleanolic acid derivatives as osteoclast inhibitors for osteoporosis. MedChemComm 7, 371–377.
Wu, J.P., Wang, J., Abeywardane, A., Andersen, D., Emmanuel, M., Gautschi, E., Goldberg, D.R., Kashem, M.A., Lukas, S., Wang, M., Martin, L., Morwick, T., Moss, N., Pargellis, C., Patel, U.R., Patnaude, L., Peet, G.W., Skow, D., Snow, R.J., Ward, Y., Werneburg, B., White, A., 2007. The discovery of carboline analogs as potent MAPKAP-K2 inhibitors. Bioorg. Med. Chem. Lett. 17, 4664–4669.
Wu, Q., Wang, R., Shi, Y., Li, W., Li, M., Chen, P., Pan, B., Wang, Q., Li, C., Wang, J., Sun, G., Sun, X., Fu, H., 2020. Synthesis and biological evaluation of panaxatriol derivatives against myocardial ischemia/reperfusion injury in the rat. Eur. J. Med. Chem. 185, 111729.
Xiao, H., Li, P., Li, X., He, H., Wang, J., Guo, F., Zhang, J., Wei, L., Zhang, H., Shi, Y., Hou, L., Shen, L., Chen, Z., Du, C., Fu, S., Zhang, P., Hao, F., Wang, P., Xu, D., Liang, W., Tian, X., Zhang, A., Cheng, X., Yang, L., Wang, X., Zhang, X., Li, J., Chen, S., 2017. Synthesis and biological evaluation of a series of bile acid derivatives as FXR agonists for treatment of NASH. ACS Med Chem Lett 8, 1246–1251.
Xu, J., Li, Z., Luo, J., Yang, F., Liu, T., Liu, M., Qiu, W.W., Tang, J., 2012. Synthesis and biological evaluation of heterocyclic ring-fused betulinic acid derivatives as novel inhibitors of osteoclast differentiation and bone resorption. J. Med. Chem. 55, 3122–3134.
Xu, H., Zhang, K., Lv, M., Hao, M., 2021. Construction of cholesterol oxime ether derivatives containing isoxazoline/isoxazole fragments and their agricultural bioactive properties/control efficiency. J. Agric. Food Chem. 69, 8098–8109.
Yang, S.S., Hu, Y.B., Wang, X.D., Gao, Y.R., Li, K., Zhang, X.E., Chen, S.Y., Zhang, T.Y., Gu, J., Deng, J.Y., 2017. Deletion of sigB causes increased sensitivity to para-aminosalicylic acid and sulfamethoxazole in mycobacterium tuberculosis. Antimicrob. Agents Chemother. 61.

Yang, R., Ma, M., Lv, M., Zhang, S., Xu, H., 2021. Non-food bioactive products for pesticides candidates (III): Agricultural properties of isoxazole esters from the plant product podophyllotoxin as botanical pesticides. Ind. Crop. Prod. 174.
Yang, X., Sun, G., Yang, C., Wang, B., 2011. Novel rhein analogues as potential anticancer agents. ChemMedChem 6, 2294–2301.
Yang, H., Zhu, X.Q., Wang, W., Chen, Y., Hu, Z., Zhang, Y., Hu, D.X., Yu, L.M., Agama, K., Pommier, Y., An, L.K., 2021. The synthesis of furoquinolinedione and isoxazoloquinolinedione derivatives as selective Tyrosyl-DNA phosphodiesterase 2 (TDP2) inhibitors. Bioorg. Chem. 111, 104881.
Yao, H., Liu, J., Xu, S., Zhu, Z., Xu, J., 2017. The structural modification of natural products for novel drug discovery. Expert Opin. Drug Discovery 12, 121–140.
Ye, Q., Li, M., Zhou, Y., Pang, T., Xu, L., Cao, J., Han, L., Li, Y., Wang, W., Gao, J., Li, J., 2013. Synthesis and biological evaluation of 3-benzisoxazolyl-4-indolylmaleimides as potent, selective inhibitors of glycogen synthase kinase-3β. Molecules 18, 5498–5516.
Yin, L., Niu, C., Liao, L.X., Dou, J., Habasi, M., Aisa, H.A., 2017. An isoxazole chalcone derivative enhances melanogenesis in B16 melanoma cells via the Akt/GSK3β/β-catenin signaling pathways. Molecules 22.
You, Y.J., Kim, Y., Nam, N.H., Ahn, B.Z., 2003. Synthesis and cytotoxic activity of A-ring modified betulinic acid derivatives. Bioorg. Med. Chem. Lett. 13, 3137–3140.
Yu, L.M., Hu, Z., Chen, Y., Ravji, A., Lopez, S., Plescia, C.B., Yu, Q., Yang, H., Abdelmalak, M., Saha, S., Agama, K., Kiselev, E., Marchand, C., Pommier, Y., An, L. K., 2018. Synthesis and structure-activity relationship of furoquinolinediones as inhibitors of Tyrosyl-DNA phosphodiesterase 2 (TDP2). Eur. J. Med. Chem. 151, 777–796.
Zhang, H., Li, F., Zhu, P., Liu, J., Yao, H., Jiang, J., Ye, W., Wu, X., Xu, J., 2015. Synthesis and biological evaluation of oxygen-containing heterocyclic ring-fused 23-hydroxy-betulinic acid derivatives as antitumor agents. Chem. Biol. Drug Des. 86, 424–431.
Zhang, W.M., Yao, Y., Yang, T., Wang, X.Y., Zhu, Z.Y., Xu, W.T., Lin, H.X., Gao, Z.B., Zhou, H., Yang, C.G., Cui, Y.M., 2018. The synthesis and antistaphylococcal activity of N-sulfonaminoethyloxime derivatives of dehydroabietic acid. Bioorg. Med. Chem. Lett. 28, 1943–1948.
Zhang, L., Zhang, Z., Chen, F., Chen, Y., Lin, Y., Wang, J., 2016. Aromatic heterocyclic esters of podophyllotoxin exert anti-MDR activity in human leukemia K562/ADR cells via ROS/MAPK signaling pathways. Eur. J. Med. Chem. 123, 226–235.
Zhang, H., Zhou, C., Geng, R., Ji, Q., 2011. Recent advances in syntheses of oxazole compounds. Chin. J. Org. Chem. 31, 1963–1976.
Zhao, L., Li, Y., Wang, Y., Qiao, Z., Miao, Z., Yang, J., Huang, L., Tian, C., Li, L., Chen, D., Yang, S., 2019. Discovery of 4H-chromen-4-one derivatives as a new class of selective rho kinase (ROCK) inhibitors, which showed potent activity in ex vivo diabetic retinopathy models. J. Med. Chem. 62, 10691–10710.
Zhu, J., Mo, J., Lin, H.Z., Chen, Y., Sun, H.P., 2018. The recent progress of isoxazole in medicinal chemistry. Bioorg. Med. Chem. 26, 3065–3075.
Zhu, S., Shen, Q., Gao, Y., Wang, L., Fang, Y., Chen, Y., Lu, W., 2020. Design, synthesis, and biological evaluation of HSP90 inhibitor-SN38 conjugates for targeted drug accumulation. J. Med. Chem. 63, 5421–5441.
Zuccato, C., Cosenza, L.C., Tupini, C., Finotti, A., Sacchetti, G., Simoni, D., Gambari, R., Lampronti, I., 2024. New synthetic isoxazole derivatives acting as potent inducers of fetal hemoglobin in erythroid precursor cells isolated from β-thalassemic patients. Molecules 29, 8.